



THE APPLICATION OF EMPIRICALLY DETERMINED  
FREQUENCY RESPONSE FUNCTIONS TO SBWR DATA

BY  
E.G. PITTS

REPORT NO. 259  
1988



INSTITUTE OF  
OCEANOGRAPHIC SCIENCES  
DEACON LABORATORY

**INSTITUTE OF OCEANOGRAPHIC SCIENCES  
DEACON LABORATORY**

---

**Wormley, Godalming,  
Surrey, GU8 5UB, U.K.**

**Telephone: 0428 79 4141  
Telex: 858833 OCEANS G  
Telefax: 0428 79 3066**

Director: Dr. C.P. Summerhayes

INSTITUTE OF OCEANOGRAPHIC SCIENCES

DEACON LABORATORY

REPORT No. 259

The application of empirically determined  
frequency response functions to SBWR data

E.G. Pitt

1988



# DOCUMENT DATA SHEET

AUTHOR	PITT, E.G.	PUBLICATION DATE 1988
<b>TITLE</b> The application of empirically determined frequency response functions to SBWR data.		
<b>REFERENCE</b> Institute of Oceanographic Sciences Deacon Laboratory, Report, No.259, 82pp.		
<b>ABSTRACT</b> <p>A method is described for applying empirically determined frequency response functions to Shipborne Wave Recorder (SBWR) measurements of wave spectra. A Froude number scaling of the available response measurements, as proposed by Crisp (1987), is used. The relative merits of a number of different length scales are discussed, as are two methods of fitting the response data to mathematical formulae.</p> <p>The correction formulae are then applied to spectral data from the I.O.S. routine SBWR wave data collection programme and the results evaluated. This is done by</p> <ul style="list-style-type: none"> <li>(a) Considering the "reasonableness" of the spectra themselves.</li> <li>(b) Comparing <math>H_s</math> and <math>T_z</math> estimated from the spectra with the corresponding quantities estimated from the simultaneous chart records.</li> <li>(c) In the case of the Seven Stones L.V. data, comparing <math>H_s</math> and <math>T_z</math> from the SBWR spectra with <math>H_s</math> and <math>T_z</math> from the Scilly Isles Waverider spectra which was operating in the same general area.</li> </ul> <p>It is found that the new correction procedure gives reasonable results for (a) and (c), but that there exist considerable discrepancies between <math>H_s</math> estimated from the spectra corrected using the new formulation and <math>H_s</math> from the chart records corrected using the old method.</p> <p>In view of this a method is developed for recorrecting historical SBWR data to the new correction standard.</p>		
<b>ISSUING ORGANISATION</b> <p>Institute of Oceanographic Sciences Deacon Laboratory Wormley, Godalming Surrey GU8 5UB. UK.</p>		<b>TELEPHONE</b> 0428 79 4141  <b>TELEX</b> 858833 OCEANS G  <b>TELEFAX</b> 0428 79 3066
<b>KEYWORDS</b> <p>SHIPBORNE WAVE RECORDER FREQUENCY RESPONSE WAVE SPECTRA</p>		<b>CONTRACT</b>  <b>PROJECT</b>  <b>PRICE</b> £22.00

Copies of this report are available from:  
The Library, Institute of Oceanographic Sciences Deacon Laboratory.



<u>CONTENTS</u>	<u>Page</u>
<b>INTRODUCTION</b>	7
The Analysis of SBWR data	7
Choice of Method of Analysis of Digital Data	8
<b>THE OPERATION OF THE SBWR AND ITS FREQUENCY RESPONSE</b>	9
<b>FREQUENCY SCALING OF MEASURED RESPONSE DATA</b>	10
<b>FITTING FORMULAE TO MEASURED RESPONSE DATA</b>	13
<b>APPLICATION OF THE RESPONSE CORRECTION</b>	14
The SBWR microcomputer data collection programme	15
Operation of the onboard microcomputer	15
On-shore processing	16
<b>EVALUATION OF THE SPECTRA</b>	17
<b>COMPARISON BETWEEN <math>H_s</math> AND <math>T_z</math> DERIVED FROM CHART RECORDS AND THE CORRESPONDING SPECTRAL MEASURES</b>	18
<b>RECORRECTING HISTORICAL WAVEHEIGHT DATA</b>	21
Differences between the T-D and the spectral estimates of $H_s$	21
The Characteristic Period	22
Recorrection of $H_s$ (T-D)	26
<b>CONCLUSIONS</b>	27
<b>ACKNOWLEDGEMENT</b>	28
<b>REFERENCES</b>	29
<b>FIGURES</b>	33-82



## 1. INTRODUCTION

The Shipborne Wave Recorder (SBWR) was devised by M.J. Tucker in the early 1950's, (TUCKER, 1956). Since then it has been used extensively for the routine measurement of waves in sea areas around the British Isles and in the North-East Atlantic, as well as in other parts of the world. Although considerable advances have been made in wave measuring instruments over the last 30 years, the SBWR remains a uniquely reliable and cost-effective system in those areas where a suitable station keeping ship is available, and so information about its performance continues to be of interest. Because the SBWR in effect uses the ship upon which it is mounted as a wave sensor, not only does the response of the instrument to waves of different wavelengths differ, but the responses of instruments mounted on different ships differ one from another. Thus, uncertainties regarding the wavelength response, or equivalently, the frequency response of the SBWR have limited the accuracy of wave measurement.

Several measurements of the frequency response of the SBWR have been undertaken on different ships over the years, and in view of the continuing interest in the instrument another such experiment was conducted in 1980 aboard the Trinity House Lightvessel at the Channel Station. This work is described in a report (CRISP, 1987) which attempts, as far as possible, to be a definitive account of the performance of the SBWR as a wave measuring instrument. This will be referred to frequently as "Crisp".

The present report describes a method of applying measured frequency response information to SBWR spectra, which since 1982 have become available on a routine basis from a number of stations around the British Isles and the near Atlantic Ocean. The approach proposed in Crisp is followed, i.e. what is essentially a Froude number scaling is used in an attempt to reconcile the available measured frequency response data.

### 1.1 The Analysis of SBWR data

When the SBWR came into use pen and paper chart was the only practical method of recording bearing in mind that the instrument is used on ships of

opportunity and operated by non-specialist personnel. In fact, the method has many advantages, two of the most important being the simplicity and reliability of the equipment and the ease with which the record can be scanned to ensure correct operation of the instrument.

The records are analysed by the so-called Tucker-Draper (T-D) method, (TUCKER, 1963; DRAPER, 1967) which is based on work on the statistics of waves by CARTWRIGHT, 1958 and CARTWRIGHT & LONGUET-HIGGINS, 1956.

Essentially, the method allows estimates of the significant waveheight,  $H_s$  and the mean zero-crossing period  $T_z$  to be made from 5 basic measurements from the chart record. There are 4 height measurements and  $T_z$  is estimated from the number of zero crossings and the record length. The heights require a correction for the response of the instrument and this is calculated as the reciprocal of the instrument's response evaluated at the frequency  $1/T_z$ . Statistical aspects of this procedure are reviewed by TANN, 1976, and the correction method is discussed by Crisp.

The advantages of chart roll recording have persisted right up to the present as regards simplicity and reliability of operation, but the expense and slowness of the manual analysis method have increasingly been seen as unacceptable. Thus around 1980 it was decided to install microcomputers onboard the ships fitted with SBWRs and to process the data at source, the results being written to magnetic tape.

It was decided to use spectral analysis of the digital data and the reasons for this decision are discussed in the next section.

## 1.2 Choice of method of analysis of digital data

It was realised that the change from analogue to digital recording and from manual to machine analysis of the data would lead to some differences in the results since wave statistics are notoriously sensitive to such changes, particularly as regards the period parameters. In the case of the SBWR whose

response is such a strong function of frequency, differences in the determination of the period parameters produce changes in the height parameters as well.

While in principle it would be possible to implement the Tucker-Draper analysis as routine on the shipboard microcomputer the results would not be the same as a Tucker-Draper analysis of the corresponding pen chart record. The reasons for this include the following:

- (i) The human analyst consistently under-estimates the number of zero-crossings in the record, particularly at low sea states.
- (ii) The digital record consistently underestimates the heights of the crests and the depth of the troughs.
- (iii) Low frequency noise, which is occasionally present in SBWR records, is allowed for in a subjective way by the human analyst but would upset a simple machine analysis.

In principle, (iii) could be dealt with by high pass digital fitting of the record before analysis and an approximate correction for (ii) can be applied, PITT *et al.*, 1978. A carefully tuned algorithm for counting zero crossings which included hysteresis might emulate the combination of pen chart and human analyst.

However, the spectral method allows the response correction function to be properly applied, and the frequency band for the calculation of the wave statistics can be simply defined. If compatibility of the period statistic with the pen chart results is considered essential, then the spectral method allows a number of period parameters to be defined in a clear and consistent way. And of course the spectrum itself is available to users. In short, the spectral method offers advantages of consistency and flexibility which make its use hard to resist.

## 2. THE OPERATION OF THE SBWR AND ITS FREQUENCY RESPONSE

Crisp describes a simple model of the operation of the SBWR which leads to the result that, considering only the hydrodynamical aspects of the measuring

system (i.e. disregarding the response of the electronics etc.), the response is equivalent to the transfer function of the measured pressure fluctuations to the surface waves. Thus, the problem of defining the frequency response of the SBWR is equivalent to determining how the pressure at the measurement position on the ship's hull is related to the surface waves. The simplest assumption that can be made is that the pressure beneath the waves is the same as it would be in the absence of the ship. Then, according to the linearised theory of water waves and assuming that the ship is operating in deep water, the amplitude response,  $R$ , is given by:

$$R(k) = \exp(-kd) \quad (2.1)$$

i.e.  $R(f) = \exp\left(-\frac{(2\pi f)^2 d}{g}\right)$

where  $k$  is the wavenumber

$f$  is the frequency of the waves

$d$  is the mean depth of immersion of the pressure sensors

$g$  is the acceleration due to gravity

Some early measurements of the response suggested that it fell more quickly than indicated by (2.1) and so the depth was multiplied by a factor  $\alpha$  (usually called  $k$ ).  $\alpha$  is set to 2.5 in the Tucker-Draper analysis method. In spite of this modification the response is still negative exponential, and in Section 3 we investigate to what extent it agrees with the more recent measurements at our disposal. Crisp points out that a more realistic theory for the pressure should include the effect of the interaction of the ship with the waves, and develops an "interface theory" as a first step in this direction.

### 3. FREQUENCY SCALING OF MEASURED RESPONSE DATA

Five sets of data are used in this work, three of which have already been considered by Crisp. These are those made onboard Weather Reporter by CANHAM *et al.*, 1962, those made onboard Cumulus by VAN AKEN & BOUWS, 1974 and Crisp's own measurements on the Channel lightvessel. To these we add a set of measurements taken on the S.S. Cairndhu, 1965 and a set made on R.V. Ernest Holt, 1965. These latter results are based on comparatively little data, each set being the mean of

just three determinations of the response each of which was based on a single wave record.

Table 3.1 sets out the main dimensions of the 5 ships.

**TABLE 3.1 (all dimensions in metres)**

Ship	Pressure Sensor Depth	Length	Beam	Draught	Water Depth
Channel L.V.	2.0	35.0	8.7	3.5	60
O.W.S. Cumulus	1.5	62.0	12.6	4.5	$\approx 1500$
O.W.S. Weather Reporter	2.2	72.0	10.9	4.3	$\approx 1500$
R.V. Ernest Holt	1.95	53.3	9.1	4.4	$\approx 1000$
S.S. Cairndhu	3.7	128.0	18.3	5.8	$\approx 1000$

Figure 3.1 is a plot of the experimental estimates of  $|R|^2$  against frequency, and as can be seen there is a wide scatter in the results.

Now consider equation (2.1). If (like Crisp) we define a scaled frequency variable

$$\xi_2 = \sqrt{\frac{2\pi d}{g}} f \quad (3.1)$$

$$(2.1) \text{ gives } R^2(\xi_2) = \exp(-4\pi \xi_2^2) \quad (3.2)$$

for the "classical" formula

$$\text{and } R^2(\xi_2) = \exp(-10\pi \xi_2^2) \quad (3.3)$$

for the "modified" formula.

In Figure 3.2 are plotted the experimental estimates of  $|R|^2$  against  $\xi_2$  as well as (3.2) and (3.3) for comparison.

It will be seen from this plot that although in general the measured responses do not agree well with either of the exponential forms, the scaling has reduced the spread between the different ships, (although the measurements from Cumulus stand out somewhat in the middle of the frequency range).

Now, (3.1) is essentially a Froude number scaling with  $d$  as the length scale. In ship motion work it is more usual to use the ship's length  $L$ , to give a scaled frequency variable

$$\xi_1 = \sqrt{\frac{2\pi L}{g}} f \quad (3.4)$$

and Figure 3.3 shows the experimental estimates of  $|R|^2$  plotted against  $\xi_1$ . This scaling provides some reconciliation of the results from the several ships, however Crisp argued that a scaling based on the product of  $L$  and  $d$  did rather better for the observations at his disposal. He thus defined the frequency variable

$$\xi_3 = \sqrt{\frac{2\pi Ld}{g}} f \quad (3.5)$$

which has dimensions of  $(\text{length})^{\frac{1}{2}}$ .

Figure 3.4 shows the experimental estimates of  $|R|^2$  plotted against  $\xi_3$ . It will be seen that this does indeed bring the results from the several ships together, except that the results for Cairndhu (by far the biggest ship) stand well apart.

(3.5) can be made non-dimensional by using the harmonic mean of  $L$  and  $d$  rather than their product to give the frequency variable

$$\xi_4 = \sqrt{\frac{2\pi}{g}} (Ld)^{\frac{1}{4}} f \quad (3.6)$$

Figure 3.5 shows the experimental estimates of  $|R|^2$  plotted against  $\xi_4$ . It will be seen that it provides a reduction in scatter between the ships which is comparable to that obtained by the use of  $\xi_1$ . In fact  $\xi_4$  was selected as the best scaling, for reasons which are discussed later.

#### 4. FITTING FORMULAE TO THE MEASURED RESPONSE DATA

Since neither the "classical" nor "modified" formulations of the SBWR response fit the experimental data well, it was decided to use a completely empirical approach. To start with the measured data were fitted by non-linear least squares to a polynomial in the scaled frequency variable  $\xi_4$ . A standard NAG library computer program was used for this. 3rd, 4th and 5th order polynomials were tried, but since the 4th order was substantially better than the 3rd, while the 5th order did not result in a significant improvement over the 4th, the 4th order polynomial was selected as the most appropriate formulation. Thus,

$$R_H^2 = A_0 + A_1 \xi_4 + A_2 \xi_4^2 + A_3 \xi_4^3 + A_4 \xi_4^4 \quad (4.1)$$

A disadvantage of this formulation is that the values of  $R_H^2$  evaluated for a particular value of  $\xi_4$  can only be expected to be reliable estimates of  $|R|^2$  within the range of  $\xi_4$  for which the original data were measured. Moreover from physical considerations  $R_H^2$  is expected to approach unity for small values of  $\xi_4$ , and empirically we note that the response approximates a constant at high values of  $\xi_4$ . Accordingly we introduce two further parameters: the values of  $\xi_4$  below which  $R_H^2$  should be taken as unity, and above which it should stay constant. We thus arrive at a 7-parameter specification of the response.

In order to reduce the number of parameters a different formulation was sought which embodied more clearly the known characteristics of the response.

Eventually the following form was adopted:

$$R_H^2 = 1 - A_0 \{1 - \exp[-A_1 \xi_4 - A_2 \xi_4^2 - A_3 \xi_4^3]\} \quad (4.2)$$

This tends to unity at low frequencies and to a constant  $(1 - A_0)$  at high frequencies.

The experimental data can be expected to be progressively less reliable as the frequency decreases below 0.1 Hz, and so in order to force the fitted curve

to adopt a physically reasonable shape at the lower frequencies, a group of five points was added to the data for each ship. These were specified at frequencies 0.0, 0.005, 0.010, 0.015, 0.020 Hz, the response being set to unity. Using this technique, it was possible to use (4.2) throughout the required range of  $\xi_4$ .

In fact, the differences between the responses estimated from 4.1 and 4.2 are marginal, especially considering the scatter in the experimental data, but 4.2 is considered more convenient.

Figures 4.1 to 4.5 show the fits obtained using data from the 5 ships separately and Figure 4.6 shows the fit obtained for the whole data set.

Table 4.1 gives the corresponding values of the four constants and the rms error. N is the number of points, including the 5 manufactured ones.

TABLE 4.1

Ship	A <sub>0</sub>	A <sub>1</sub>	A <sub>2</sub>	A <sub>3</sub>	$\varepsilon$ rms	N
Channel L.V.	0.8468	0.4876	-6.4058	26.691	0.0443	30
O.W.S. Cumulus	0.7734	1.0832	-19.048	64.048	0.0260	28
O.W.S. Weather Reporter	0.8258	-1.0047	8.9790	3.7864	0.0440	22
Ernest Holt	0.83725	2.2130	-21.234	54.182	0.0877	23
Cairndhu	0.82108	0.27094	-7.4233	40.096	0.0531	24
All Ships	0.81027	0.50723	-8.1996	35.790	0.0690	127

## 5. APPLICATION OF THE RESPONSE CORRECTION

According to the simple model described in Crisp, the spectral data must be corrected as follows:-

$$S_{\text{corrected}} = S_{\text{measured}} \times \frac{1}{R_H^2} \times \frac{1}{R_E^2}$$

where  $R_E$  is the response function of the electronic double integrator. Before going on to describe the application of the correction method it will be useful to document the SBWR spectral data collection programme.

### **5.1 The SBWR microcomputer data collection programme**

The Hewlett-Packard H9915 microcomputer has been in use in the I.O.S. routine wave data collection programme since 1983 when one was installed at the shore station for the Isles of Scilly Waverider which was located at the Coastguard tower on St. Mary's. Since then they have been used successfully at a number of coastal sites.

In 1980, a microcomputer was installed on one of the ships attending Ocean Station Lima, MV Starella, on a trial basis. Subsequently, the second ship attending the site, OWS Cumulus, was also equipped with a microcomputer, and it is proposed to accept the spectral data as the main data source from 1984 onwards.

### **5.2 Operation of the onboard microcomputer**

The microcomputer is programmed to initiate a wave recording (hereafter called an "observation") at intervals of 3 hours at Ocean Station Lima and of 1.5 hours on the Lightvessels attending Seven Stones, Channel and Dowsing. The wave observation consists of 4096 measurements of the SBWR output separated by 0.5 seconds, giving a total length of 2048 seconds. In the subsequent processing, the observation is divided into two sections of 1024 seconds. Firstly, each section is subjected to a number of quality control checks, and depending on the outcome of these the section is either 'accepted' or 'rejected'. If a section is accepted its Digital Fourier Transform is calculated using an FFT method and the sample spectrum is estimated in the way outlined in PITT, 1981. The main parameters of this calculation are as follows: the section is cosine-tapered over  $1/8$  of its length at each end; each sample estimate consists of the mean of 7 adjacent elementary (periodogram) estimates giving a frequency resolution of 0.006836 Hz; and 14 degrees of freedom for each estimate. The

spectrum is then corrected for the response of the double integrator and also for the hydrodynamic response using the inverse of the classical formula (3.2). A number of integrated properties of the spectrum are derived including the spectral moments of integer order from -2 to +4,  $H_s$  and  $T_z$  and Goda's (1970)  $Q_p$ . These are then written to magnetic tape. If a section is rejected a single-record no-data observation is written. In the subsequent on-shore processing, where there are spectra for two valid sections, these are averaged to give a final spectrum with 28 degrees of freedom.

### 5.3 On-shore Processing

The microcomputer tapes were returned to the laboratory at regular intervals dictated by the changeover of ships attending O.S. Lima or by the relief of the Lightvessels. Here, they were transcribed onto computer compatible tape and subsequently written to disk. Further processing consisted of:

- (a) Assembling the data into monthly files with the correct representation of missing data.
- (b) Recorrecting the spectra by multiplying by the classical formula (3.2) and dividing by the empirical response (4.2). Both of these corrections are ship dependent, and (in the case of Lima) in any given month the site may have been attended by either or both ships.
- (c) Recalculating the integrated properties of the spectra i.e. the spectral moments,  $Q_p$ ,  $H_s$  and  $T_z$ .

The recorded data were then written to disk file in the standard I.O.S. spectral wave data format.

## 6. EVALUATION OF THE SPECTRA

The success of the correction method was judged rather subjectively by checking if the part of the measured spectra at frequencies above the spectral peak was fitted by an  $f^{-5}$  tail (under appropriate conditions).

Fig. 6.1 shows spectra from Ocean Station Lima measured during severe conditions which show satisfactory fits to an equilibrium tail defined by  $S(f) = \alpha'f$  with  $\alpha' = 0.00076 \text{ m}^2 \text{ sec}^2$ . The numbers above each graph are year, day number, time,  $H_s$  and  $T_z$ . The last figure is the quality flag - 0 for accepted, 1 for rejected, and is set during the on-shore processing of the data.

Fig. 6.2 shows some rather poorer fits, and in particular 3 spectra which were measured with the ship underway. These show a transfer of energy from higher to lower frequencies caused by Doppler shifting as the ship ran with the waves. Note that these observations were not noted as "steaming records" which would have resulted in the quality flag being set to 1.

Fig. 6.3 includes some spectra of 'steaming records' measured when the ship was steaming into the waves.

The lightvessels at the Dowsing and Seven Stones sites are of similar length, 35 m, but the pressure sensor depths were 0.8 m and 2.6 m respectively. In section 3 it was explained that scaling of the frequency by ship's length only (3.4) and by the harmonic mean of ship's length and pressure sensor depth (3.6) gave rather similar results in that they both gave a similar degree of reconciliation of the measured responses of the different ships.

However, we note that (3.4) predicts an identical response for the Dowsing and the Seven Stones Lightvessels (since they have the same length), while (3.6) will make some allowance for the substantially different pressure sensor depths.

Fig. 6.4 and Fig. 6.5 show spectra for the Seven Stones corrected using the two scaling options, and Fig. 6.6 and Fig. 6.7 show data from Dowsing.

The differences between the two scaling options are small, but with perhaps a slightly better fit for the Seven Stones data with Scale 4 (3.6). It was therefore decided to adopt (3.6) as the best frequency scaling option. It is recognised that this is a highly subjective assessment, made more difficult by the fact that these coastal sites are affected by tidal currents and their associated Doppler shifts.

Fig. 6.8 and Fig. 6.9 show spectra from Channel Lightvessel corrected using Crisp's results from Channel as fitted by the curve in Fig. 4.1.

Another aspect of the response curves should be considered: this is the tendency for the response to approach a constant value at a scaled frequency of about  $\frac{1}{2}$ . It is possible that this may be due to noise dominating the signal at the higher frequencies and Crisp investigated the effect of non-linear interaction due to the changing mean depth of the pressure sensor as the ship heaved. More extensive and detailed calculations were undertaken by the present writer, but did not satisfactorily explain the form of the response. In view of this uncertainty, the information from the instrument may be considered suspect above scaled frequency 0.5, and an equilibrium tail substituted for the measured spectrum. This method was tried, but the differences between  $H_s$  and  $T_z$  derived from the 'corrected' spectra and the 'substituted' spectra proved to be negligible. It was decided to use the empirical correction throughout the frequency range. At least this has the merit that the measured values of the spectrum are recoverable by reversing the correction.

## 7. COMPARISONS BETWEEN $H_s$ AND $T_z$ DERIVED FROM CHART RECORDS AND THE CORRESPONDING SPECTRAL MEASURES

Comparisons were made between the wave parameters estimated from the chart records using the Tucker-Draper method and those from the spectral technique. In each case linear regression was used with the line constrained to pass through the origin. Figures 7.1.1 to 7.1.3 show data from Lima measured during the early months of 1984. They respectively show comparisons of  $H_s$  derived from chart records i.e.  $H_s(T-D)$ , with  $H_s$  derived from the spectra, the same for  $T_z$ , and a comparison between  $T_z(T-D)$  and  $T_1$ , the first moment period from the spectrum.

Figures 7.2.1 to 7.2.3 show similar comparisons for the Seven Stones Lightvessel, 7.3.1 to 7.3.3 are for the Dowsing Lightvessel and 7.4.1 to 7.4.3 are for the Channel Lightvessel.

Table 7.1 gives a summary of the main results of these comparisons.

TABLE 7.1

Measurement site	Parameters		Number of Data Pairs	Correlation Coeff	Slope
	Ind	Dep			
Lima	$H_s(T-D)$	$H_s(\text{Spec})$	451	0.9646	0.8806
	$T_z(T-D)$	$T_z(\text{Spec})$	451	0.8370	0.8473
	$T_z(T-D)$	$T_1(\text{Spec})$	451	0.8550	0.9296
Seven Stones	$H_s(T-D)$	$H_s(\text{Spec})$	765	0.9287	0.7875
	$T_z(T-D)$	$T_z(\text{Spec})$	322	0.9387	0.9146
	$T_z(T-D)$	$T_1(\text{Spec})$	322	0.9405	0.9841
Dowsing	$H_s(T-D)$	$H_s(\text{Spec})$	656	0.9768	1.0317
	$T_z(T-D)$	$T_z(\text{Spec})$	656	0.9179	0.8116
	$T_z(T-D)$	$T_1(\text{Spec})$	656	0.9421	0.8624
Channel	$H_s(T-D)$	$H_s(\text{Spec})$	336	0.9547	0.8084
	$T_z(T-D)$	$T_z(\text{Spec})$	336	0.9372	0.8972
	$T_z(T-D)$	$T_1(\text{Spec})$	336	0.9370	0.9872

It is clear that major discrepancies exist in the estimates for both  $H_s$  and  $T_z$ . In all cases except Dowsing, the chart-roll estimates of  $H_s$  are higher (on average) than those for the spectra. In the case of Lima, however, it should be noted that for waveheights up to about 7 m the two measures are in reasonable agreement. The two very high chart values were the highest to be measured that winter and the highest was the world record. This discrepancy is clearly a

statistical effect rather than one associated with the correction procedure. For Lima,  $T_z$  from the chart rolls is on average 15% larger than from the spectra.

For Seven Stones,  $H_s$  from the charts is fully 21% higher on average than from the spectra. For the lower waveheights, the chart roll value often exceeds the spectral value by 50% or more. This is a matter of some concern, as it is the different analysis and correction methods which have caused the discrepancy. Seven Stones has the deepest pressure sensor of the vessels considered in this report, the depth being 2.6m, which results in large corrections being applied at the shorter periods in the chart roll method. The chart-roll  $T_z$ 's exceed the spectral  $T_z$ 's by 8½% on average.

During 1985 there was a period during which the Waverider (W/R) to the West of St Mary's, Isles of Scilly and the HP9915 on the Seven Stones Lightvessel were both operational. Now, while the two sites are some distance apart ( $\approx 22$ km) and the Scilly Isles Waverider is considered to be better exposed, nevertheless the comparison of simultaneous observations from the two systems is of interest. Figure 7.5 shows the comparison for  $H_s$ . The values from the two sources of spectral data over the range from 1 to 8 m differ by about 7½%, the W/R giving higher values. Remarkably, considering the geographical separation of the two sites, the measurements are well correlated with a correlation coefficient of 0.93. Fig. 7.6 shows the corresponding comparison for  $T_z$ . This shows that the Seven Stones (SBWR) values exceed the Scilly Isles (W/R) values by 4% on average, with a tendency for the values to approximate each other closely at the longer periods, and to diverge at the shorter periods. This is as one would expect given the higher frequency limit to which the moments are summed in the W/R analysis scheme (0.64 Hz) compared with 0.48 Hz for the SBWR system.

This is a useful indication that the SBWR correction scheme is yielding sensible results, and suggests that it is the chart-roll method which has produced waveheights which are too high. By contrast, the Dowsing results show that the chart-roll values of  $H_s$  are lower than the spectral results. The chart-roll values of  $T_z$  exceed those from the spectra by 19% on average. Note that the comparison is for a very restricted range of  $H_s$  and  $T_z$ . The measured  $H_s$  does not exceed 4m, and the great bulk of the values are less than 2m, while  $T_z$  is between 3 and 8 seconds.

For the Channel Lightvessel, the value of  $H_s(T-D)$  exceed the spectral values by 19% while the chart-roll  $T_z$ 's exceed the spectral values by 10% on average.

Since the chart-roll method is expected to overestimate  $T_z$ , and the comparisons confirm this expectation, it is of interest to investigate other period parameters of the spectrum to see if they better approximate the chart-roll  $T_z$ 's. The comparison with  $T_1$  (the first moment period) is good for Seven Stones and Channel, rather less good for Lima (chart-roll 7% longer than  $T_1$ ) and poor for Dowsing with the chart-roll results about 14% in excess of the spectral  $T_1$ .

## 8. RECORRECTING HISTORICAL WAVEHEIGHT DATA

Because there are considerable differences between the T-D and the spectral data there is some interest in developing a method of reconciling the results from the two methods so that the currently accumulating spectral data can be combined with the historical T-D data.

### 8.1 Differences between the T-D and the spectral estimates of $H_s$

There are essentially three important differences between the T-D and spectral estimates of  $H_s$ :-

- (1) There are differences in the statistics of the estimates derived by each method. Assuming the ideal Gaussian narrow-band sea surface (and perfect measurements) the r.m.s. error in the estimation of  $H_s$  is about 6% in the case of the T-D method and perhaps 3-4% in the spectral method, and they are both unbiased estimates of the true  $H_s$ . The latter point in particular is illustrated in Fig.8.1.1-8.1.4 which show  $H_s$  calculated from the uncorrected spectra plotted against the uncorrected values of  $H_s(T-D)$ .

(2) The correction method is fundamentally different. In the spectral method the response correction function is applied to each spectral estimate and then the corrected spectrum is summed to estimate  $m_0$ , and then  $H_s$  is calculated as  $4\sqrt{m_0}$ . In the T-D method, the uncorrected  $H_s$  is estimated and then a scalar correction is derived as the correction function evaluated at a (single) characteristic frequency, which is the reciprocal of the mean zero crossing period of the record.

(3) And, of course, the correction functions used are different.

## 8.2 The Characteristic Period

Clearly, there is little we can do about the statistical differences and except for the few highest values these are not expected to be significant. By and large it appears to be the correction process (2 and 3) which is responsible for the differences. In pursuing this, we first wished to find out what inaccuracy was introduced by the use of a scalar correction evaluated at a characteristic frequency, rather than by using the full procedure of correcting the spectrum frequency by frequency.

To do this we used the spectral data and plotted

$$m'_0 Q(1/T_c) \text{ against } \Delta f \sum_i' S_i' Q(f_i) \quad (\text{Primes indicate uncorrected values throughout this section})$$

where  $S_i'$  is the uncorrected spectral density at frequency  $f_i$ .  $m'_0$  is the zeroth moment of the uncorrected spectrum, i.e.

$$m'_0 = \Delta f \sum_i' S_i'$$

(in general the  $n$ th moment of the spectrum will be defined by  $m_n = \Delta f \sum_i S_i f_i^n$ )

$Q$  is the correction function to be applied and is given by

$$Q = \frac{1}{R_H^2} \times \frac{1}{R_E^2} ,$$

as previously defined.  $T_C$  is the characteristic period and was taken as  $T'_{11}$  ( $= m'_{10}/m'_{11}$ ).

The results for Lima, Seven Stones, Dowsing and Channel are shown in Figures 8.2.1-8.2.4 and summarised in Table 8.2.1. We first note the remarkably high correlation - clearly the scalar correction method can be used with very high statistical confidence. Next we see that the scalar corrected values are biased below the fully corrected values by about 11%.

Some further comparisons were made using  $T_C = \beta T'_{11}$  where  $\beta$  could be varied. It was found that at a certain value of  $\beta (< 1)$ , the bias in the results could be made to disappear, but at the expense of poorer correlation.

At first sight these results may be surprising, but consider the following.

#### 8.2.1 Why does the scalar correction work so well?

Suppose the correction function is linear in frequency:

$$C = a_0 + a_1 f, \text{ say.}$$

Then we can show very easily that  $T'_{11}$  is the appropriate characteristic period and leads to an exact correction:

$$m_0 = \Delta f \sum_i S'_{1i} (a_0 + a_1 f_i)$$

$$= a_0 m'_{10} + a_1 m'_{11}$$

$$= m'_{10} (a_0 + a_1 \frac{m'_{11}}{m'_{10}})$$

where we note that the bracketed quantity is just the correction function evaluated at frequency  $1/T'_1$ .

However,  $Q$  is not linear and we may ask if the above ideas can be extended to a more general correction function.

Suppose we fit a straight line  $C$  to  $Q$  so that the sum of the squares of the residuals (weighted by the measured spectrum) is minimized,

i.e.  $D = \sum_i (C_i - Q_i)^2 S'_i$  where  $C_i = C(f_i)$  etc.

$$\text{so that } \frac{\partial D}{\partial a_0} = 2 \sum_i (C_i - Q_i) S'_i = 0 \quad (8.2.1a)$$

$$\text{i.e. } a_0 m'_0 + a_1 m'_1 - m_0 = 0 \quad (8.2.1b)$$

$$\text{and } \frac{\partial D}{\partial a_1} = 2 \sum_i f_i (C_i - Q_i) S'_i = 0$$

$$\text{i.e. } a_0 m'_1 + a_1 m'_2 - m_1 = 0 \quad (8.2.2)$$

Equations 8.2.1 and 8.2.2 allow  $a_0$  and  $a_1$  to be estimated from the moments of the corrected and uncorrected spectra; however, for our purposes only 8.2.1 is of interest. 8.2.1a says that  $m_0$  calculated using the actual correction function  $Q$  is the same as  $m_0$  calculated using the fitted straight line correction function  $C$ . 8.2.1b shows that we may apply an exact correction by using  $C$  evaluated at  $1/T'_1$ . However, in the comparisons described above we used  $Q(1/T'_1)$  not  $C(1/T'_1)$ , so that the ordinate of each point differs from unity by a factor  $Q(1/T'_1)/C(1/T'_1)$ .

$$\text{Moreover, } C(1/T'_1) = \frac{m_0}{m'_0} = \frac{\Delta f \sum S'_i Q_i}{\Delta f \sum S'_i}$$

which is the average of  $Q$  weighted by the spectrum, call it  $\bar{Q}$ .

Evidently, for a wide class of spectra  $Q(1/T'_1)/\bar{Q}$  remains close to 0.89.

### 8.2.2 Estimating $T_1'$

When recorrecting the T-D values of  $H_S$ , the period parameter available is  $T_z(T-D)$  not  $T_1'$ . We could attempt to calculate the relationship between  $T_z(T-D)$  and  $T_1'$  for a given analytical spectrum using a given instrument response function. However, the variety of spectral forms found in nature is so wide, and the counting process used in the estimation of  $T_z(T-D)$  so difficult to model that once again we must use empirical correlations.

$T_1$  from the uncorrected spectra (i.e.  $T_1'$ ) was plotted against  $T_z$  from the T-D analysis for Lima, Seven Stones, Dowsing and Channel. The results are shown in Figures 8.2.5-8.2.8 and summarised in Table 8.2.2.

TABLE 8.2.1

**Comparison between  $m_0$  fully corrected and  $m_0$  using a scalar correction**

Station and period	Slope (Scalar: Full)	Correlation Coefficient
Lima (Jan-Mar 84)	0.8948	0.9987
Seven Stones (Apr-May 85)	0.8929	0.9997
Dowsing (Jul-Sep 85)	0.9082	0.9967
Channel (Mar-Apr 86)	0.8741	0.9988

TABLE 8.2.2

**Comparison between  $T_1$  from the uncorrected spectra and  $T_z(T-D)$**

Station and period	Slope ( $T_1':T_z$ )	Correlation Coefficient
Lima (Jan-Mar 84)	1.0724	0.8951
Seven Stones (Apr-May 85)	1.0518	0.9183
Dowsing (Jul-Sep 85)	1.0076	0.9557
Channel (Mar-May 86)	1.1262	0.8615

### 8.3 Recorrection of $H_s(T-D)$

On the basis of the previous section, we may correct  $H_s(T-D)$  as follows:

$$H_{SR} = H_s'(T-D) \times \frac{1}{\sqrt{S_{SF}}} \sqrt{Q(f_c)}$$

where  $H_{SR}$  is the corrected value of  $H_s$

$H_s'(T-D)$  is the uncorrected estimate of  $H_s$

$S_{SF}$  is the empirical coefficient relating the scalar corrected  $m_0'$  to the fully corrected  $m_0$  (as discussed in section 8.2)

$$f_c = 1/\{T_z(T-D) \times S_{T'T_z}\}$$

where  $S_{T'T_z}$  is the empirical coefficient relating  $T_1$  from the uncorrected spectrum to  $T_z(T-D)$ .

This was tried on data from Lima, Seven Stones, Dowsing and Channel. Since  $S_{SF}$  varies only slightly from ship to ship (Table 8.2.1), the mean of the four was used, i.e.  $S_{SF} = 0.8925$  with standard deviation 0.014.

$S_{T'T_z}$  differed substantially from ship to ship so the individual values were used.

$H_{SR}$  is plotted against  $H_s$  (spectral) in Figs. 8.3.1, 8.3.2, 8.3.3 and 8.3.4. The correlation and regression coefficients are shown in Table 8.3.1.

Lima, Seven Stones and Dowsing show satisfactory agreement. For Channel the recorrected heights are about 5% less than the spectral values on average. Careful investigation failed to reveal the cause of this, although it was noted that the  $T_1':T_z$  relationship was very variable.

TABLE 8.3.1

Comparison between recorrected  $H_s(T-D)$  and spectral  $H_s$ 

Station and period	Slope ( $H_{SR}:H_s(\text{spectral})$ )	Correlation Coefficient
Lima (Jan-Mar 84)	1.0482	0.9611
Seven Stones (Feb-Apr 85)	1.0026	0.9347
Dowsing (Jul-Sep 85)	0.9903	0.9751
Channel (Mar-May 86)	0.9505	0.9690

## 9. CONCLUSIONS

An empirical response function for the SBWR has been developed, based on a Froude number scaling of the frequency as proposed by Crisp.

The inverse of this function has been used to correct spectral data measured at four IOSDL SBWR wave measurement sites, and the corrected spectra have been used to estimate  $H_s$ ,  $T_z$  and  $T_1$ .

When these were compared with  $H_s$  and  $T_z$  estimated from the simultaneous chart recordings (the so-called Tucker-Draper estimates of  $H_s$  and  $T_z$ ,  $H_s(T-D)$  and  $T_z(T-D)$ ), considerable differences were noted. As far as  $T_z(T-D)$  is concerned, this agrees better with the first moment period of the spectrum,  $T_1$  than with the spectral  $T_z$ . More importantly, serious discrepancies exist between the  $H_s$  estimates for those vessels with rather deep pressure sensors. Both Seven Stones L.V. and Channel L.V. show differences of about 20%, with  $H_s(T-D)$  higher.

Some W/R measurements are presented which suggest that the new correction method is giving sensible results.

In view of the discrepancies noted in  $H_s$ , a method is proposed for recorrecting historical  $H_s(T-D)$  data and this was tried out on the four installations. For three of these, the recorrected values of  $H_s$  agreed well with

the spectral values, while for the fourth, Channel L.V., some unexplained residual error remained.

#### **10. ACKNOWLEDGEMENT**

This work was carried out as part of the IOSDL wave climate study and was supported financially by the Department of Energy.

## REFERENCES

AKEN, H.M. van & BOUWS, E. 1974 Frequency response of a shipborne wave recorder.  
pp.281-300 in, Proceedings of the International Symposium on Wave Measurement and Analysis, New Orleans, Sept. 1974, Vol.1.  
New York: American Society of Civil Engineers, 913pp.

CANHAM, H.J.S., CARTWRIGHT, D.E., GOODRICH, G.J. & HOBGEN, N. 1962 Seakeeping trials on ocean weather ship Weather Reporter.  
Transactions of the Royal Institution of Naval Architects, 104, 447-492.

CARTWRIGHT, D.E. 1958 On estimating the mean energy of sea waves from the highest waves in a record.  
Proceedings of the Royal Society of London, A247, 22-48.

CARTWRIGHT, D.E. & LONGUET-HIGGINS, M.S. 1956 The statistical distribution of the maxima of a random function.  
Proceedings of the Royal Society of London, A237, 212-232.

CRISP, G.N. 1987 An experimental comparison of a Shipborne Wave Recorder and a Waverider buoy conducted at the Channel Lightvessel.  
Institute of Oceanographic Sciences, Report, No.235, 181pp.

DRAPER, L. 1967 The analysis and presentation of wave data - a plea for uniformity.  
pp.1-11 in, Proceedings of 10th Coastal Engineering Conference, Tokyo, Sept. 1966, Vol.1.  
New York: American Society of Civil Engineers. (2 vols.)

GODA, Y. 1970 Numerical experiments on waves with spectral simulation.  
Report of the Port and Harbour Research Institute, 9(3), 57pp.

NPL 1965 Report on analysis of ship motion trials data for "Cairndhu".  
National Physical Laboratory Coordinating Committee for Research into the Seagoing Qualities of Ships, Report, No.6, 21pp.  
(Unpublished manuscript)

NPL 1965 Report on analysis of ship motion trials data for "Ernest Holt".  
National Physical Laboratory Coordinating Committee for Research into the Seagoing Qualities of Ships, Report No.7, 25pp.  
(Unpublished manuscript)

PITT, E.G., DRIVER, J.S. & EWING, J.A. 1978 Some intercomparisons between wave recorders.  
Institute of Oceanographic Sciences, Report, No.43, 63pp.

PITT, E.G. 1981 The spectral analysis of wave data.  
Institute of Oceanographic Sciences, Internal Document, No.120, 5pp. + appendices.  
(Unpublished manuscript)

TANN, H.M. 1976 The estimation of wave parameters for the design of offshore structures.  
Institute of Oceanographic Sciences, Report, No.23, 29pp.

TUCKER, M.J. 1956 A shipborne wave recorder.  
Transactions of the Royal Institution of Naval Architects, 98, 236-250.

TUCKER, M.J. 1963 Analysis of records of sea waves.  
Proceedings of the Institution of Civil Engineers, 26, 305-316.

**FIGURES**

Fig. 3.1	Measured values of response against frequency	33
Fig. 3.2	Measured values of response against $\xi_2$ with graphs of "classical" and "modified" responses for comparison	34
Fig. 3.3	Measured values of response against $\xi_1$	35
Fig. 3.4	Measured values of response against $\xi_3$	36
Fig. 3.5	Measured values of response against $\xi_4$	37
Fig. 4.1	Least squares fit to data from Channel LV	38
Fig. 4.2	Least squares fit to data from Cumulus	39
Fig. 4.3	Least squares fit to data from Weather Reporter	40
Fig. 4.4	Least squares fit to data from Ernest Holt	41
Fig. 4.5	Least squares fit to data from Cairndhu	42
Fig. 4.6	Least squares fit to complete experimental data set	43
Fig. 6.1	Spectra from O.S. Lima	44
Fig. 6.2	Spectra from O.S. Lima	45
Fig. 6.3	Spectra from O.S. Lima	46
Fig. 6.4	Spectra from Seven Stones	47
Fig. 6.5	Spectra from Seven Stones	48
Fig. 6.6	Spectra from Dowsing	49
Fig. 6.7	Spectra from Dowsing	50
Fig. 6.8	Spectra from Channel	51
Fig. 6.9	Spectra from Channel	52
Fig. 7.1.1	O.S. Lima: $H_S(T-D)$ compared with $H_S(\text{Spectral})$	53
Fig. 7.1.2	$T_Z(T-D)$ compared with $T_Z(\text{Spectral})$	54
Fig. 7.1.3	$T_Z(T-D)$ compared with $T_1(\text{Spectral})$	55
Fig. 7.2.1	Seven Stones LV: $H_S(T-D)$ compared with $H_S(\text{Spectral})$	56
Fig. 7.2.2	$T_Z(T-D)$ compared with $T_Z(\text{Spectral})$	57
Fig. 7.2.3	$T_Z(T-D)$ compared with $T_1(\text{Spectral})$	58

Fig.7.3.1	Dowsing LV:	$H_s(T-D)$ compared with $H_s(\text{Spectral})$	59
Fig.7.3.2		$T_z(T-D)$ compared with $T_z(\text{Spectral})$	60
Fig.7.3.3		$T_z(T-D)$ compared with $T_1(\text{Spectral})$	61
Fig.7.4.1	Channel LV:	$H_s(T-D)$ compared with $H_s(\text{Spectral})$	62
Fig.7.4.2		$T_z(T-D)$ compared with $T_z(\text{Spectral})$	63
Fig.7.4.3		$T_z(T-D)$ compared with $T_1(\text{Spectral})$	64
Fig. 7.5	Seven Stones LV $H_s(\text{Spectral})$ compared with Scilly Isles W/R $H_s(\text{Spectral})$		65
Fig. 7.6	Seven Stones LV $T_z(\text{Spectral})$ compared with Scilly Isles W/R $T_z(\text{Spectral})$		66
Fig.8.1.1	$H_s(\text{Spectral})$ uncorrected plotted against $H_s(T-D)$ Uncorrected: Lima		67
Fig.8.1.2	$H_s(\text{Spectral})$ uncorrected plotted against $H_s(T-D)$ Uncorrected: Seven Stones		68
Fig.8.1.3	$H_s(\text{Spectral})$ uncorrected plotted against $H_s(T-D)$ Uncorrected: Dowsing		69
Fig.8.1.4	$H_s(\text{Spectral})$ uncorrected plotted against $H_s(T-D)$ Uncorrected: Channel		70
Fig.8.2.1	$m'_0$ plotted against $m_0$ (see text): Lima		71
Fig.8.2.2	$m'_0$ plotted against $m_0$ (see text): Seven Stones		72
Fig.8.2.3	$m'_0$ plotted against $m_0$ (see text): Dowsing		73
Fig.8.2.4	$m'_0$ plotted against $m_0$ (see text): Channel		74
Fig.8.2.5	$T_1$ (Uncorrected spectrum) plotted against $T_z(T-D)$ : Lima		75
Fig.8.2.6	$T_1$ (Uncorrected spectrum) plotted against $T_z(T-D)$ : Seven Stones		76
Fig.8.2.7	$T_1$ (Uncorrected spectrum) plotted against $T_z(T-D)$ : Dowsing		77
Fig.8.2.8	$T_1$ (Uncorrected spectrum) plotted against $T_z(T-D)$ : Channel		78
Fig.8.3.1	$H_s(T-D)$ recorrected plotted against $H_s(\text{spectral})$ : Lima		79
Fig.8.3.2	$H_s(T-D)$ recorrected plotted against $H_s(\text{spectral})$ : Seven Stones		80
Fig.8.3.3	$H_s(T-D)$ recorrected plotted against $H_s(\text{spectral})$ : Dowsing		81
Fig.8.3.4	$H_s(T-D)$ recorrected plotted against $H_s(\text{spectral})$ : Channel		82

Fig. 3.1  
MEASURED VALUES OF RESPONSE PLOTTED AGAINST FREQUENCY

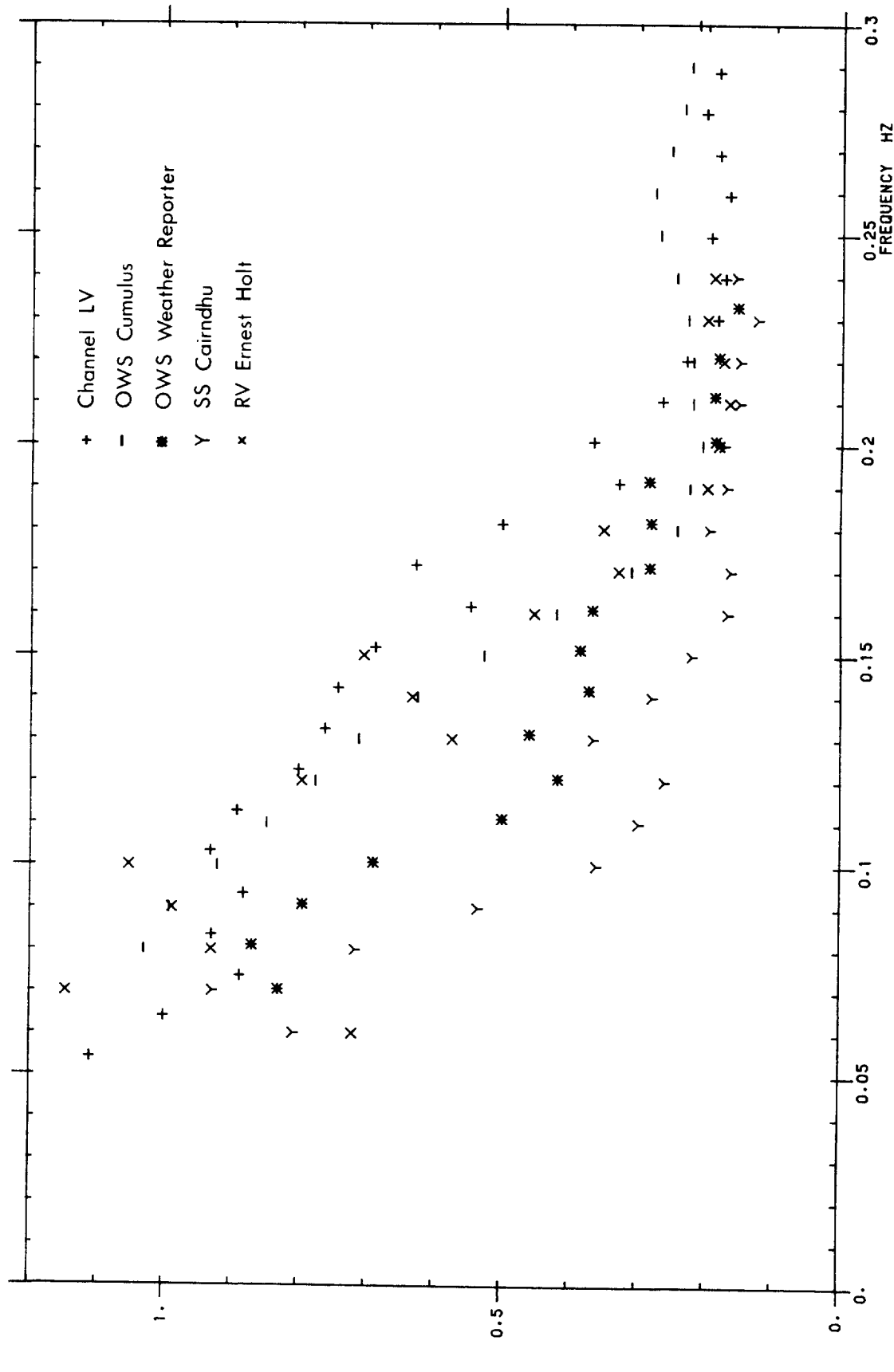


Fig. 3.2  
MEASURED VALUES OF RESPONSE PLOTTED AGAINST  $\xi_2$

Key as in Fig. 3.1

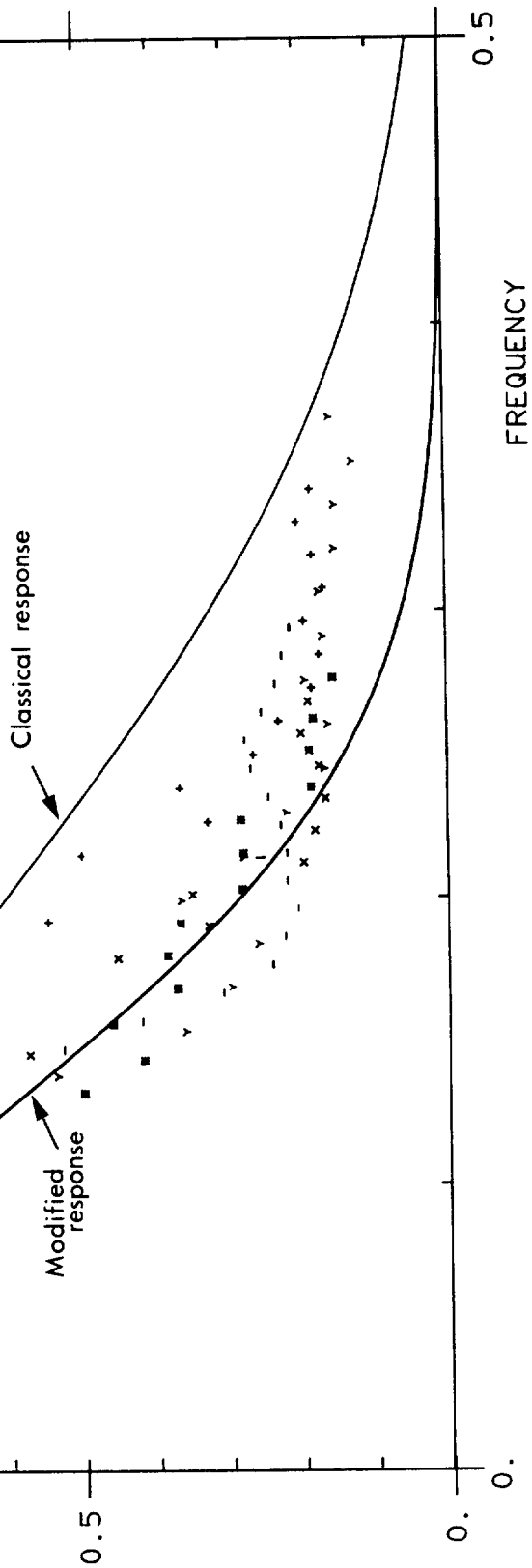
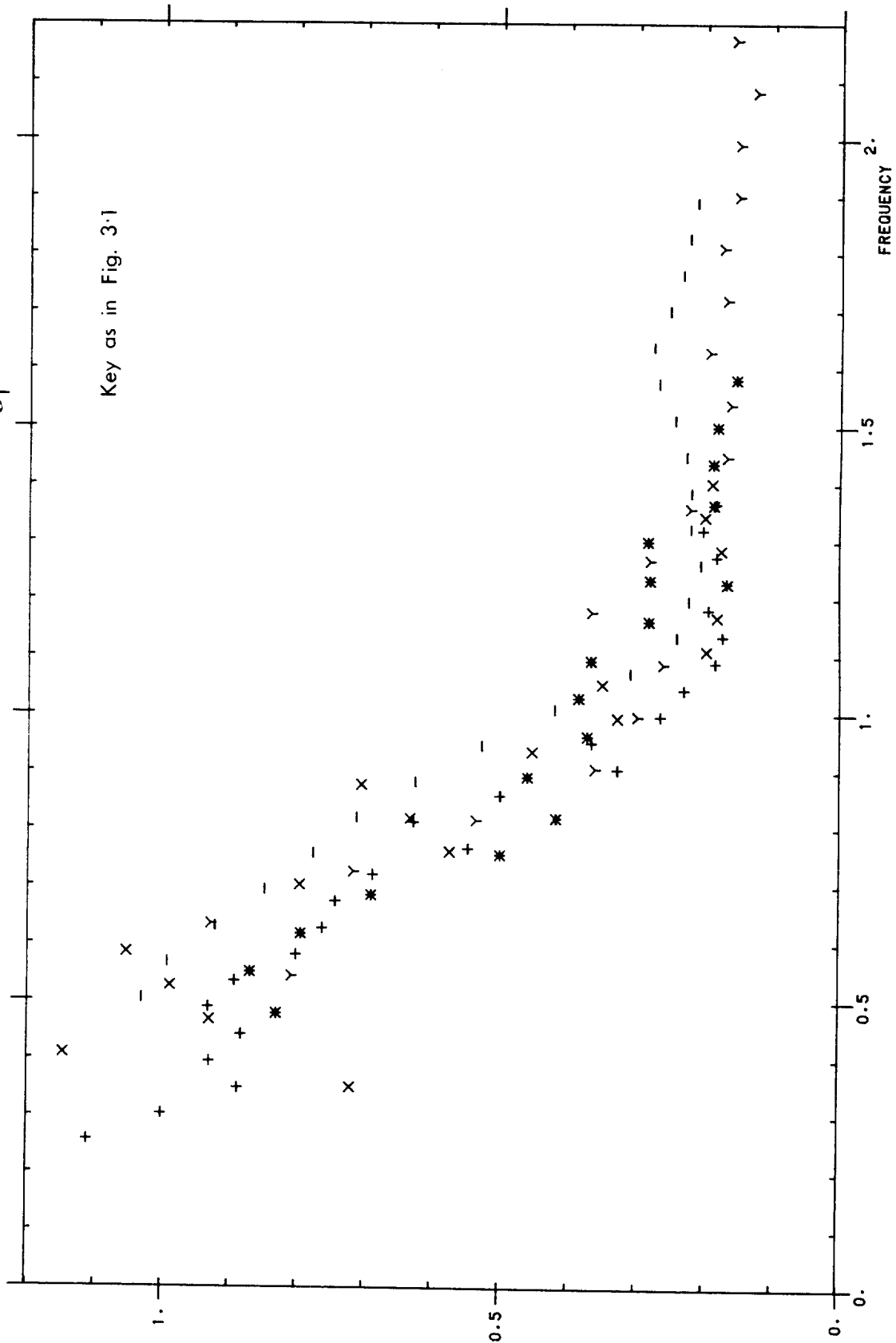
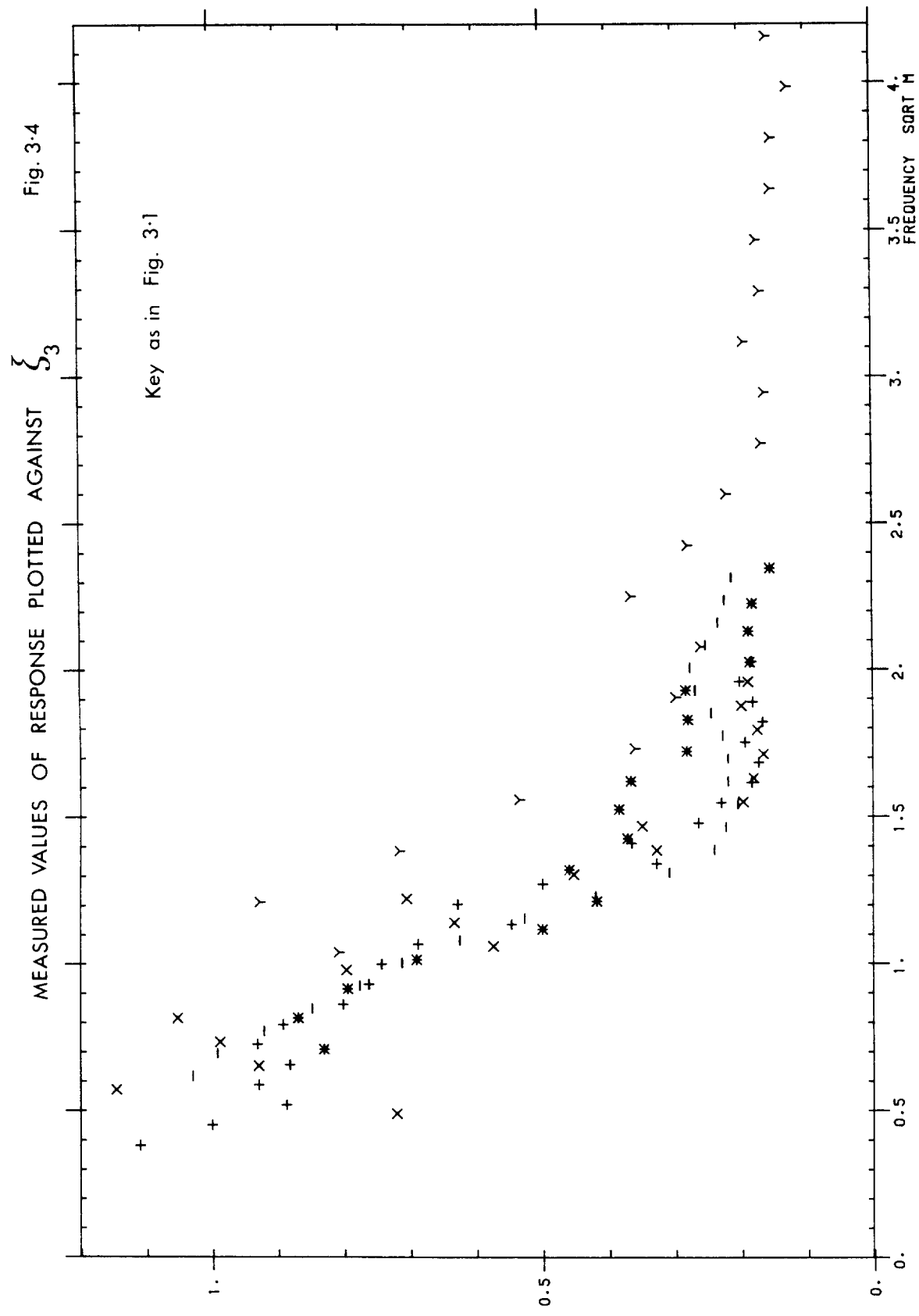


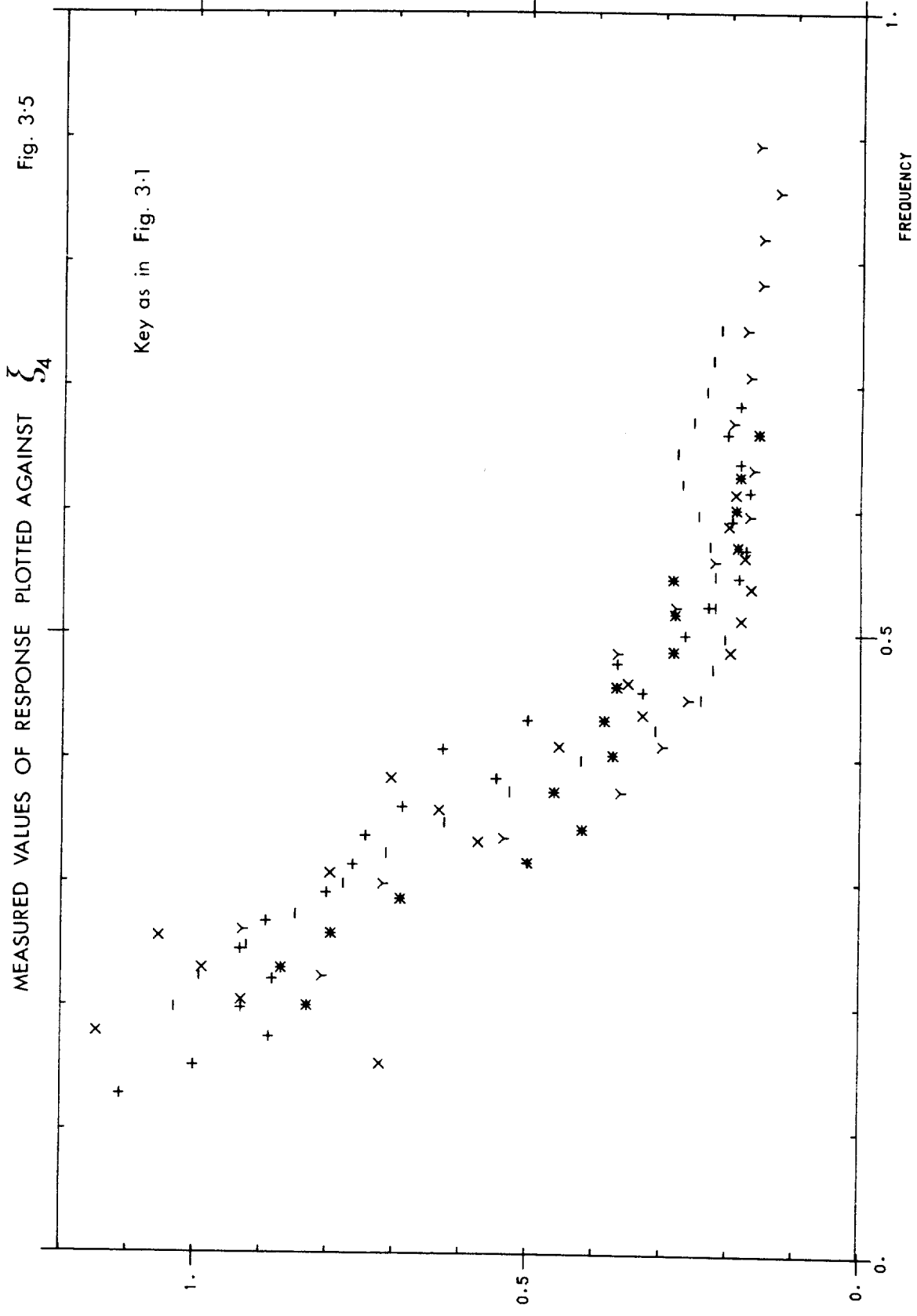
Fig. 3.3  
MEASURED VALUES OF RESPONSE PLOTED AGAINST  $\zeta_1$

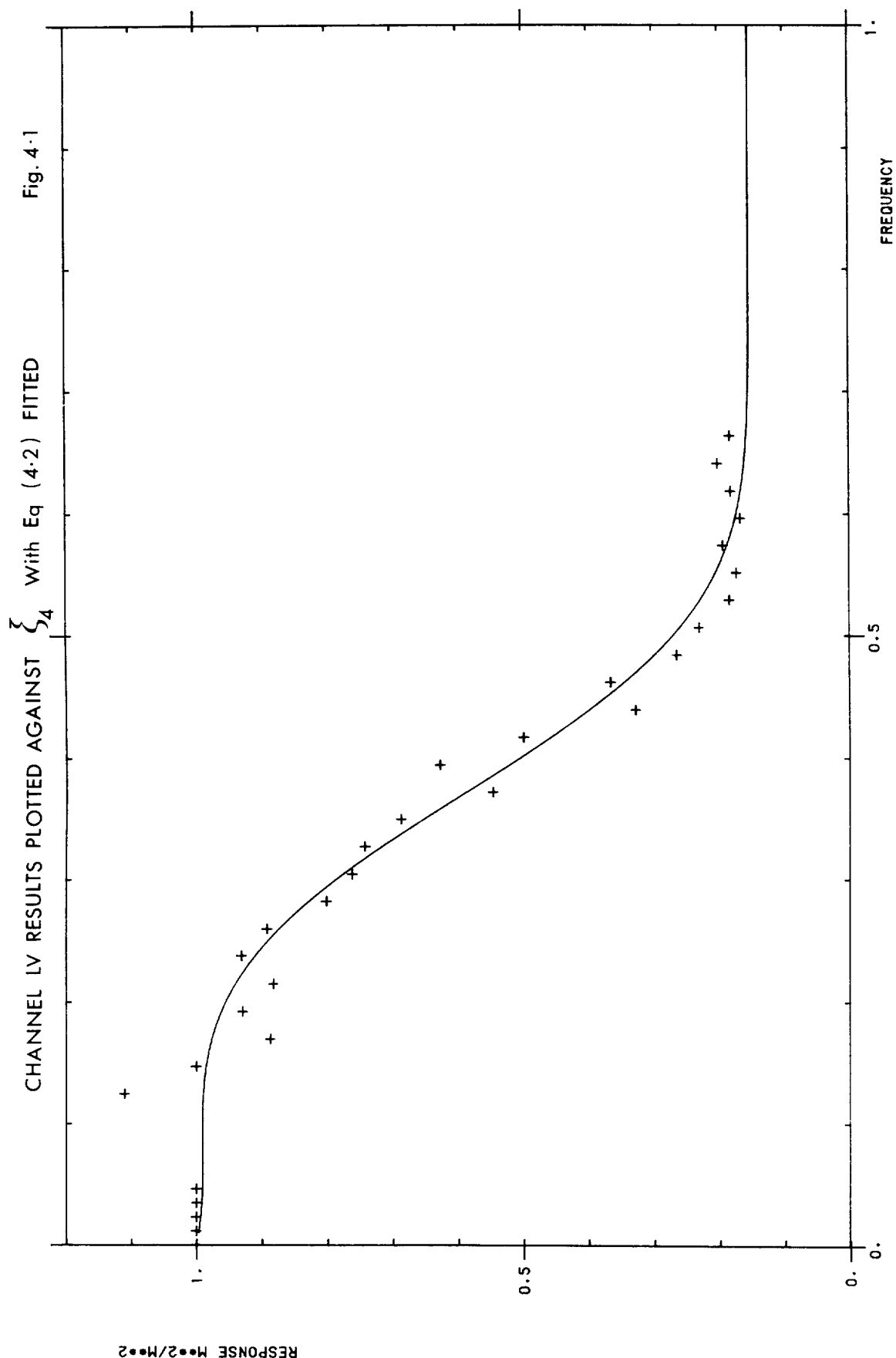
Key as in Fig. 3.1

RESPONSE  $M_{002}/M_{002}$









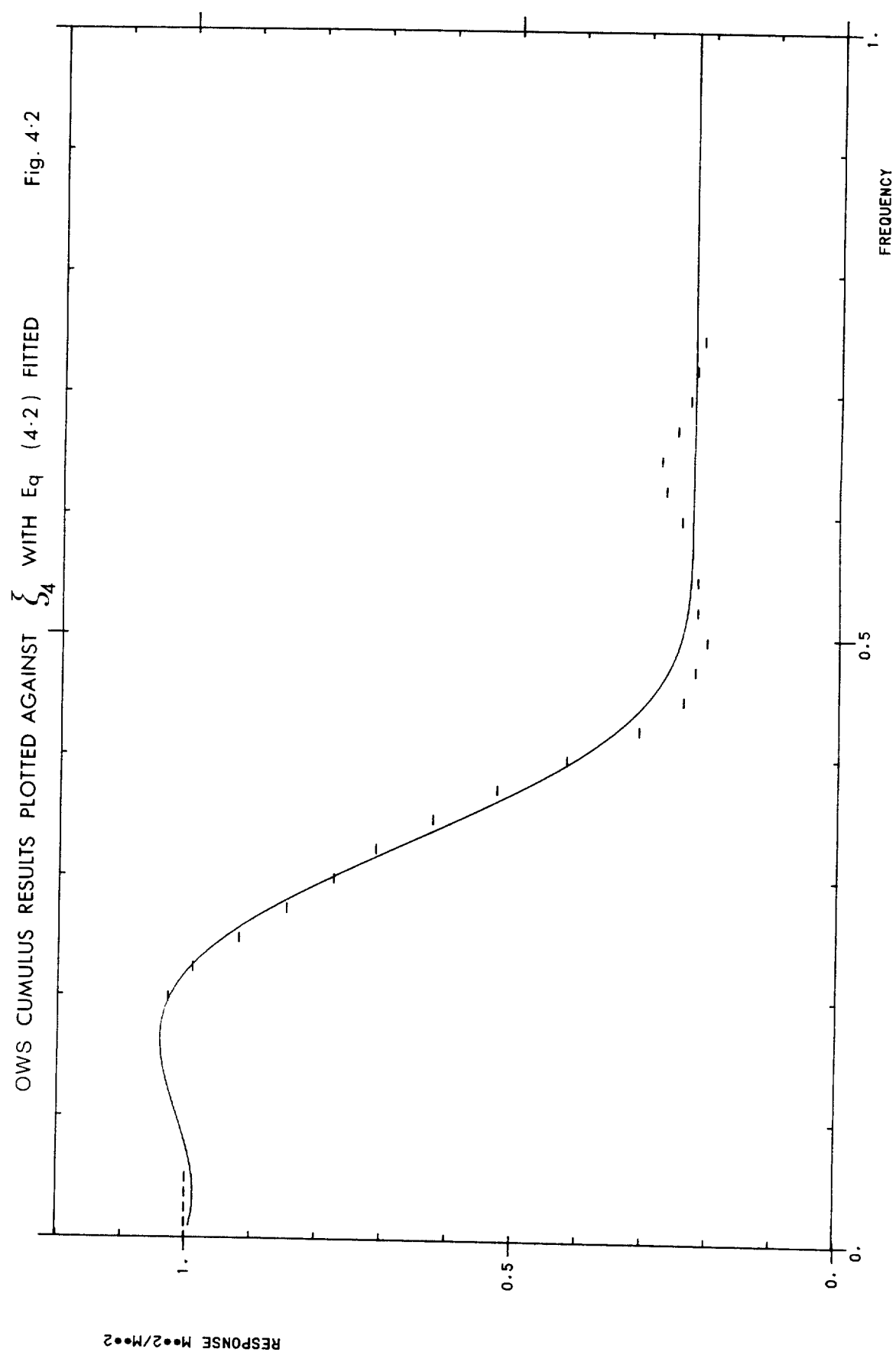
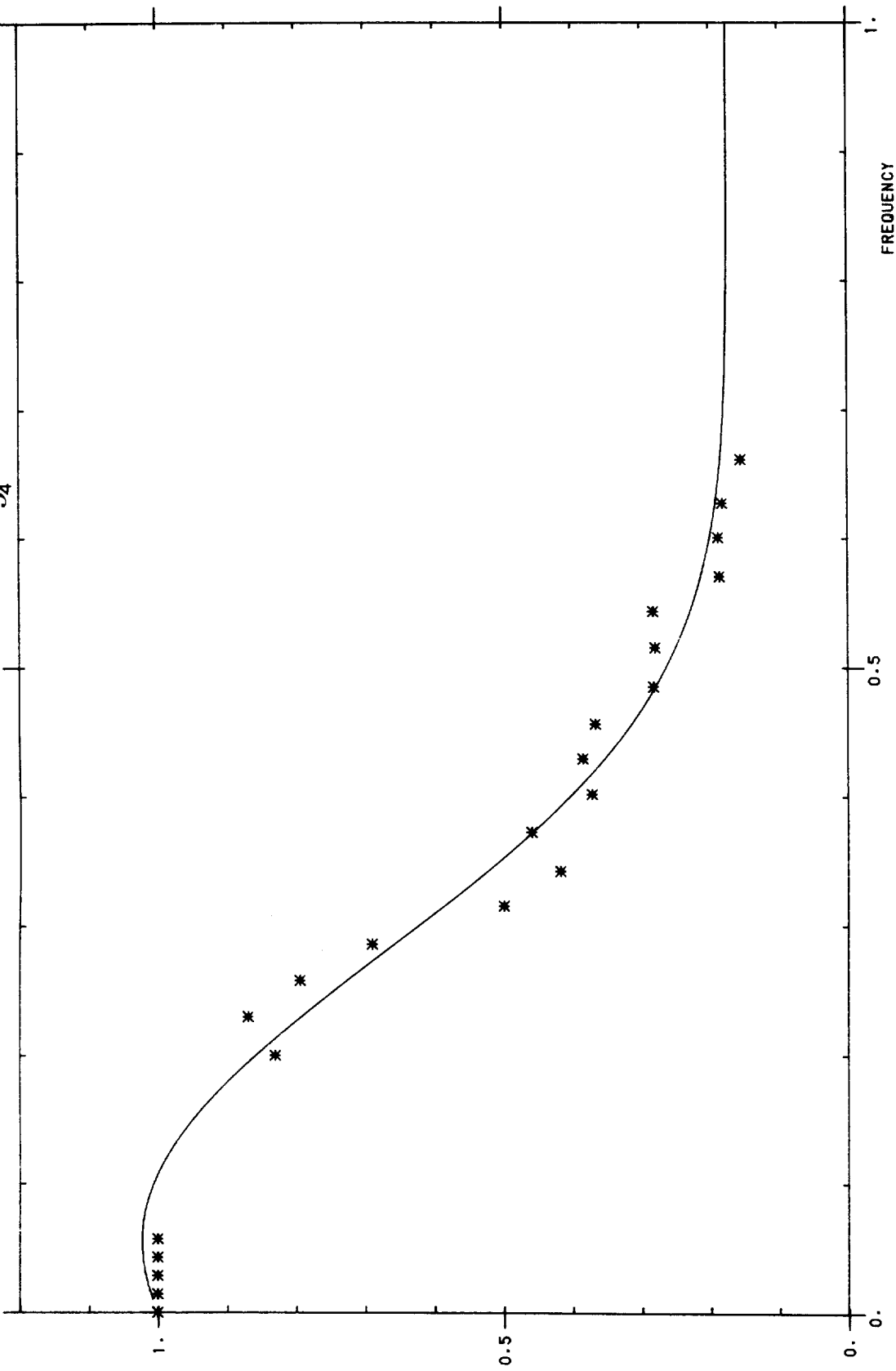
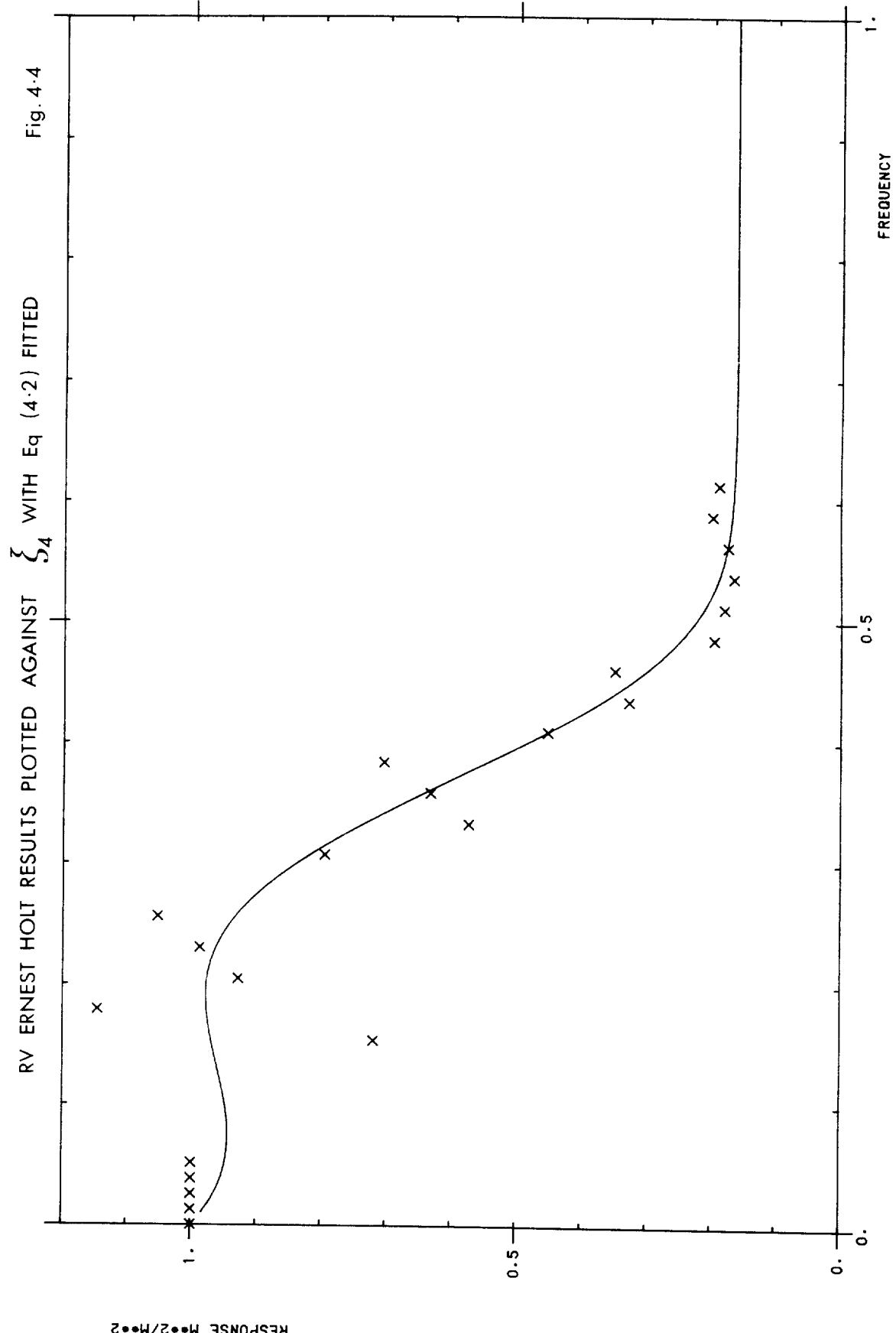
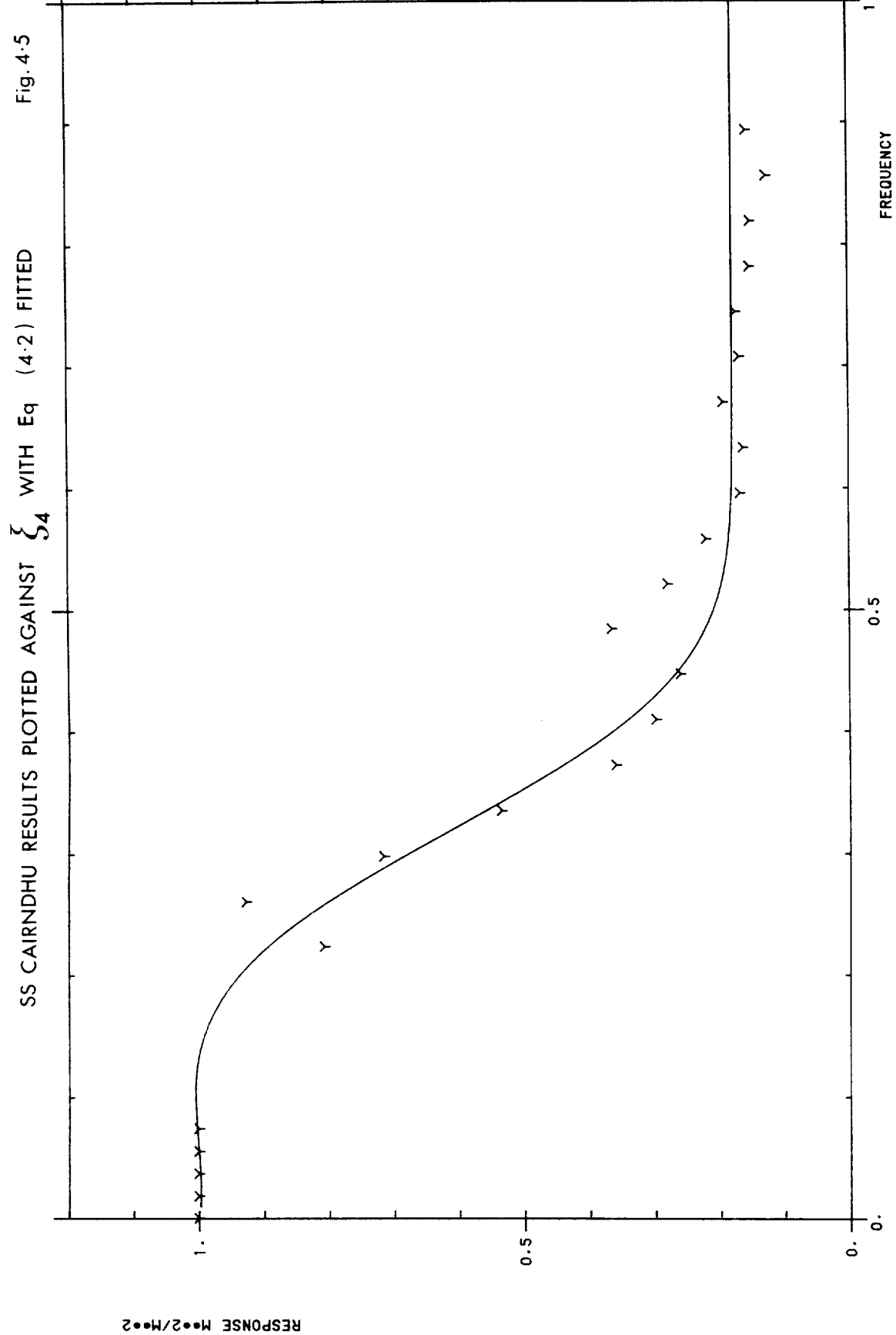
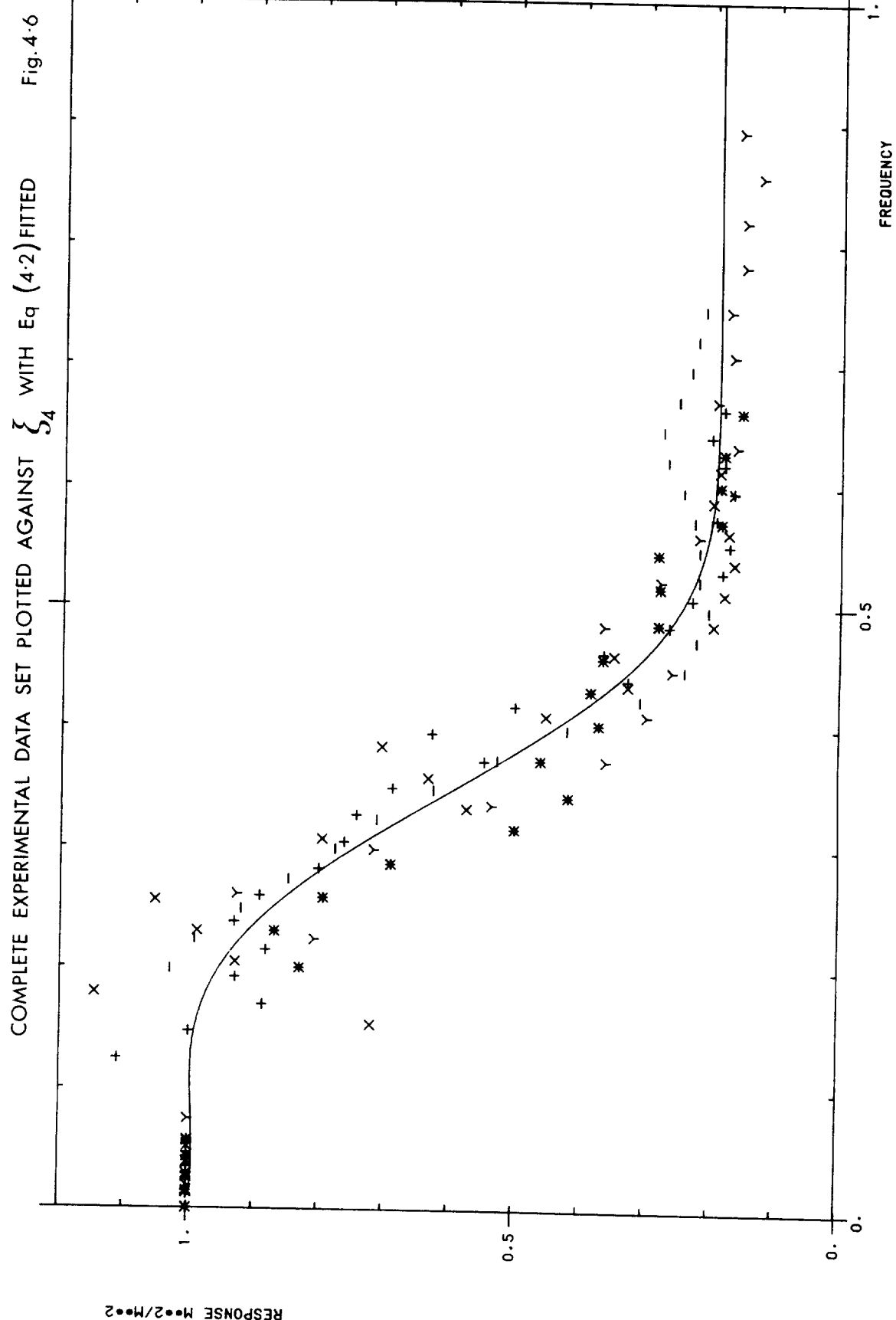


Fig. 4.3  
OWS WEATHER REPORTER RESULTS PLOTTED AGAINST  $\xi_{24}$  with Eq(4.2) FITTED





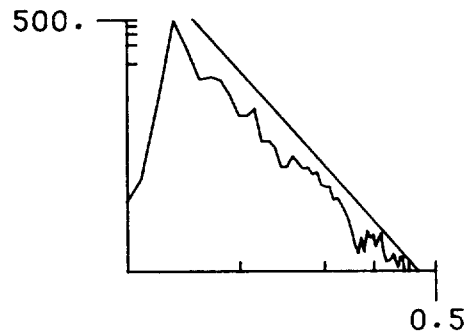
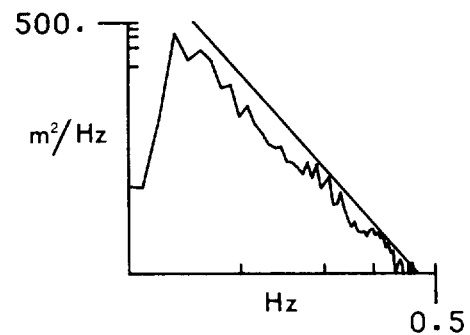




SPECTRA FROM OCEAN WEATHER STATION LIMA  
 CORRECTED USING FREQUENCY VARIABLE  $\zeta$   
 $\zeta_4$

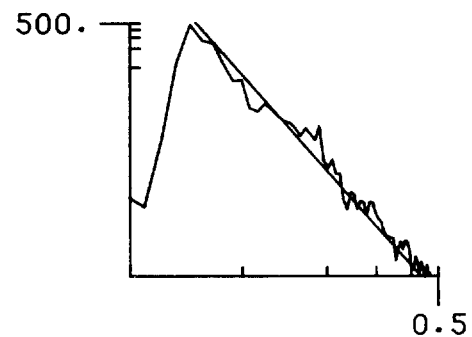
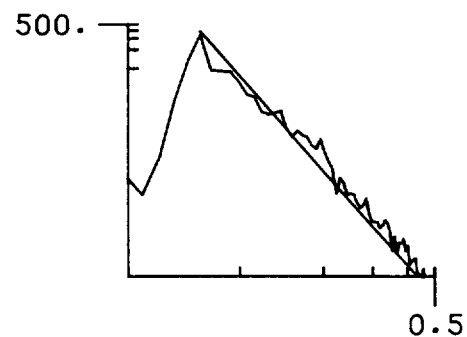
Fig. 6.1

84 1 0 0 10.37 12.37 1 84 1 3 0 10.35 13.10 1



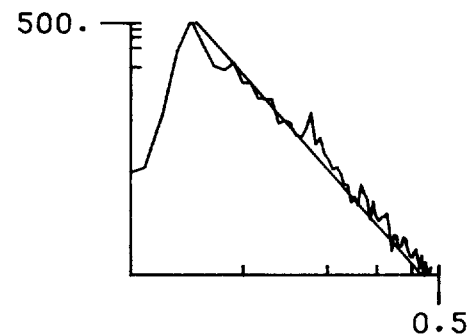
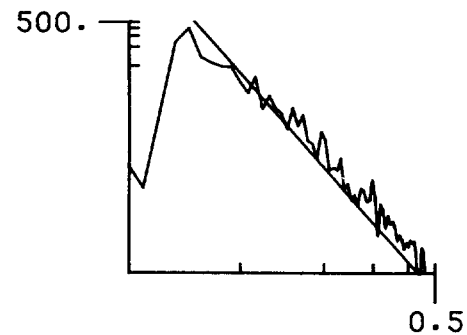
84 1 6 0 10.94 9.95 1

84 1 9 0 13.07 11.02 0



84 1 12 0 12.68 10.46 0

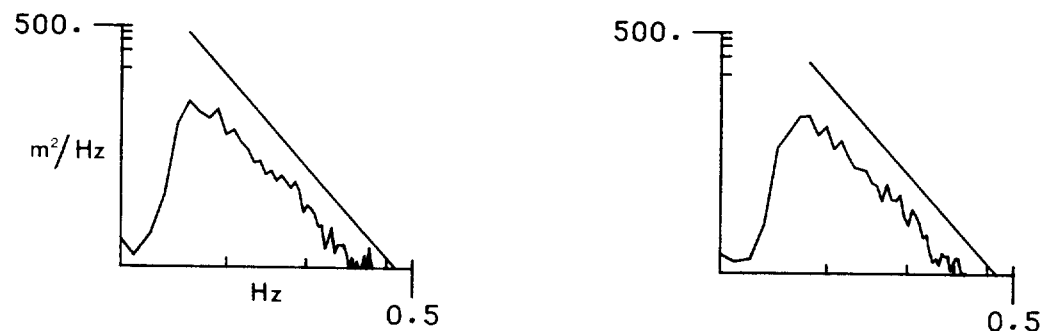
84 1 15 0 13.31 10.99 0



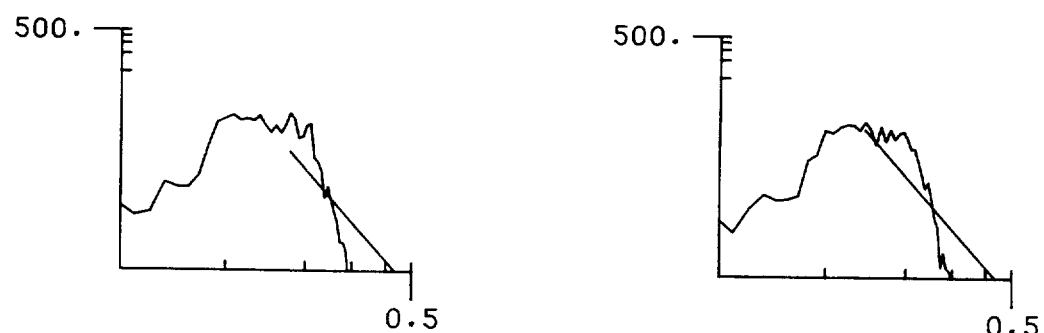
SPECTRA FROM OCEAN WEATHER STATION LIMA  
 CORRECTED USING FREQUENCY VARIABLE  $\xi$   
 $\zeta_4$

Fig. 6-2

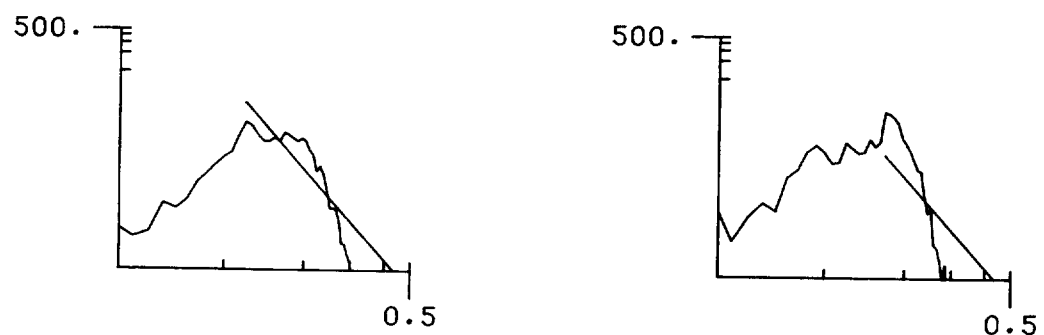
84 8 6 0 4.01 9.42 1 84 8 9 0 3.70 9.07 1



84 8 1135 5.56 6.52 0 84 8 1435 5.30 6.37 1



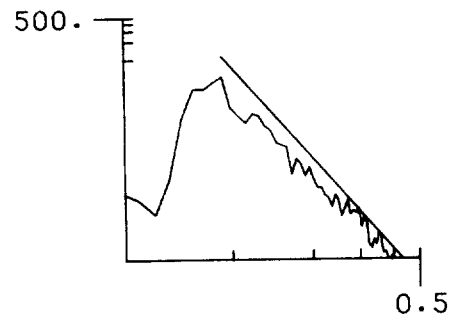
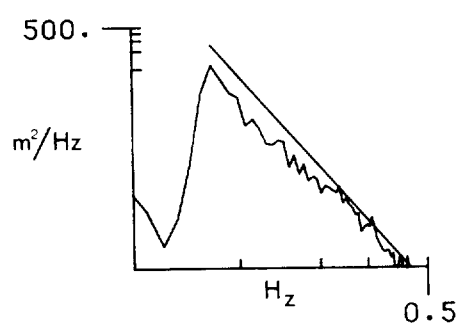
84 8 1735 4.20 6.19 1 84 8 2035 5.06 6.05 1



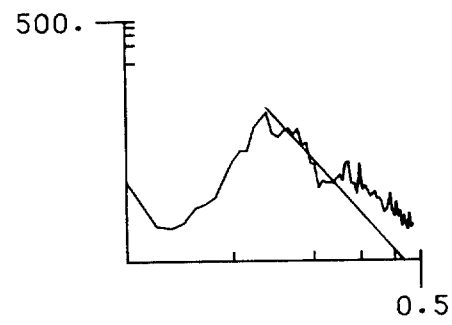
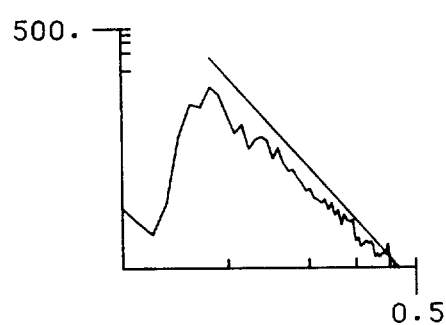
SPECTRA FROM OCEAN WEATHER STATION LIMA  
 CORRECTED USING FREQUENCY VARIABLE  $\zeta_4$

Fig. 6-3

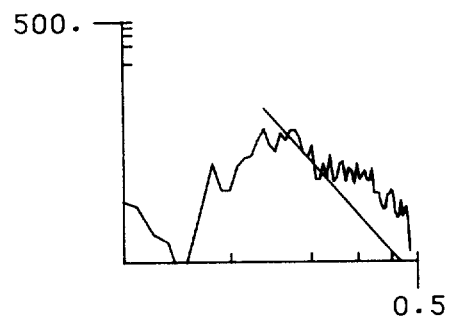
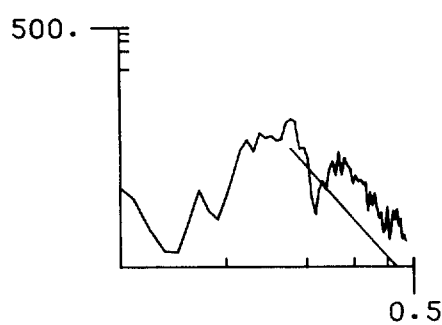
84 62 0 0 6.48 9.48 0 84 62 3 0 5.49 8.96 0



84 62 6 0 5.19 8.84 0 84 62 835 3.76 5.19 0

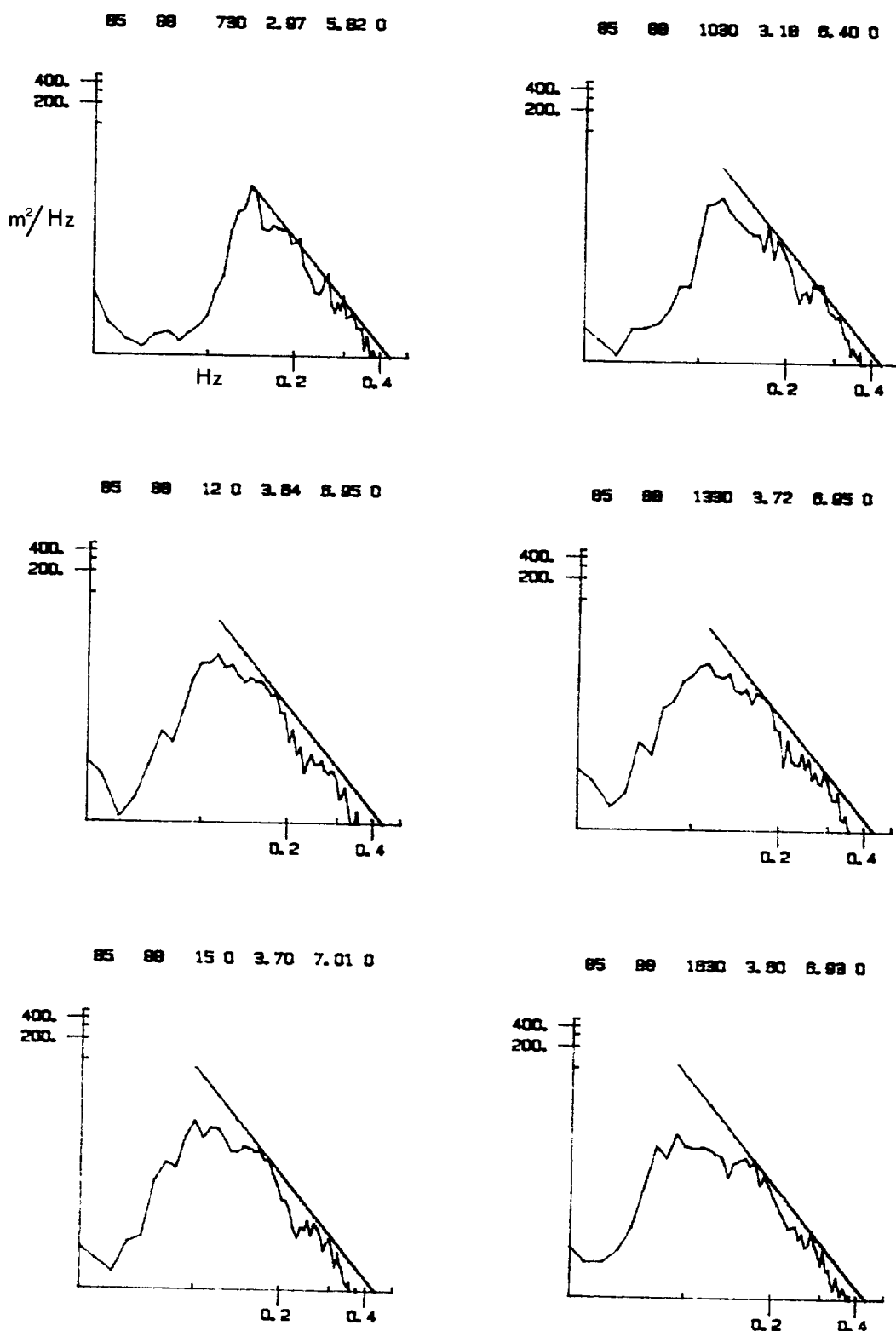


84 62 1135 4.08 4.85 0 84 62 1435 3.59 4.57 0



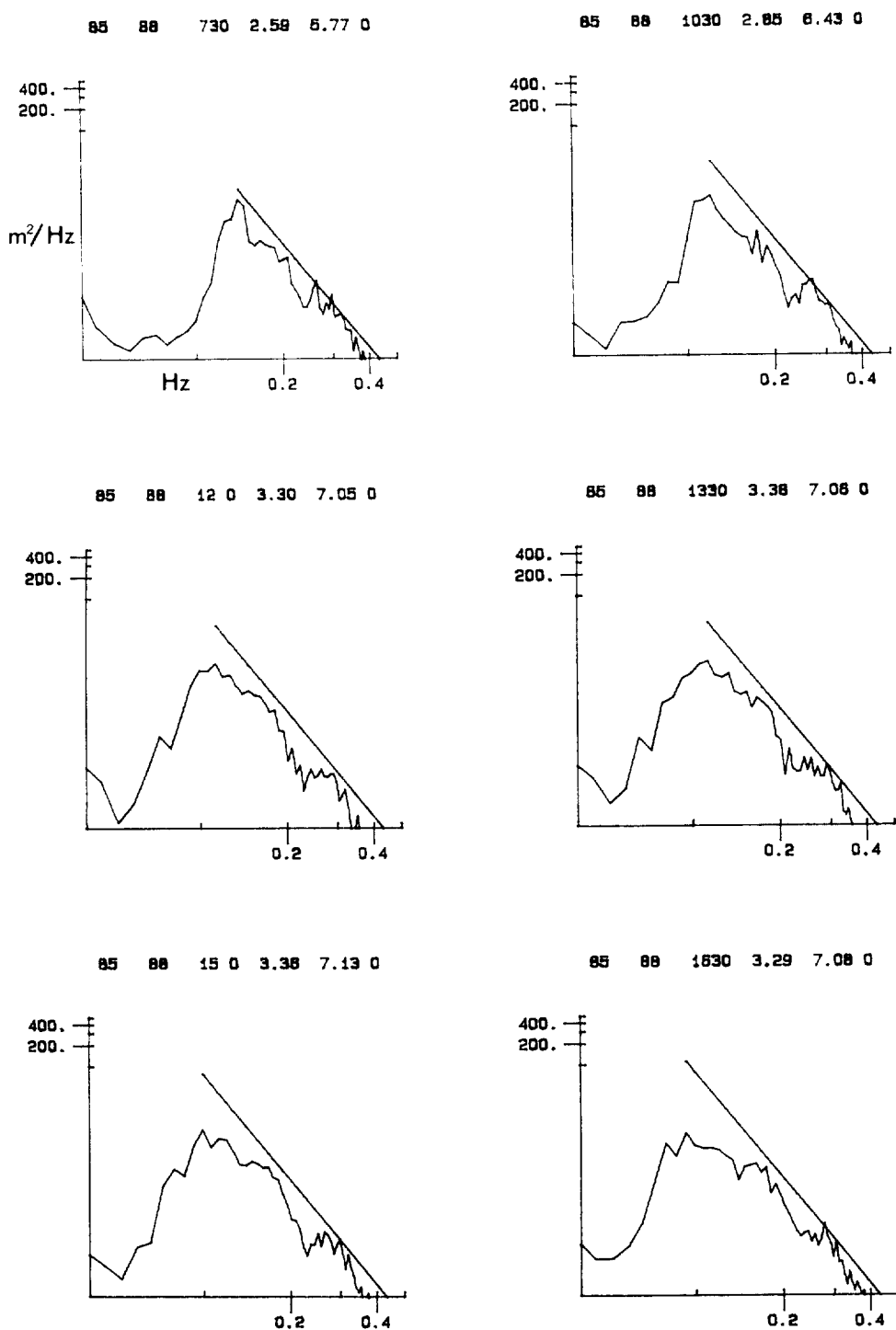
SPECTRA FROM THE SEVEN STONES LIGHTVESSEL  
CORRECTED USING FREQUENCY VARIABLE  $\xi_4$

Fig. 6·4



SPECTRA FROM THE SEVEN STONES LIGHTVESSEL  
CORRECTED USING FREQUENCY VARIABLE  $\xi_1$

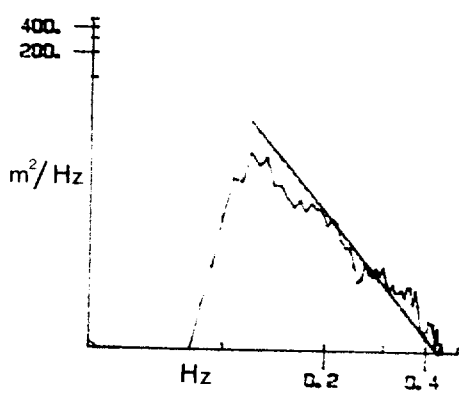
Fig. 6·5



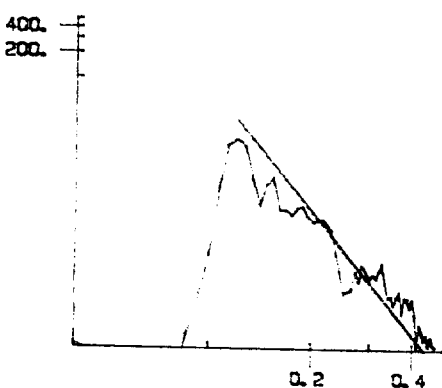
SPECTRA FROM DOWSING LIGHTVESSEL  
CORRECTED USING FREQUENCY VARIABLE  $\zeta_4$

Fig. 6.6

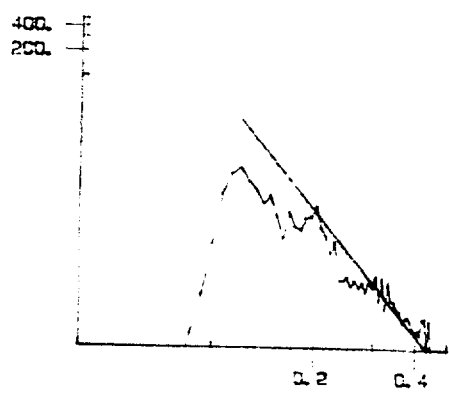
85 217 1530 3.31 5.84 0



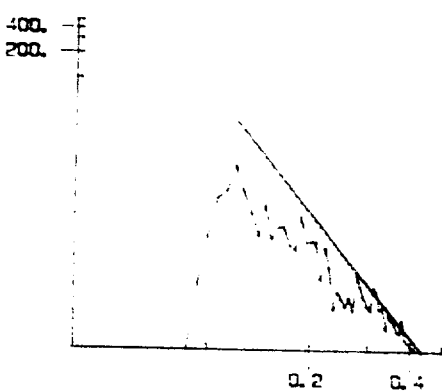
85 217 18 0 3.49 5.88 0



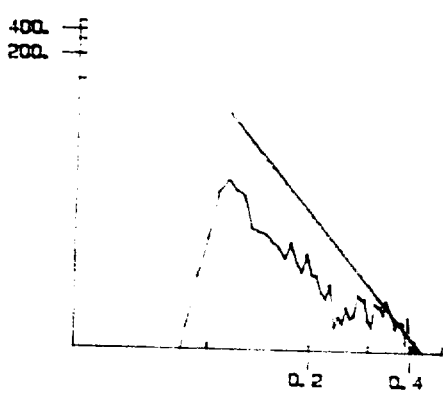
85 217 1930 2.71 5.88 0



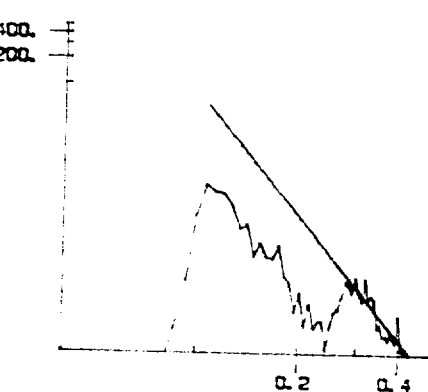
85 217 21 0 2.35 5.85 0



85 217 2230 2.08 5.95 0

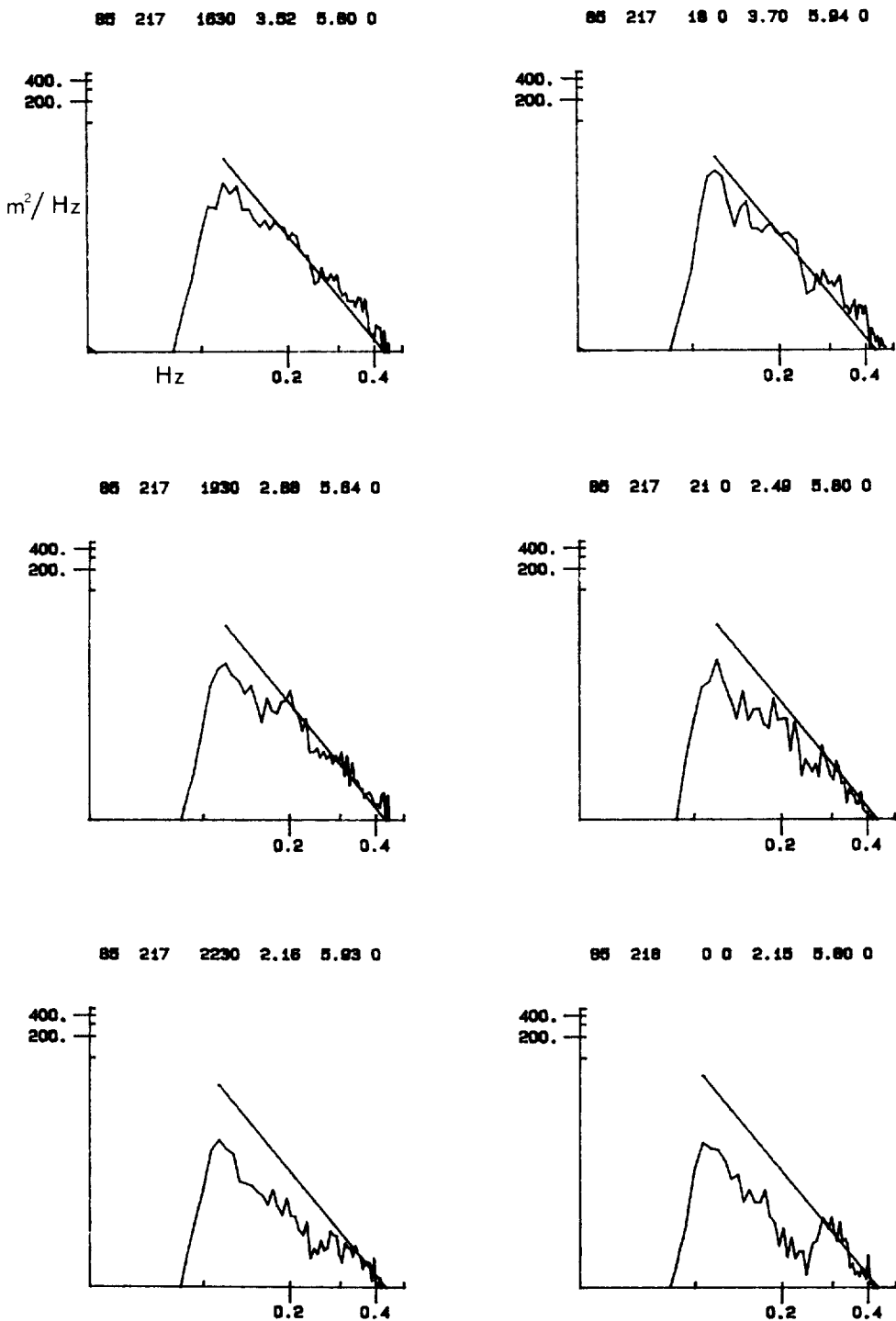


85 218 0 0 2.05 5.82 0



SPECTRA FROM DOWSING LIGHTVESSEL  
CORRECTED USING FREQUENCY VARIABLE  $\zeta_1$

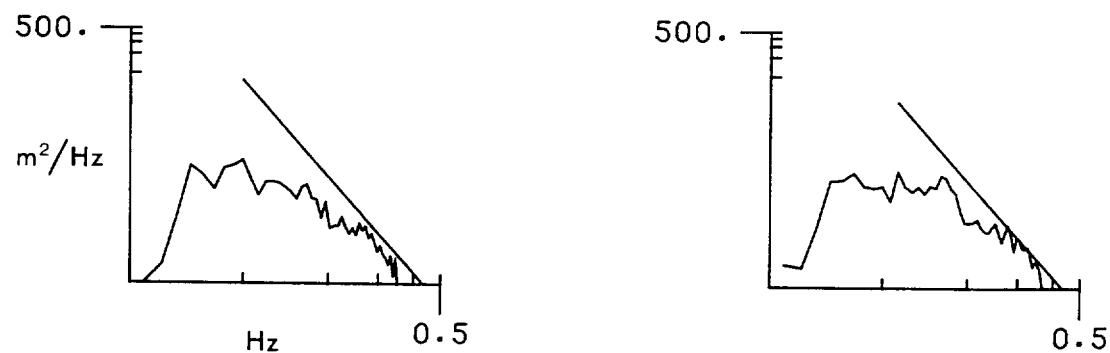
Fig. 6.7



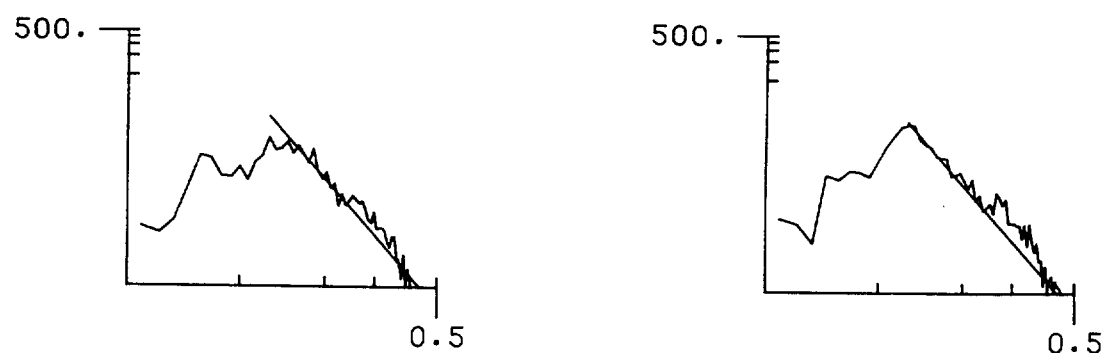
SPECTRA FROM THE CHANNEL LIGHTVESSEL  
CORRECTED USING FREQUENCY VARIABLE  $\zeta_4$

Fig. 6.8

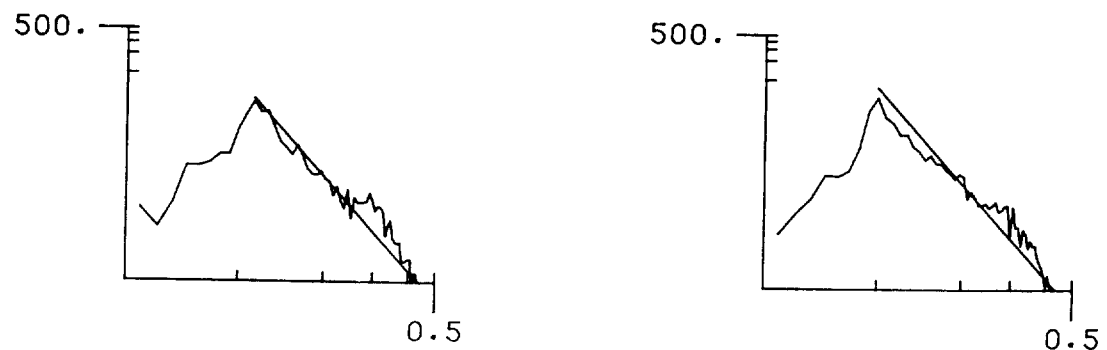
86 83 0 0 2.36 6.66 0 86 83 130 2.39 6.17 0



86 83 3 0 3.88 6.02 0 86 83 430 4.80 6.27 0



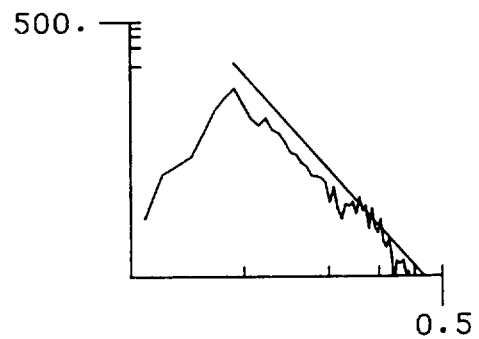
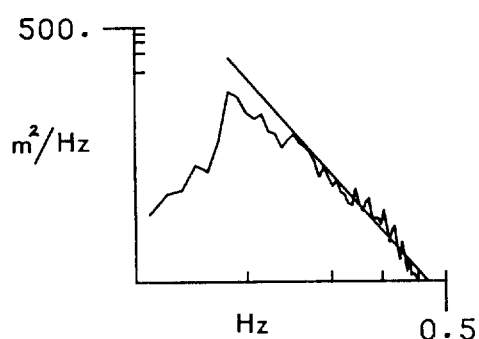
86 83 6 0 5.20 6.80 0 86 83 730 5.55 7.25 0



SPECTRA FROM THE CHANNEL LIGHTVESSEL  
CORRECTED USING FREQUENCY VARIABLE  $\zeta_4$

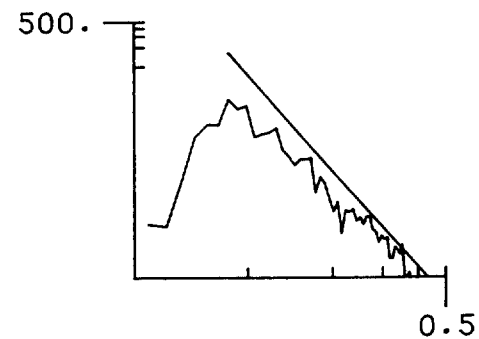
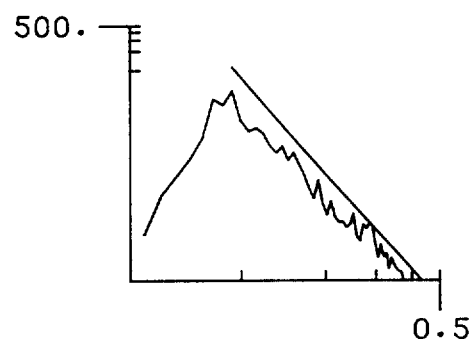
Fig. 6.9

86 83 9 0 5.47 7.72 0 86 83 1030 5.26 8.40 0



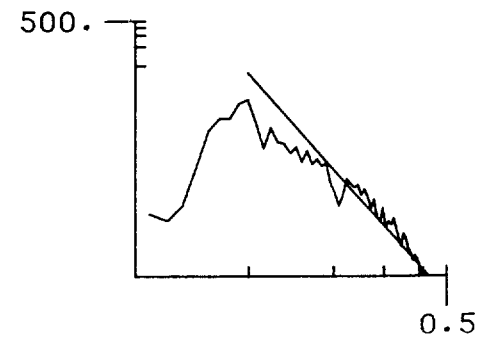
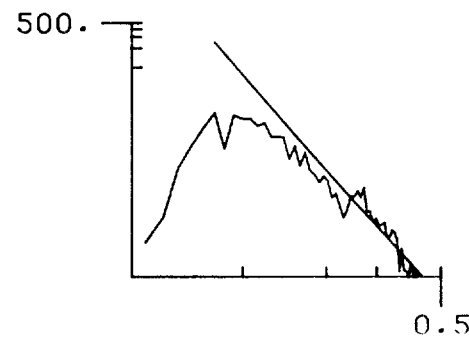
86 83 12 0 5.14 8.75 0

86 83 1330 4.69 8.39 0



86 83 15 0 4.64 7.45 0

86 83 1630 4.71 7.37 0



LIMA, JANUARY - MARCH 1984

Fig. 7.1.1.

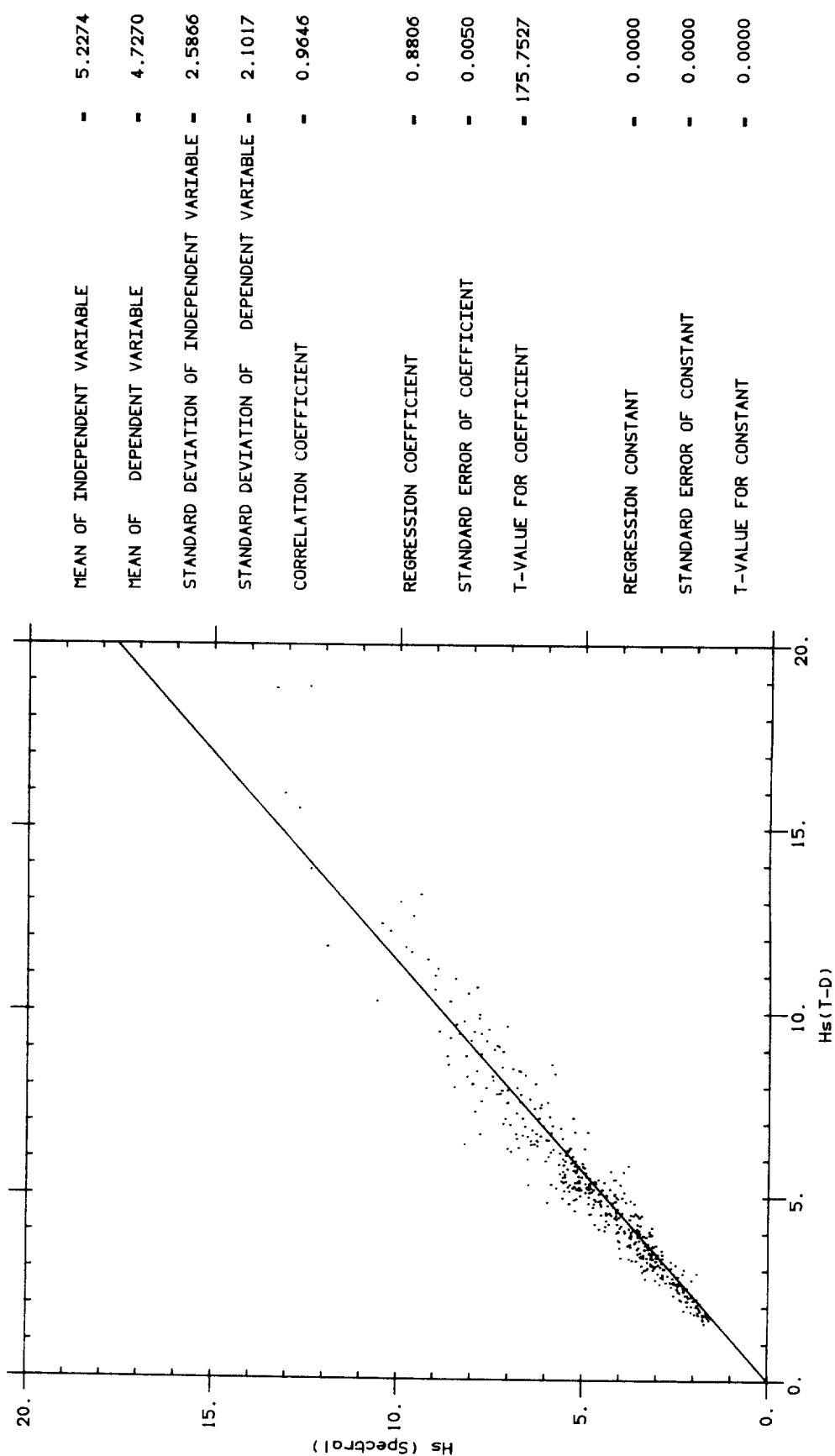


Fig. 7.1.2.

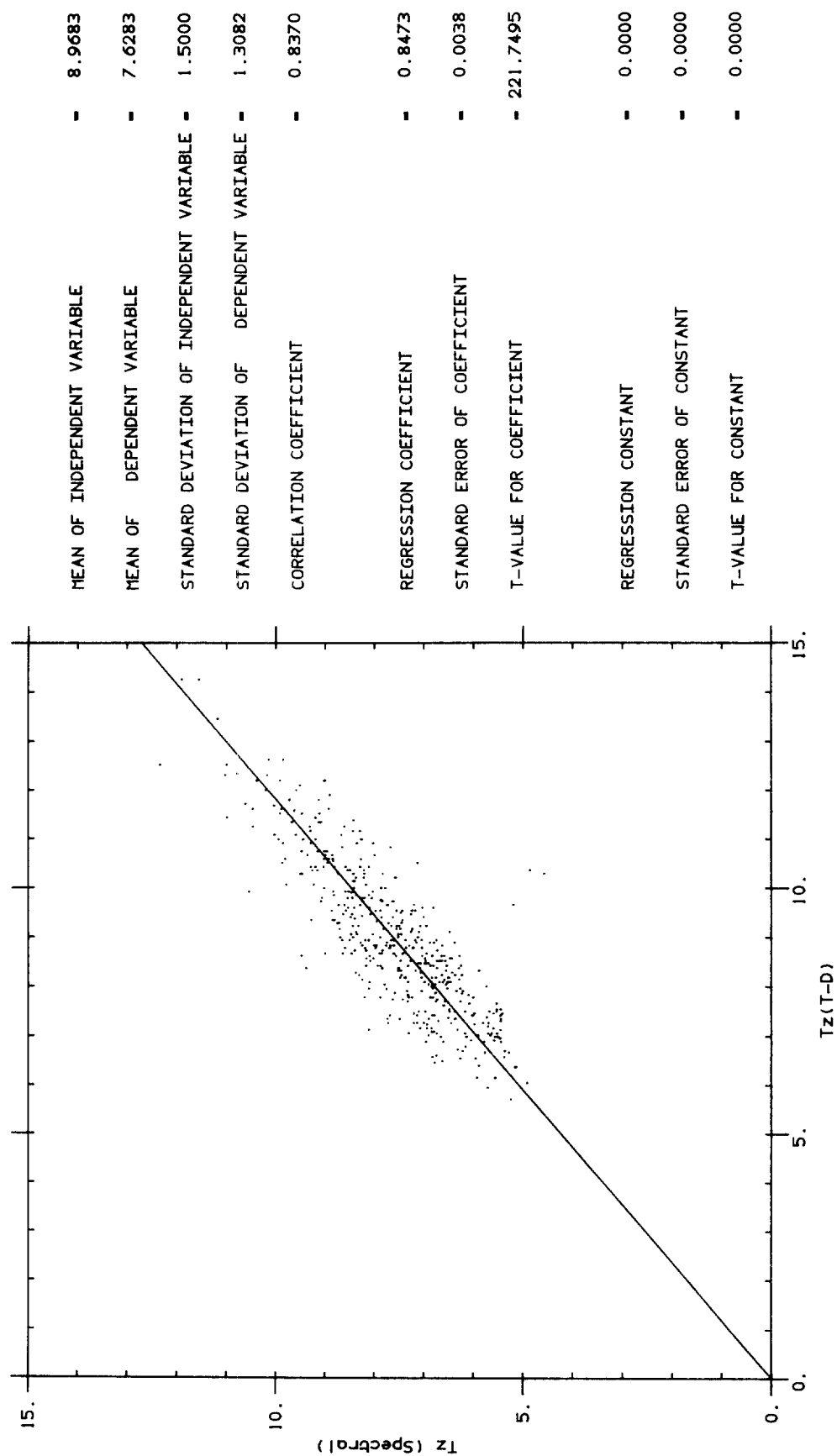


Fig. 7.1.3.

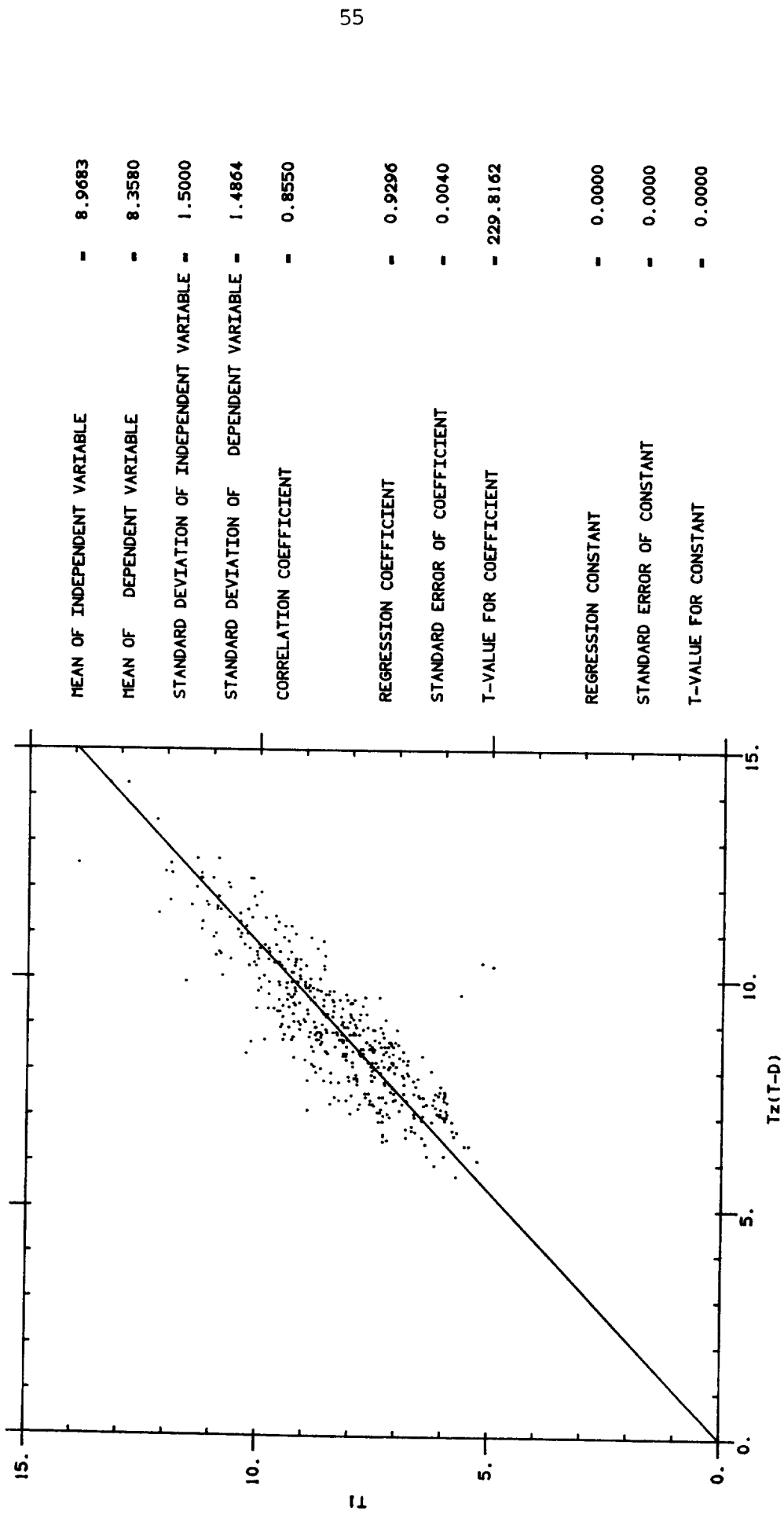
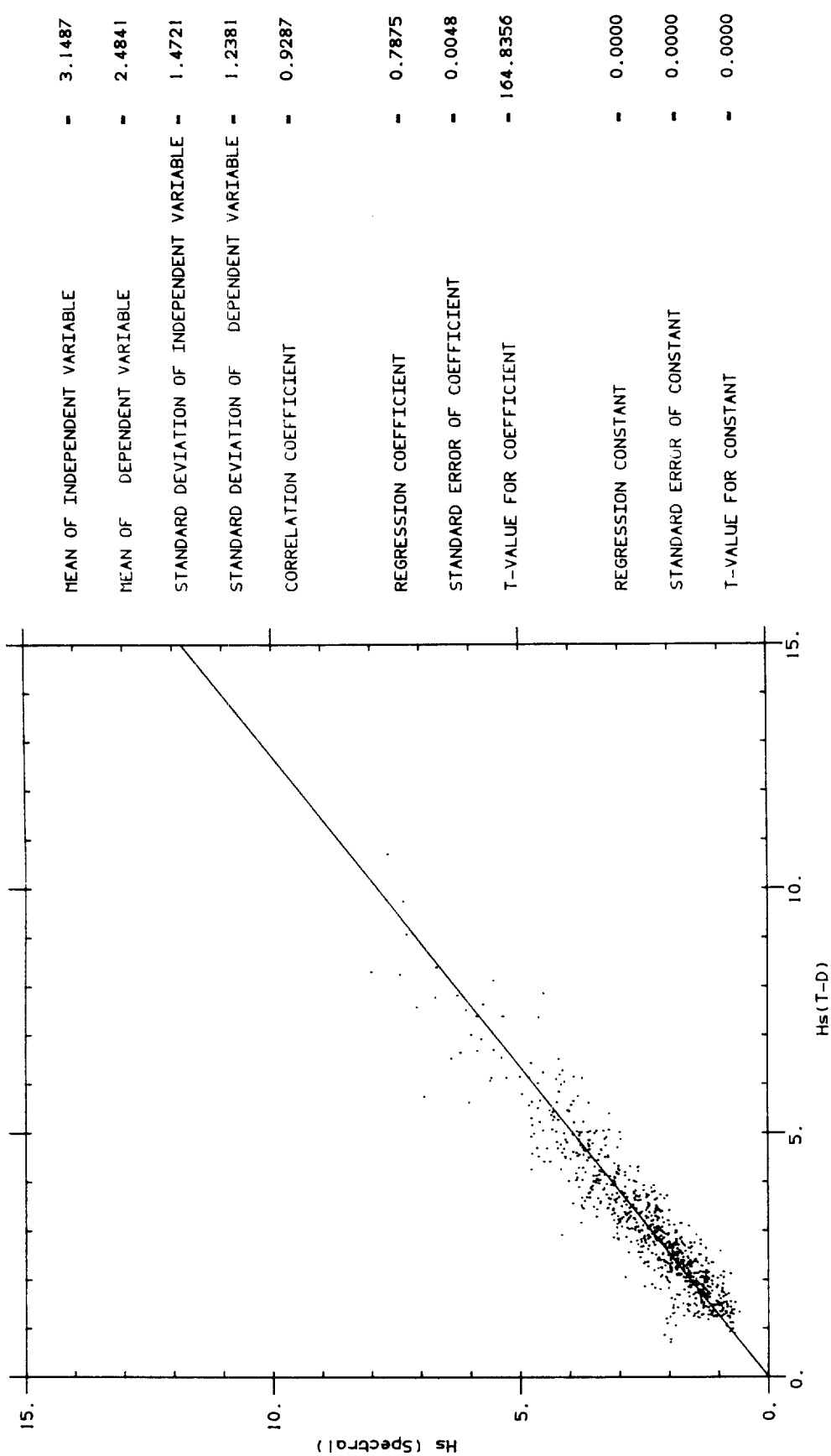


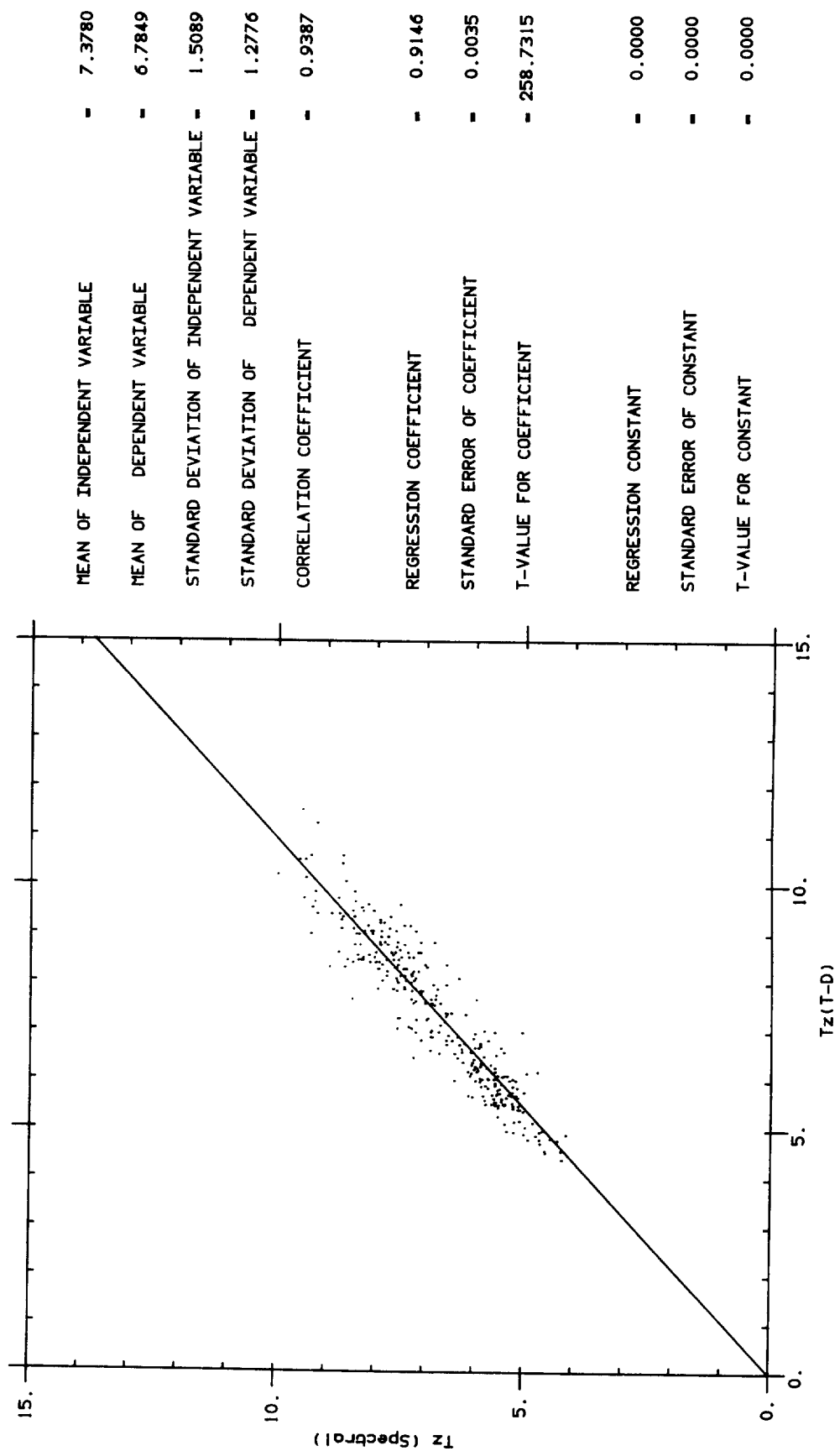
Fig. 7.2.1

SEVEN STONES, FEBRUARY - MAY 1985



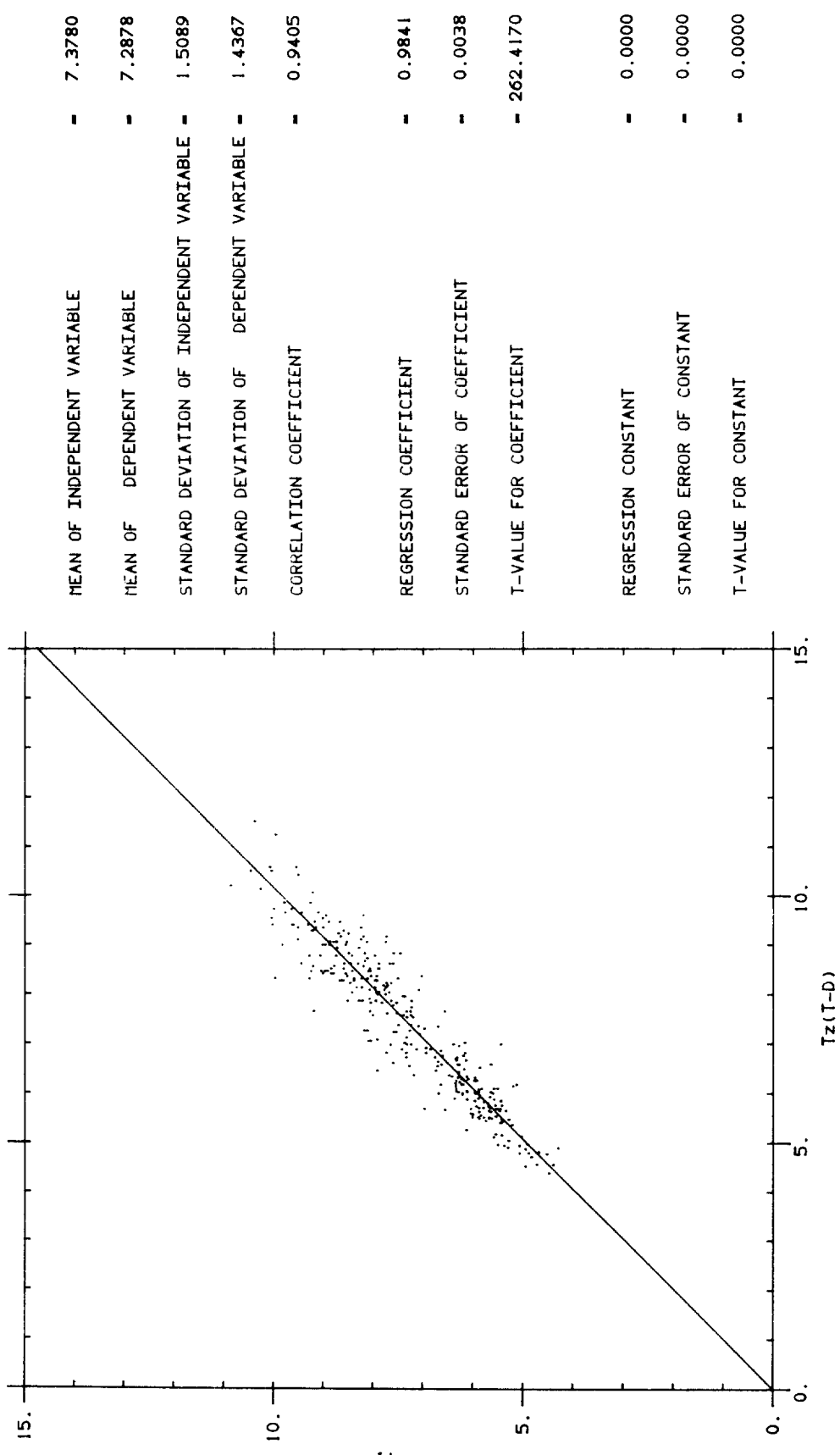
SEVEN STONES, APRIL - MAY 1985

Fig. 7.2.2.



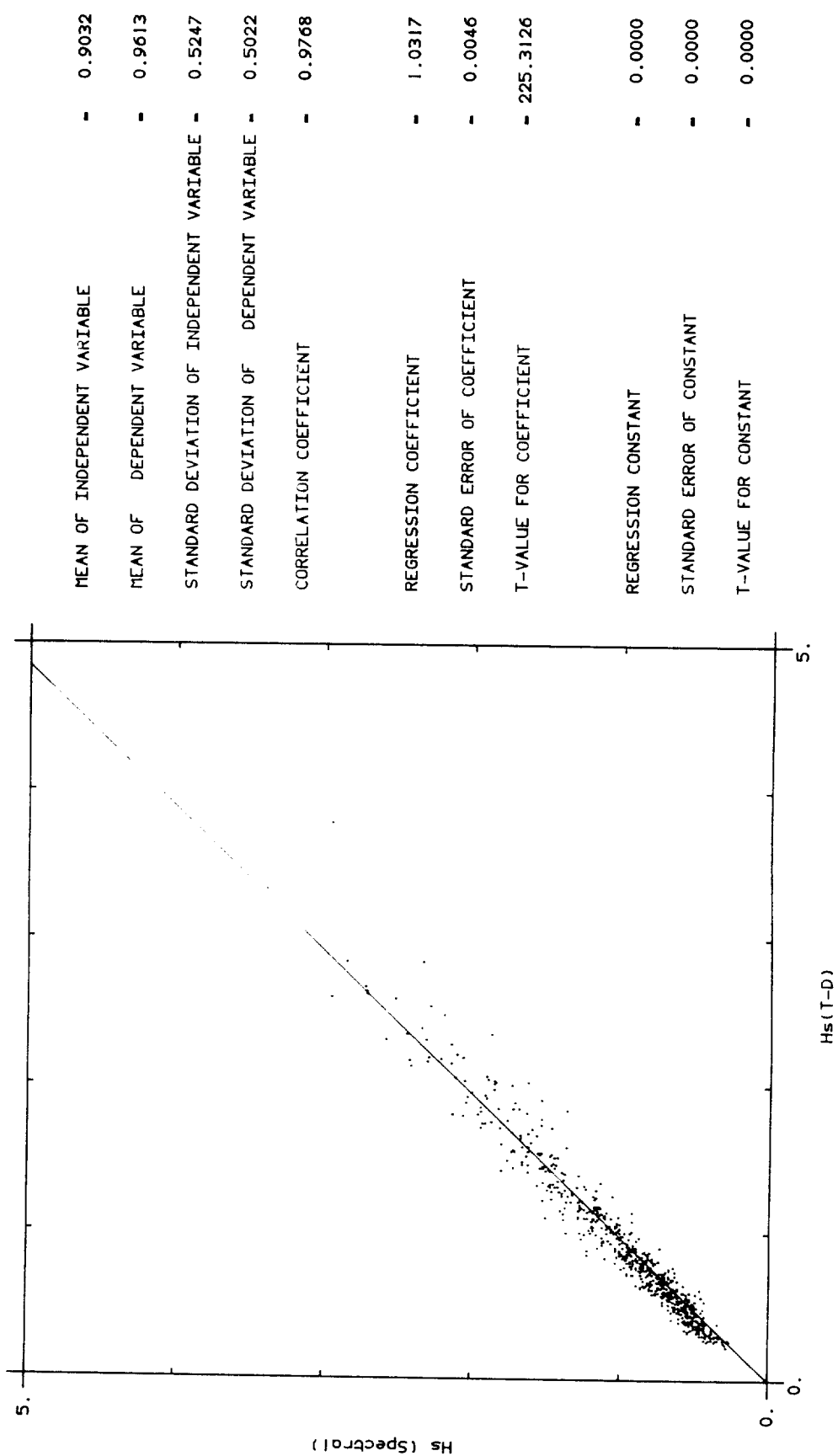
SEVEN STONES: APRIL - MAY 1985

Fig. 72.3.



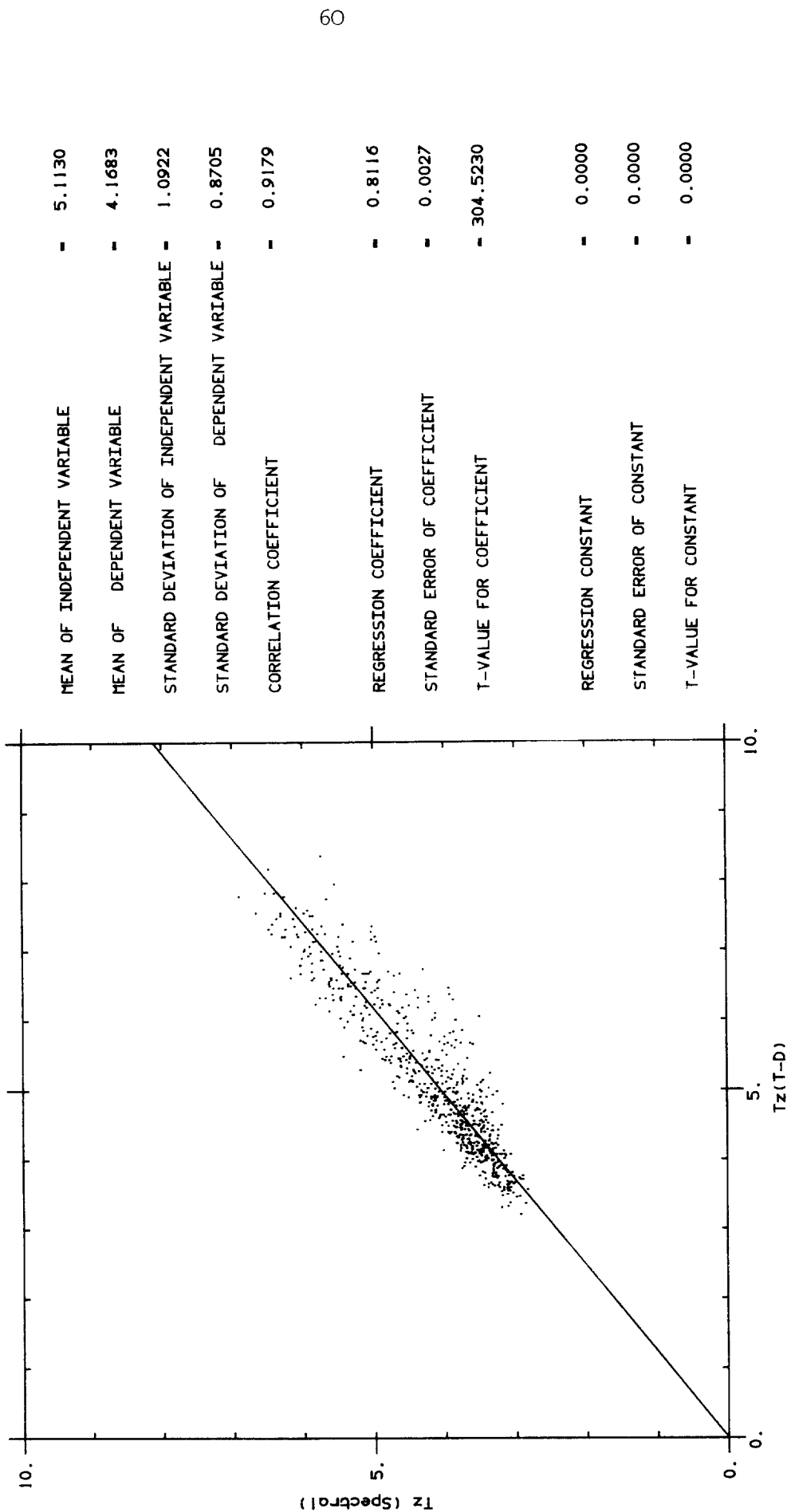
DOUSING, JULY - SEPTEMBER 1985

Fig. 7.3.1



DOHSENG, JULY - SEPTEMBER 1985

Fig. 7.3.2.



DOUISING: JULY - SEPTEMBER 1985

Fig. 7.3.3

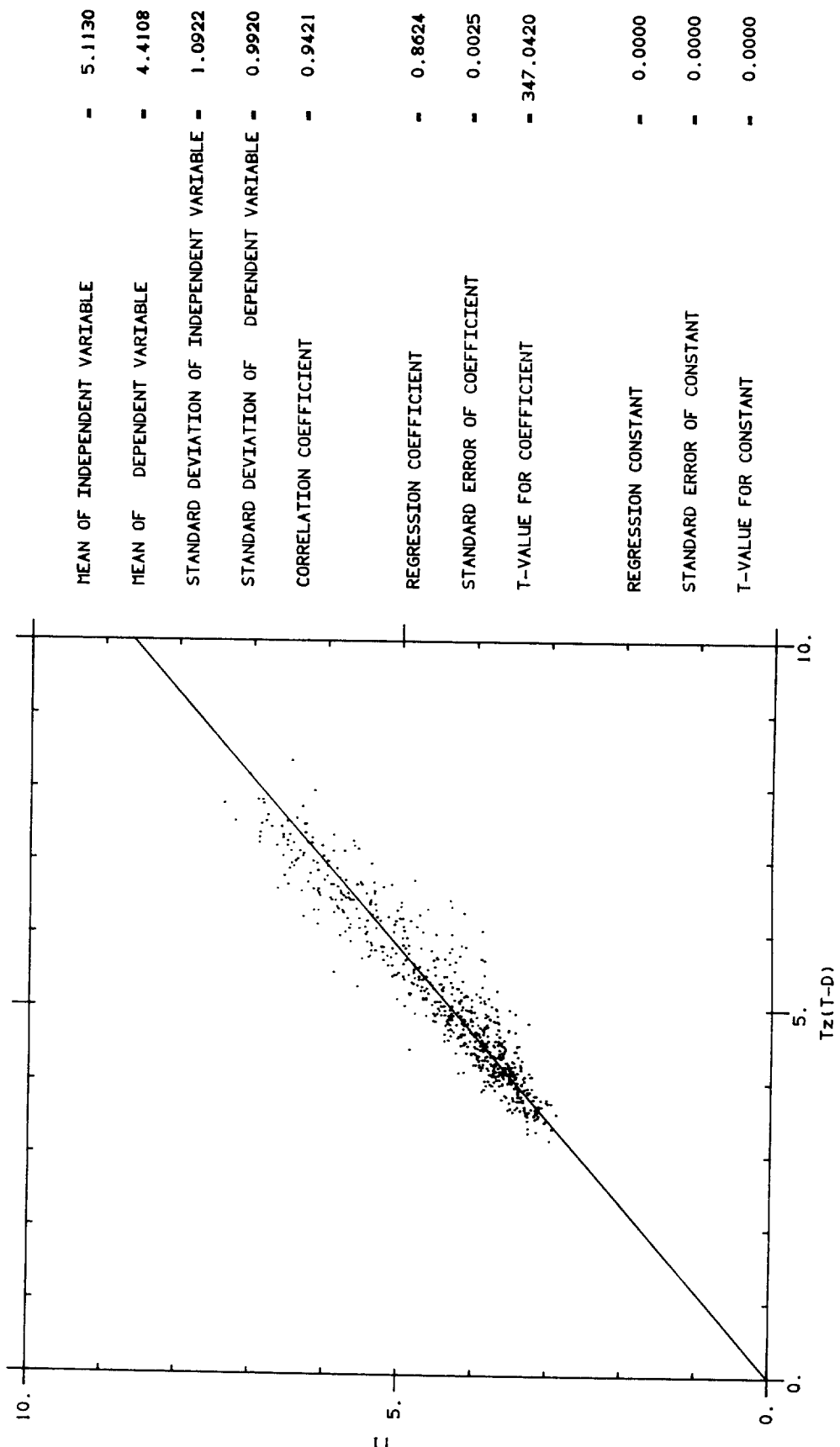
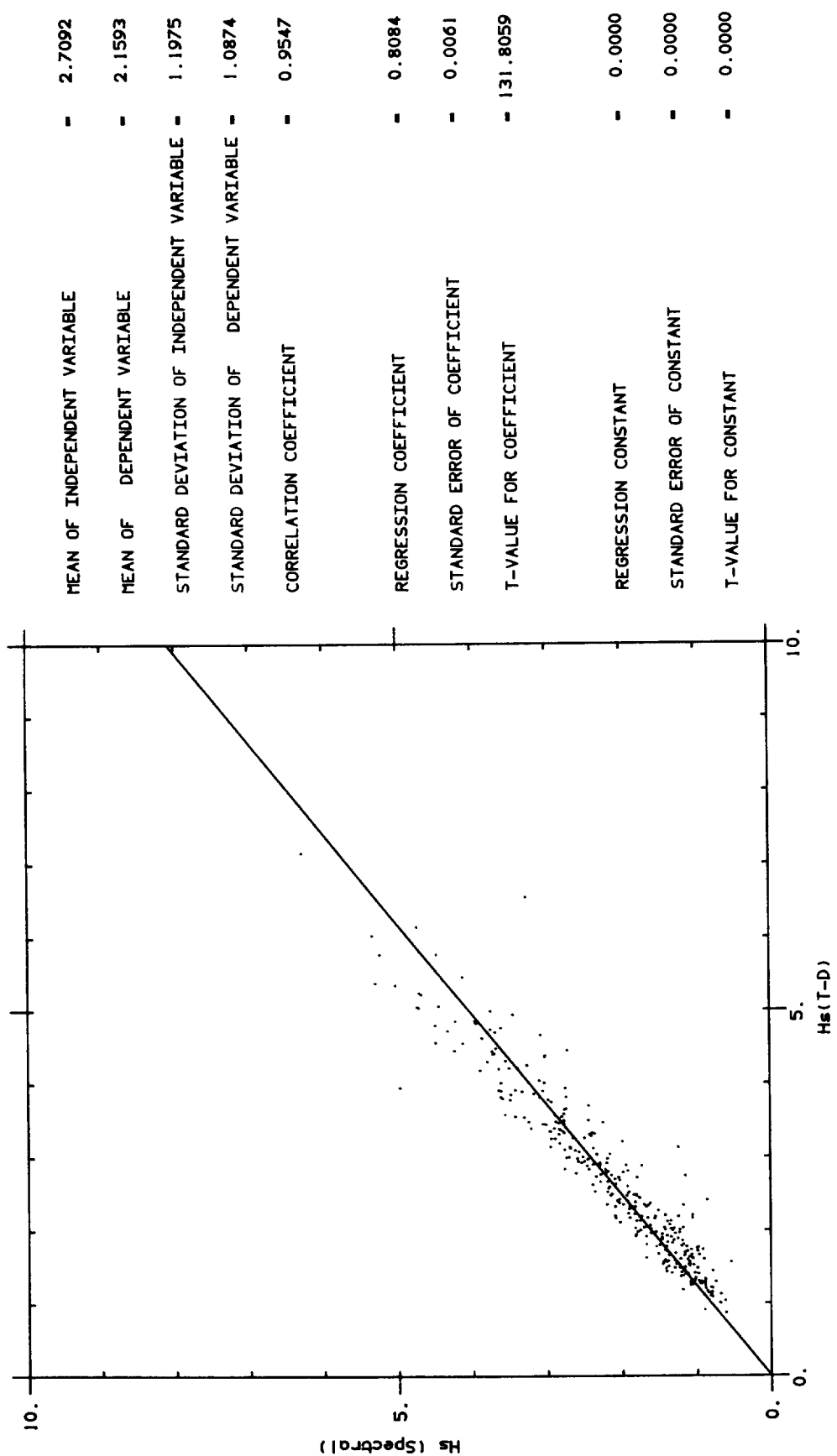


Fig. 7-4-1

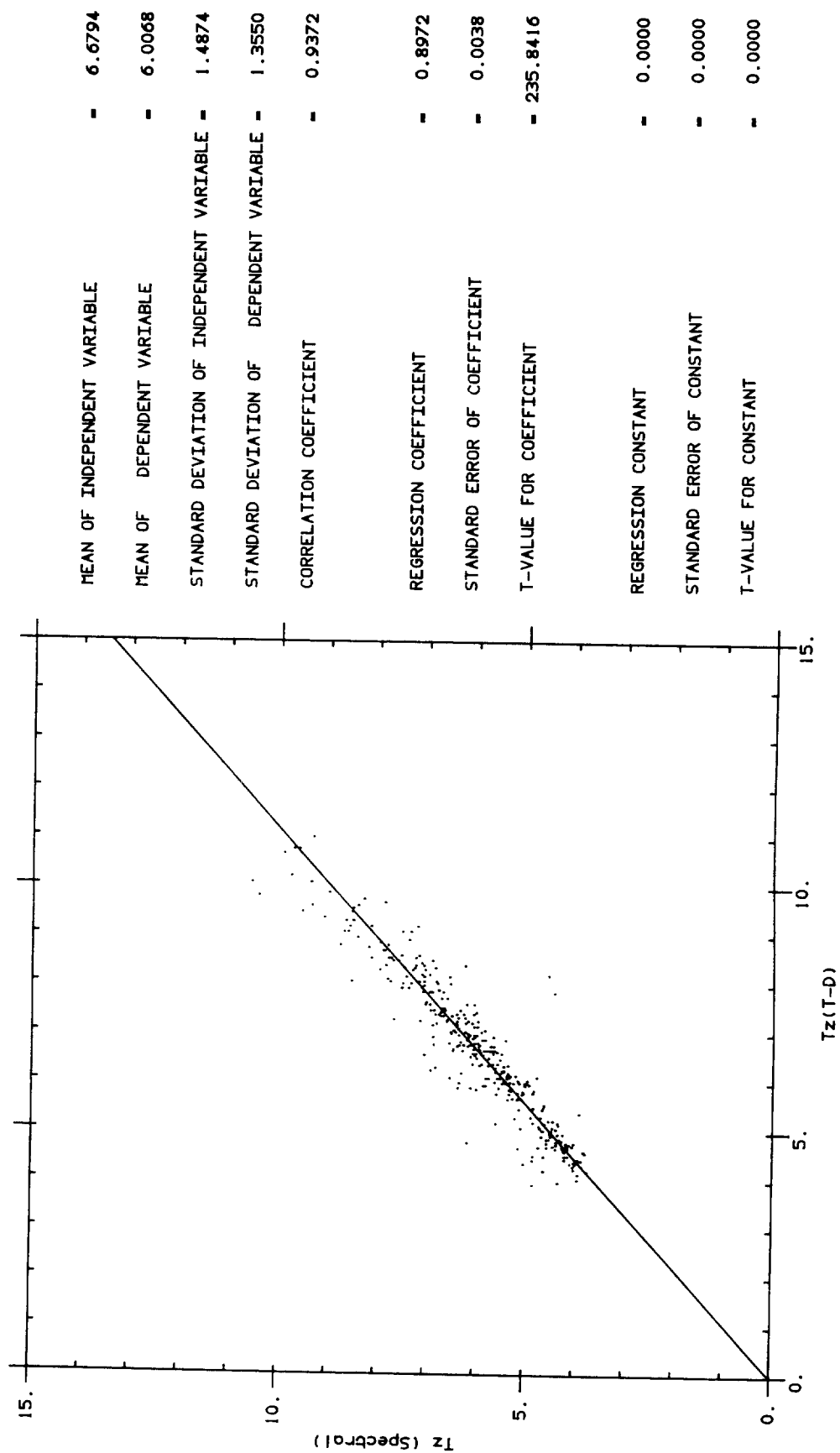
CHANNEL LV, MARCH-APRIL 1986



CHANNEL: MARCH - APRIL 1986

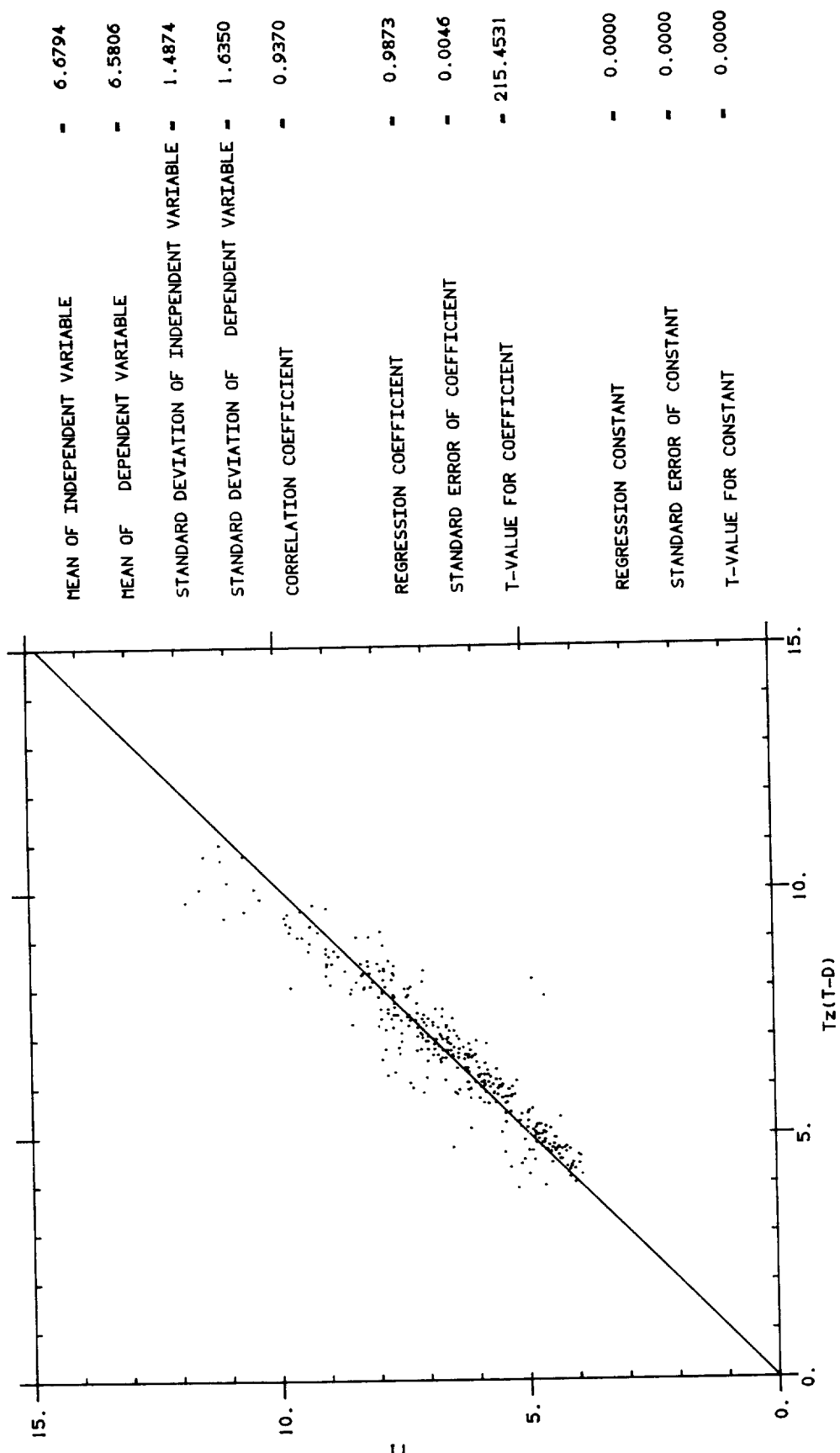
Fig. 7.4.2.

63



CHANNEL, MARCH - APRIL 1986

Fig. 7.4.3.



SEVEN STONES SBWR : SCILLY W/R

Fig. 7.5

65

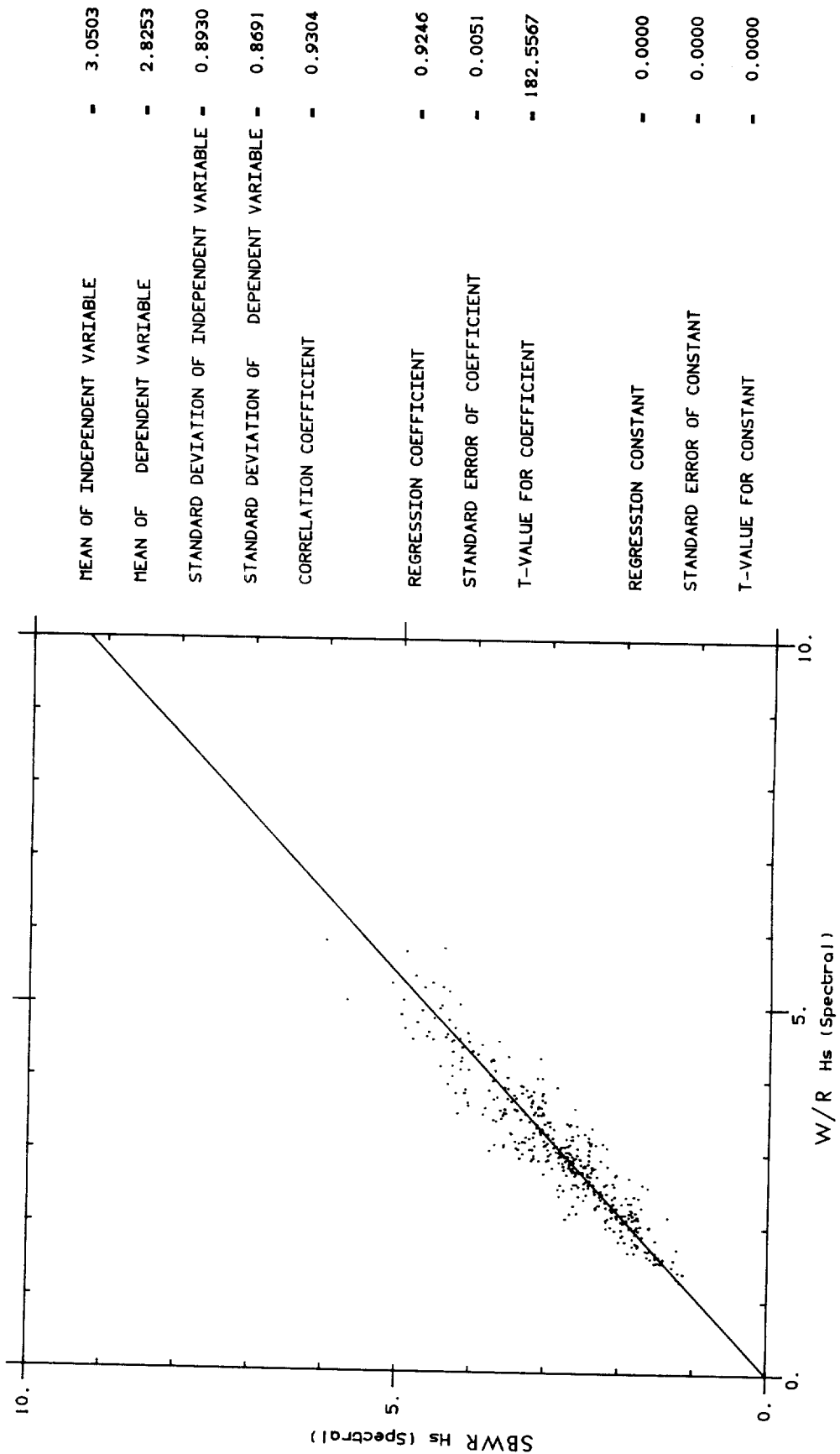
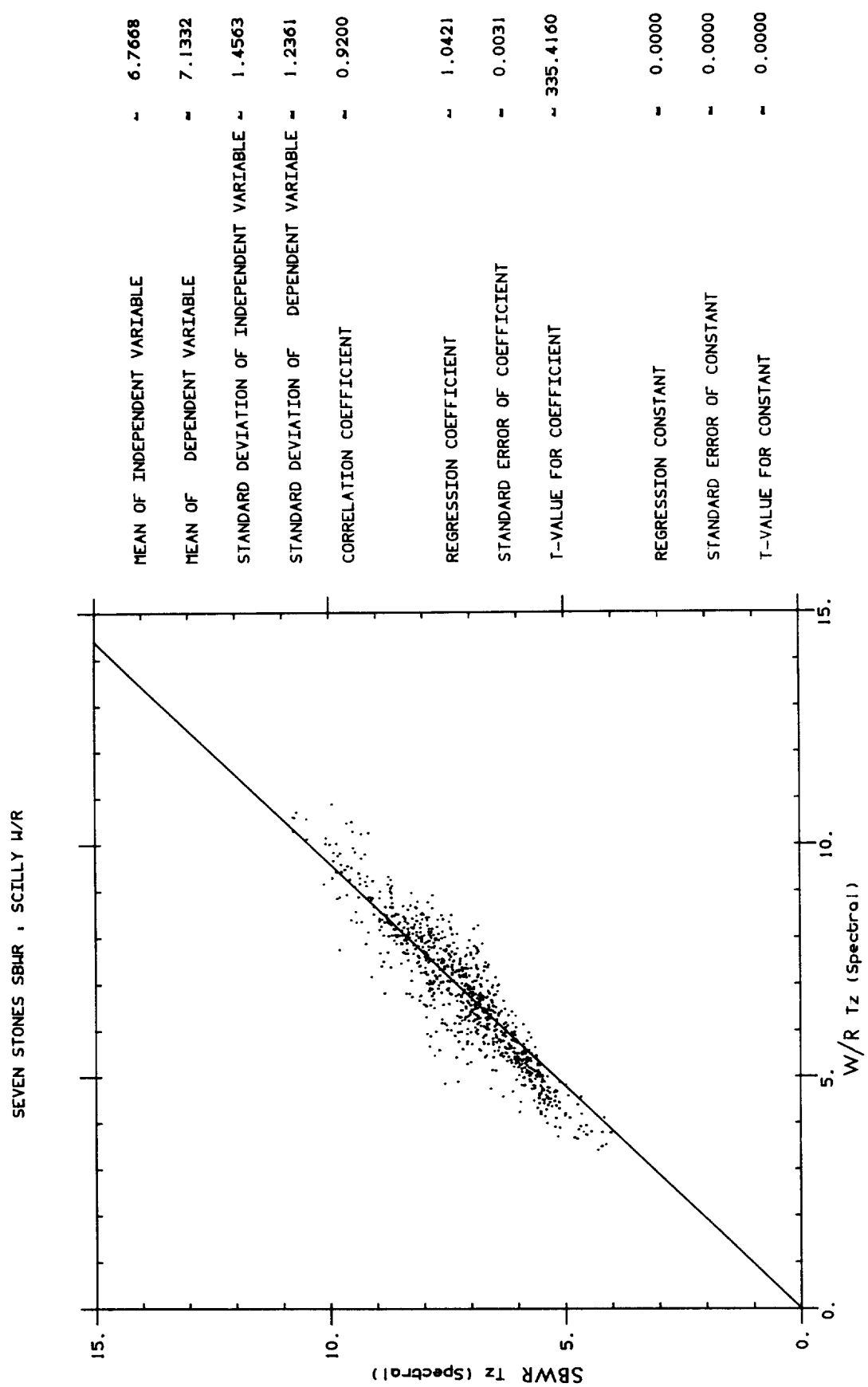


Fig. 7.6



LIMA, JANUARY - MARCH 1984

Fig. 8-1-1

67

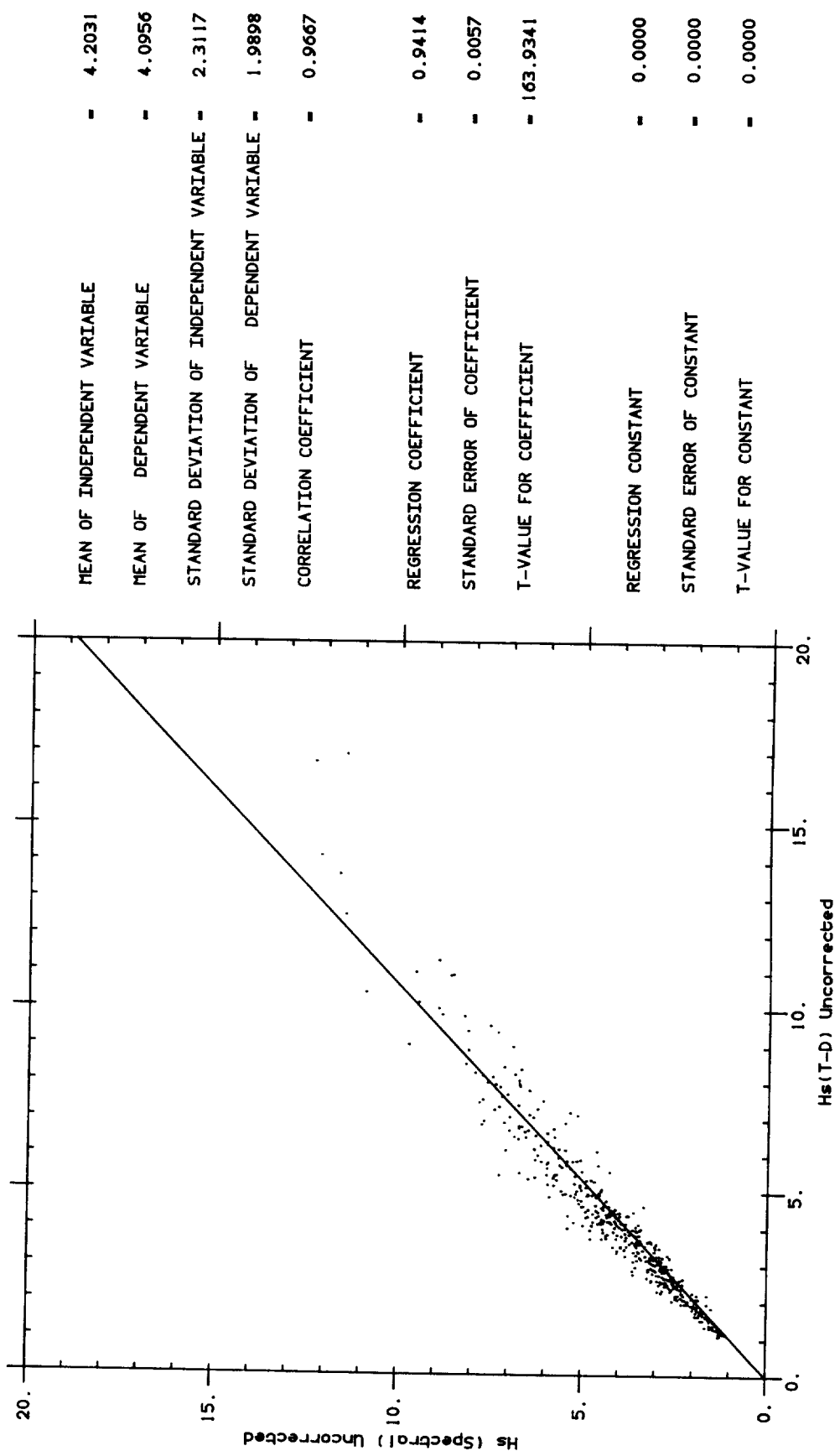
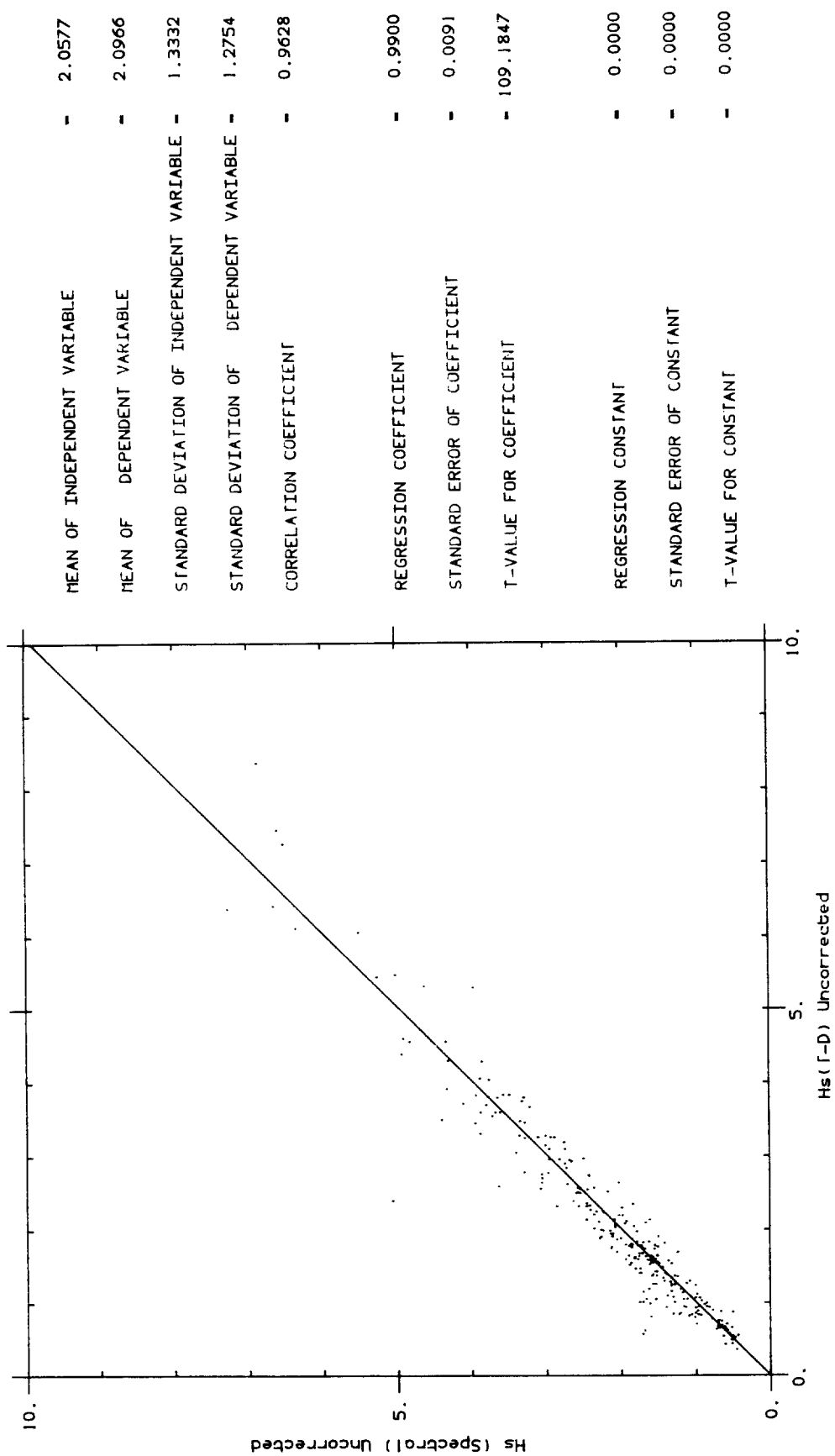


Fig. 8.1.2

SEVEN STONES, APRIL - MAY 1985



DOWSING: JULY - SEPTEMBER 1985

Fig. 8.1-3

69

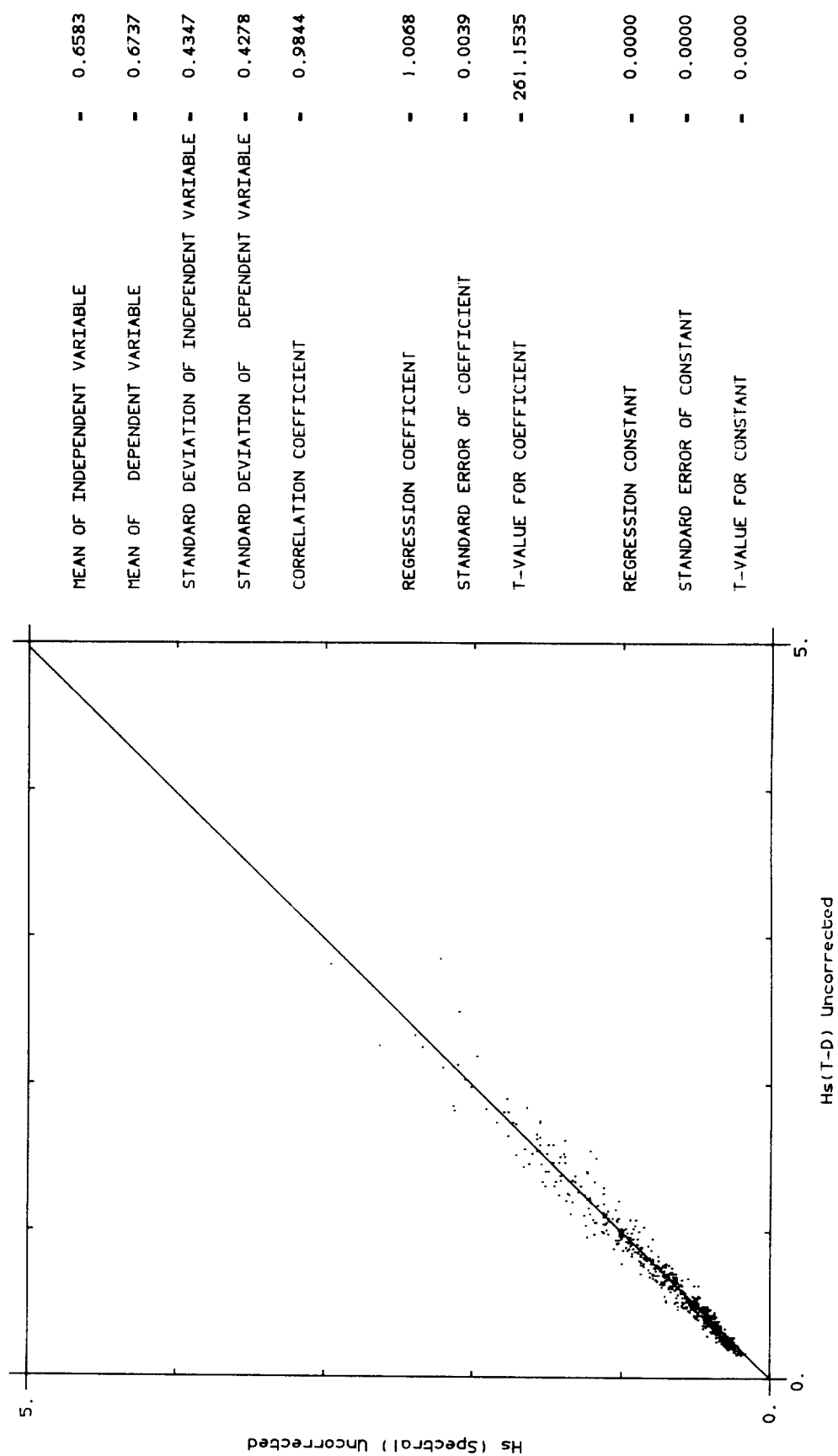
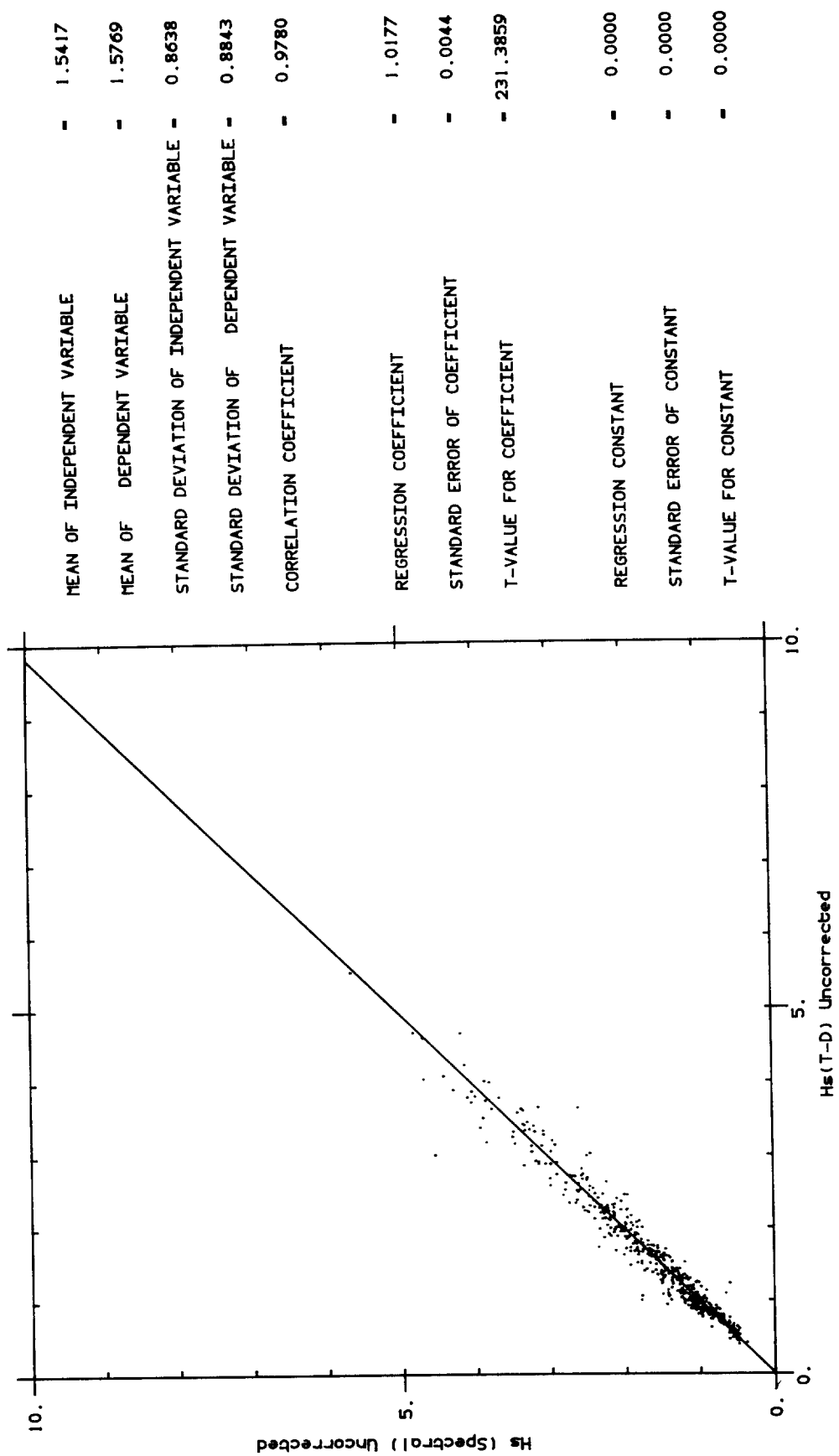


Fig. 8.1.4

CHANNEL: MARCH - MAY 1986



LIMA: JANUARY - MARCH 1984

Fig. 8-2-1

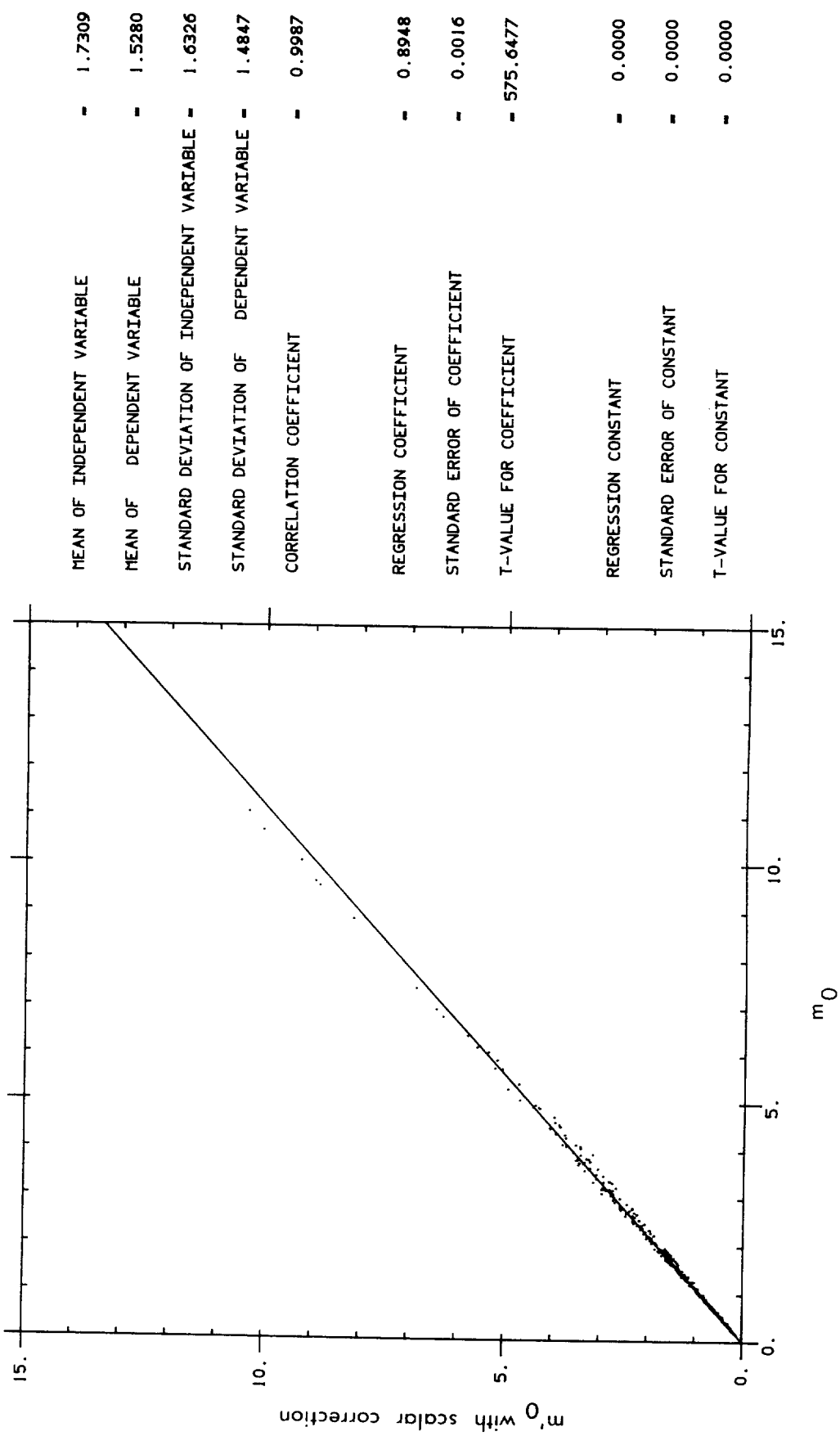
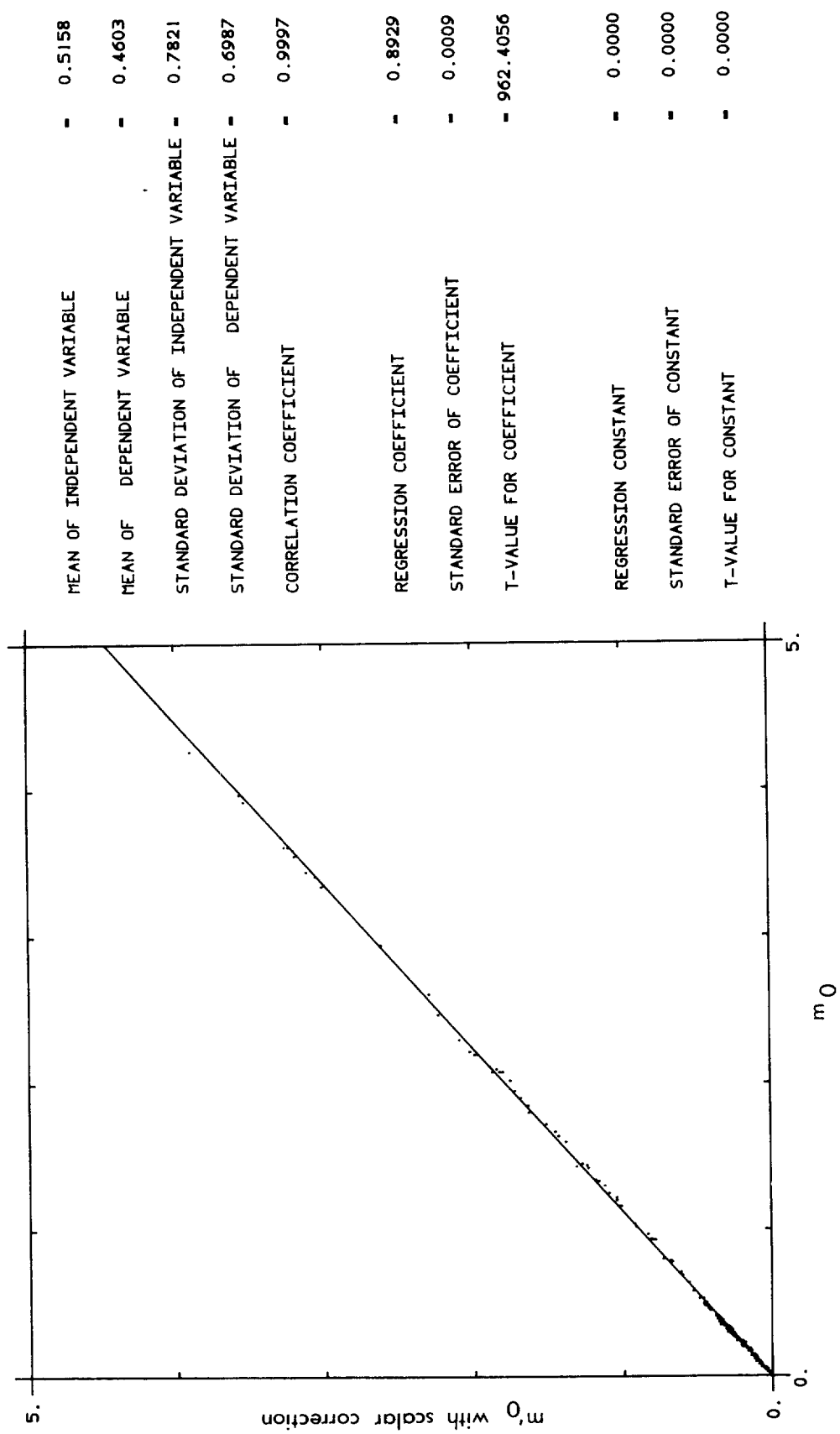


Fig. 8.2.2

SEVEN STONES, APRIL - MAY 1985



DOUSING, JULY - SEPTEMBER 1985

Fig. 8.2.3

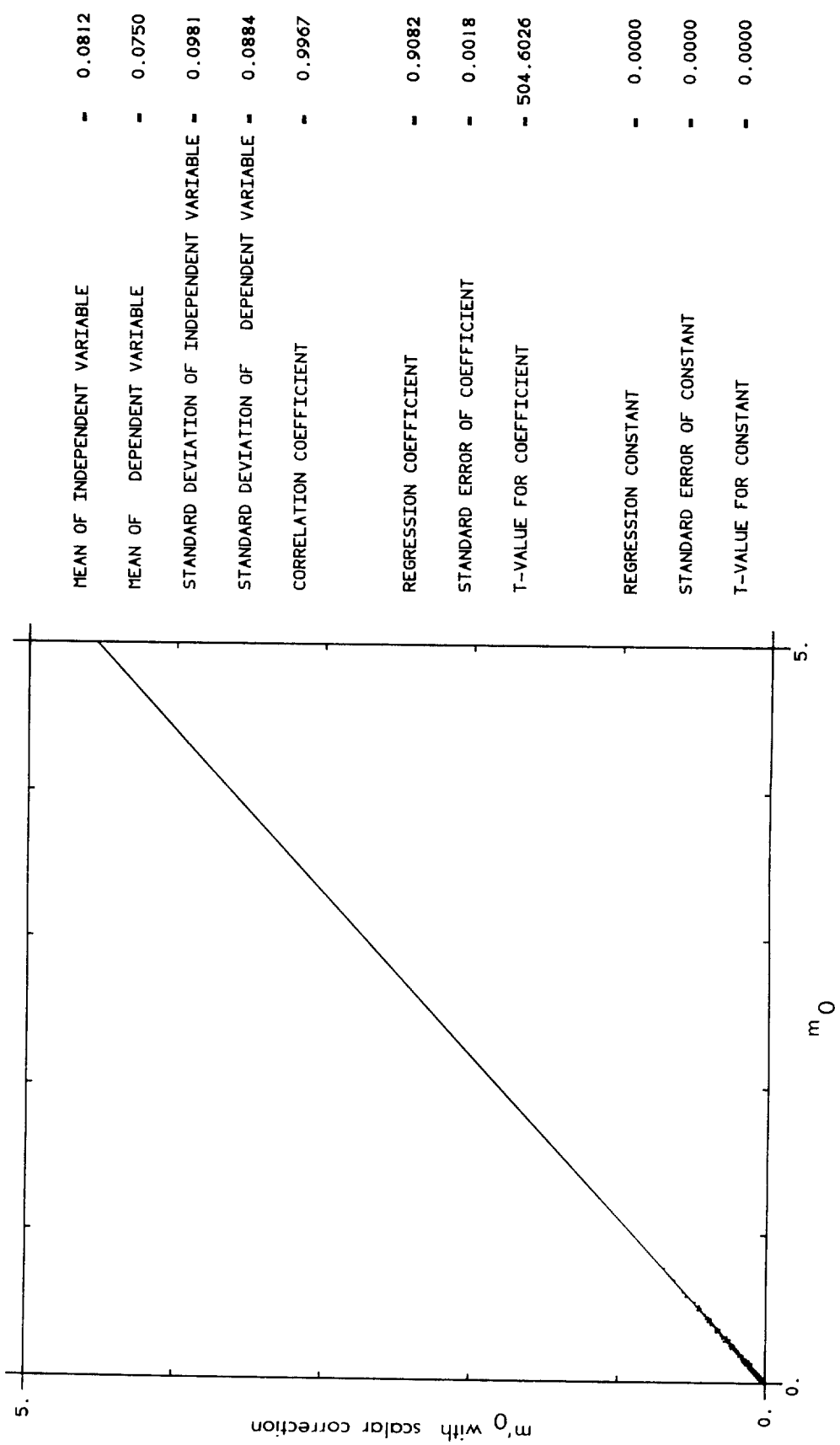
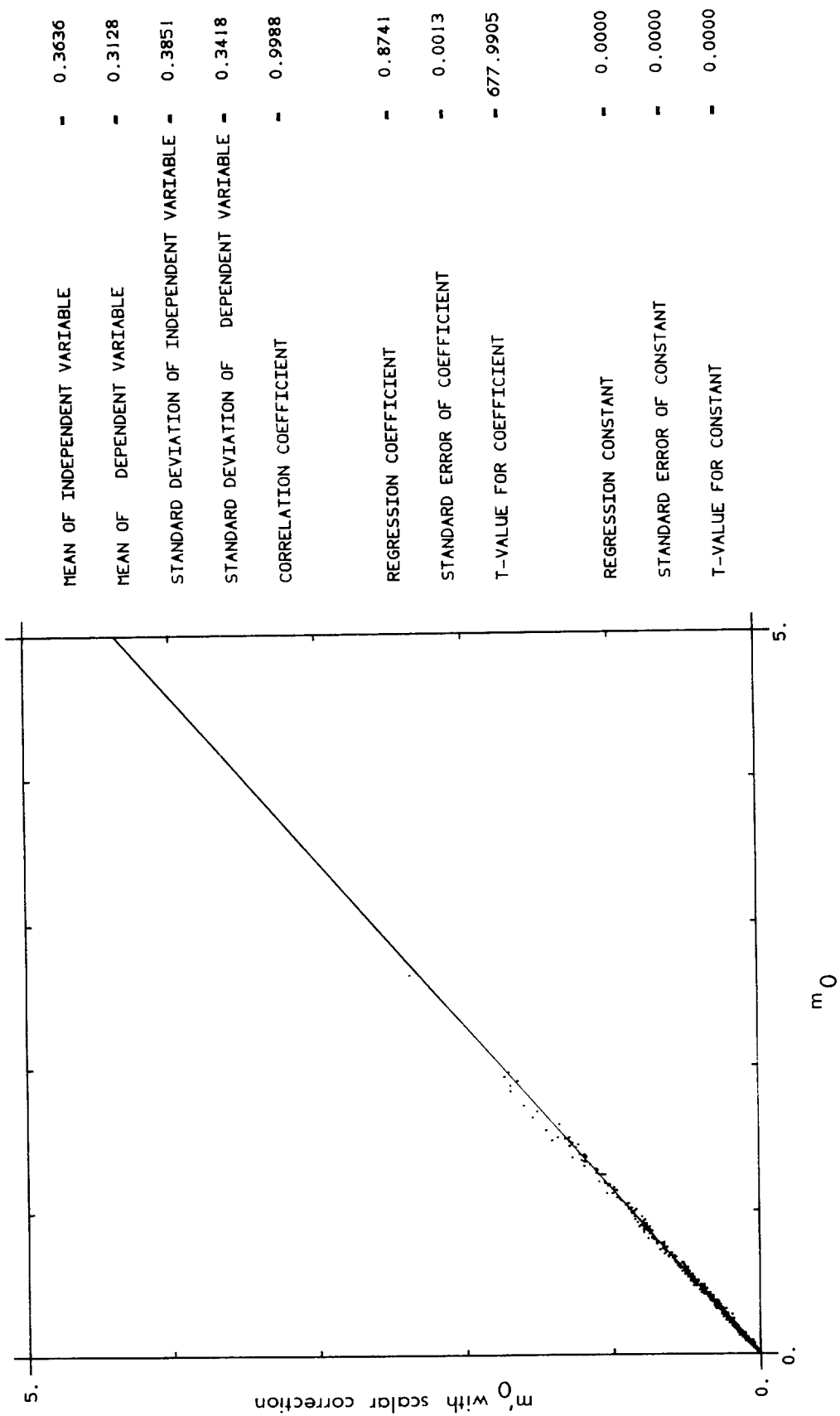


Fig. 8.2.4



LIMA(U): JANUARY - MARCH 1984

Fig. 8.2.5

75

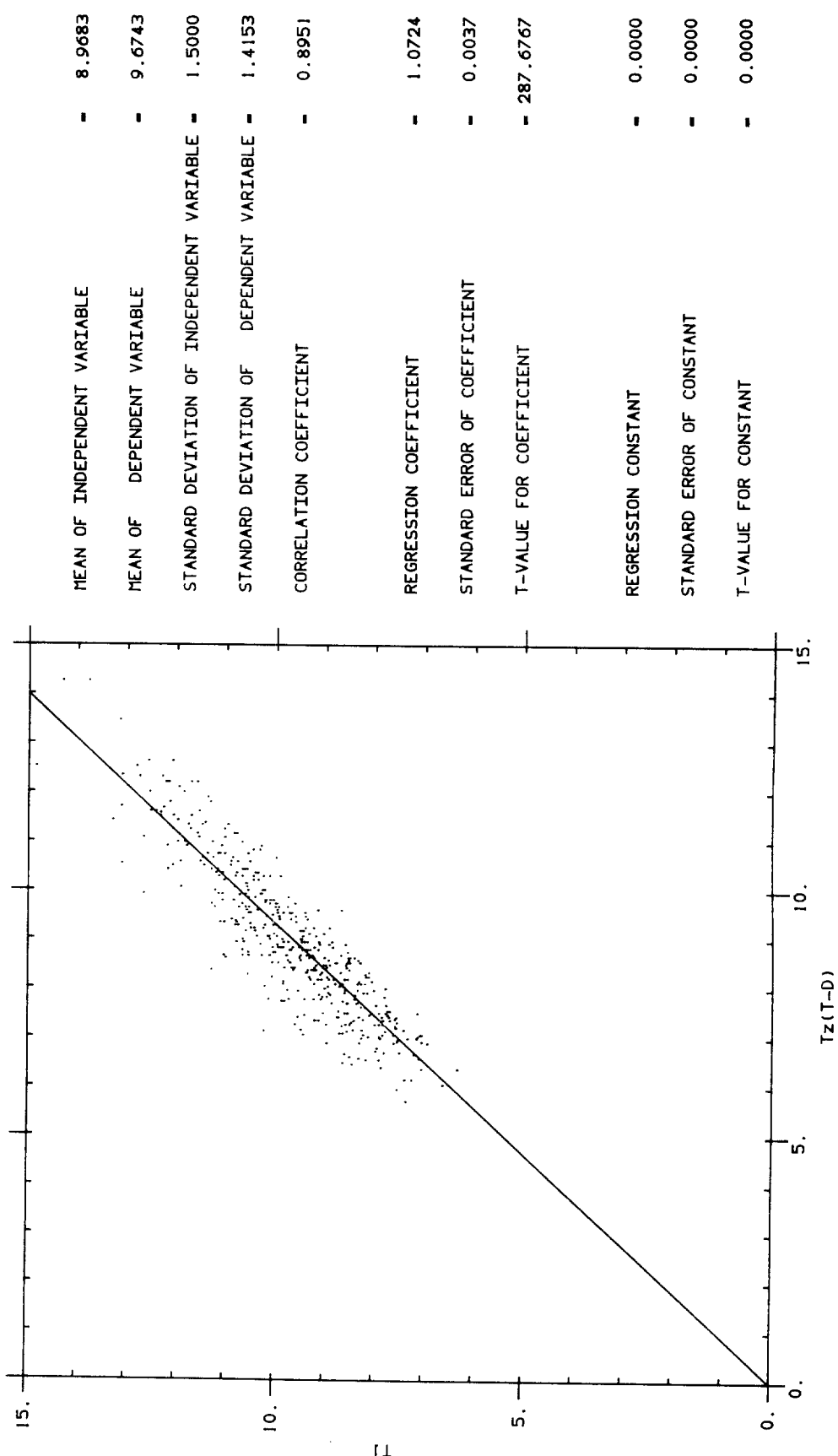
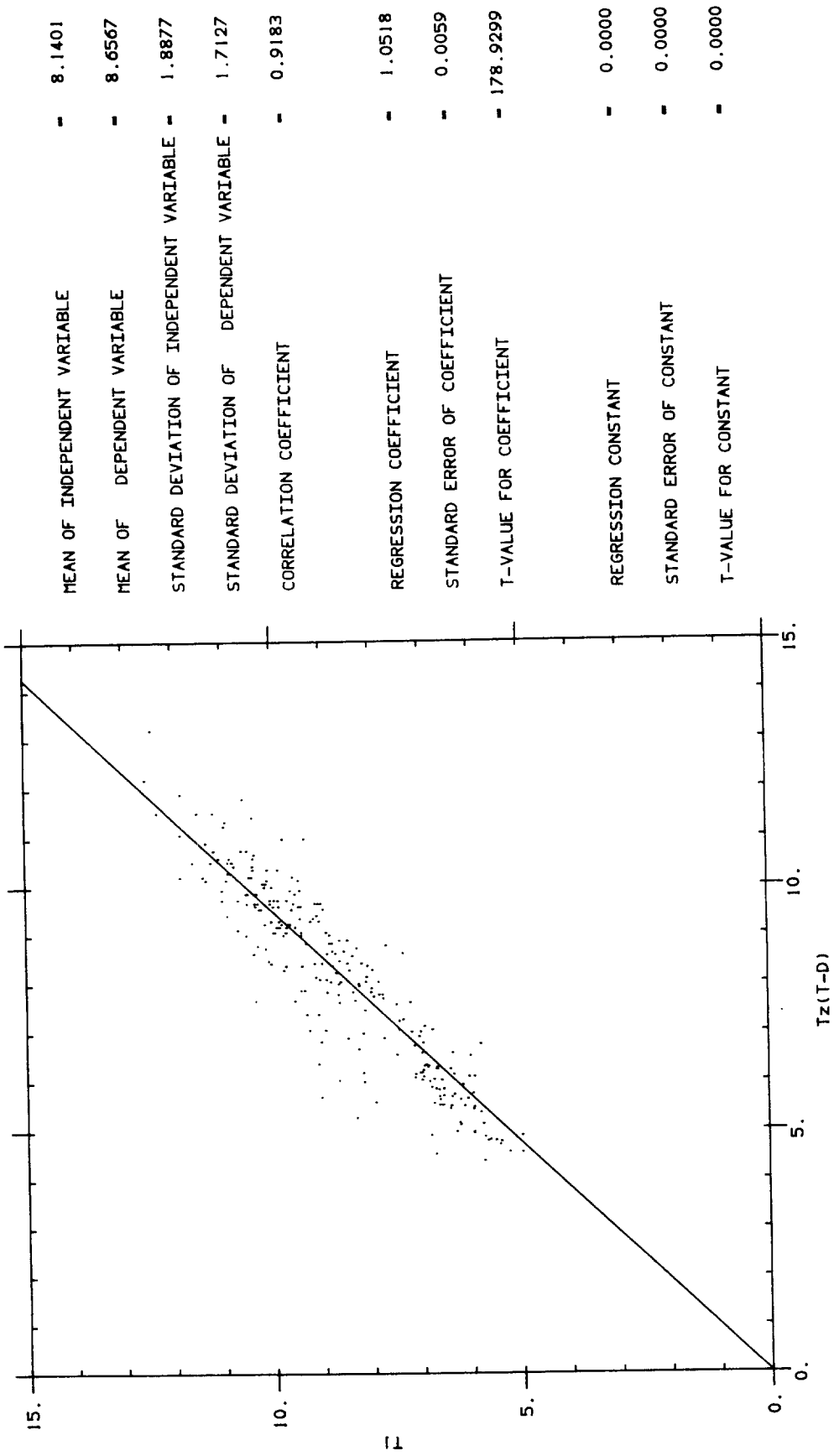


Fig. 8.2.6

SEVEN STONES(U), APRIL - MAY 1985



DOSSING(U), JULY - SEPTEMBER 1985

Fig. 8.2.7

77

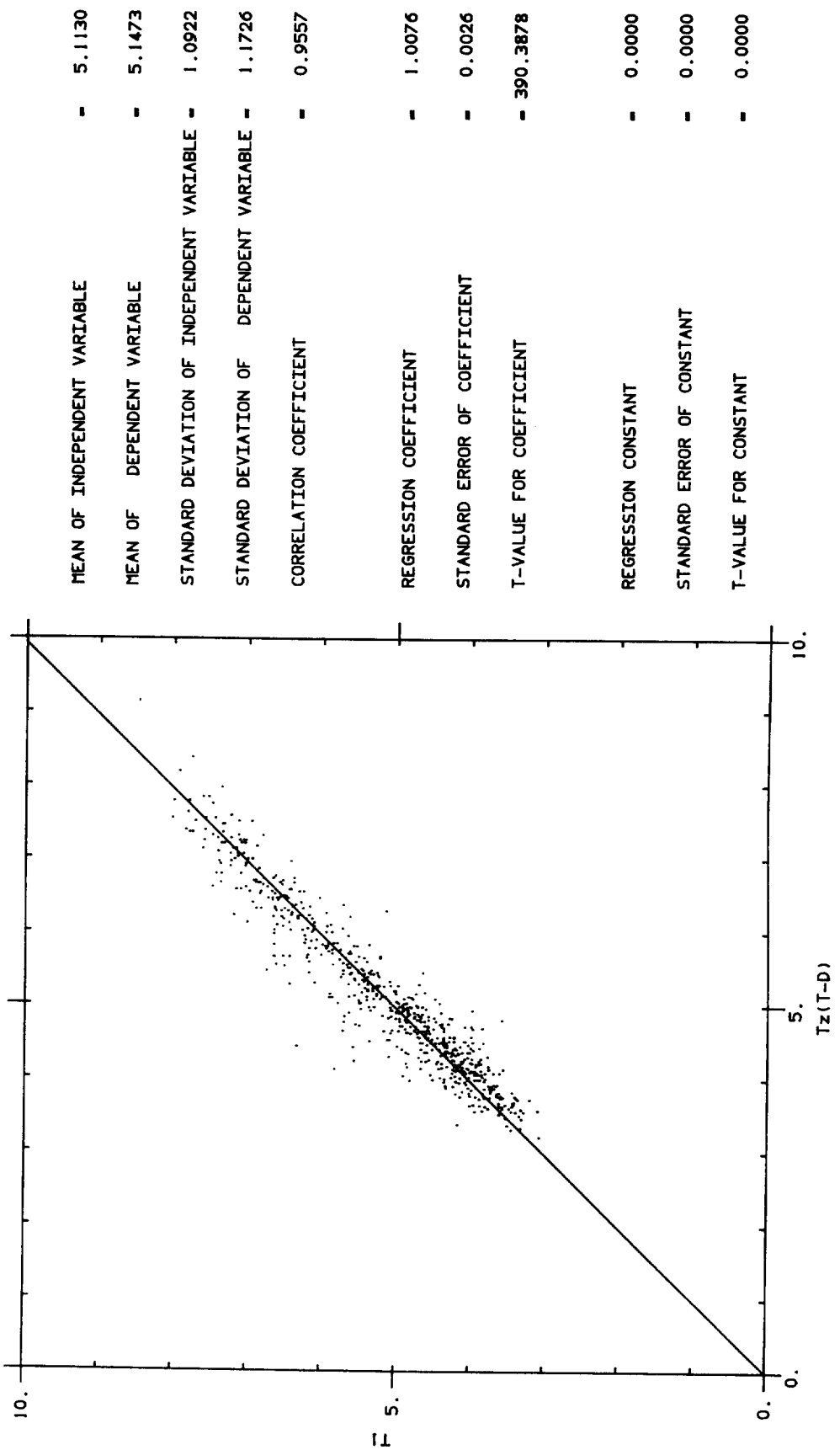
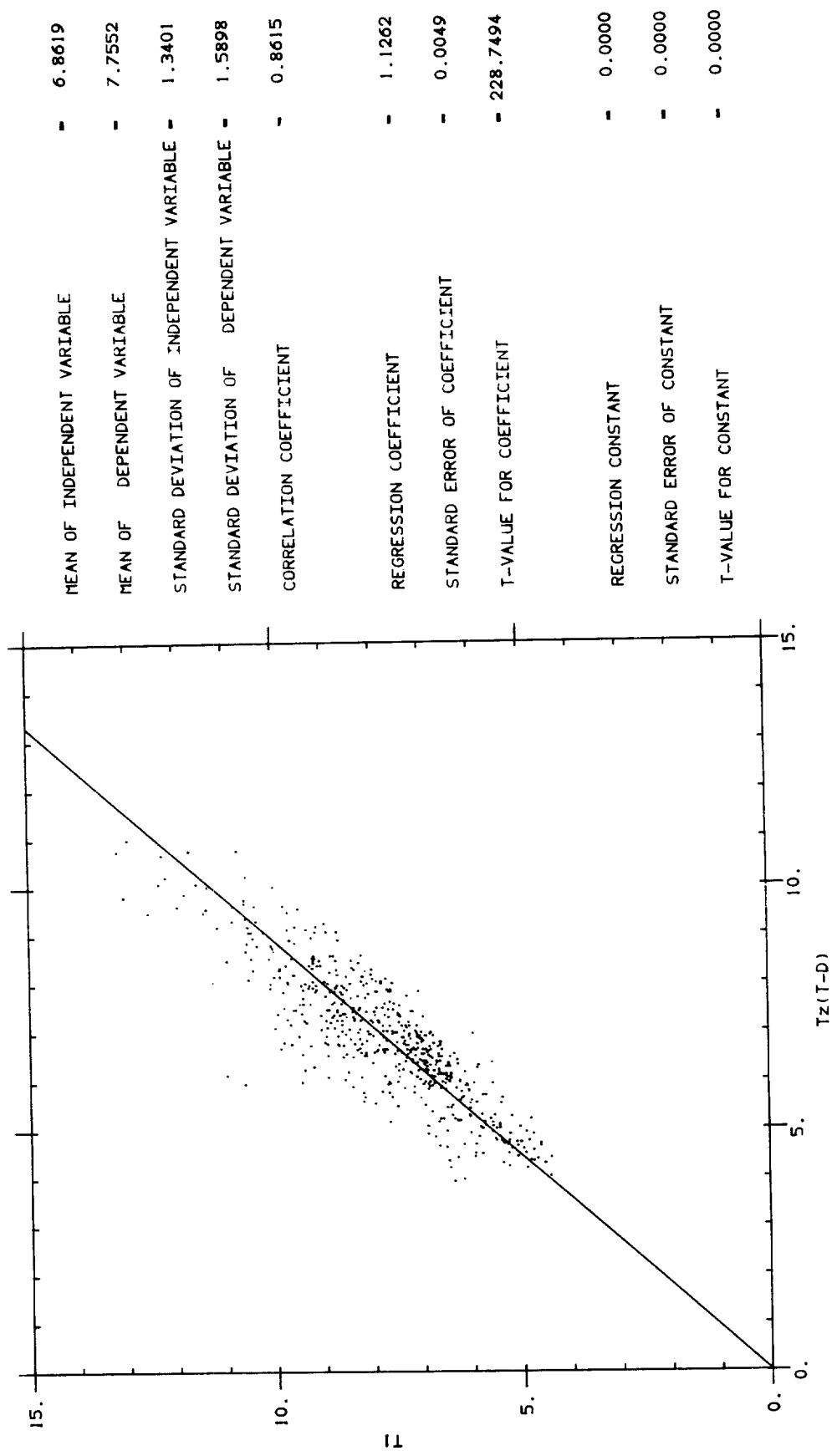


Fig. 8.2.8

CHANNEL (U), MARCH - MAY 1986



O.W.S. LIMA: JANUARY-MARCH 1984

Fig. 8-3-1

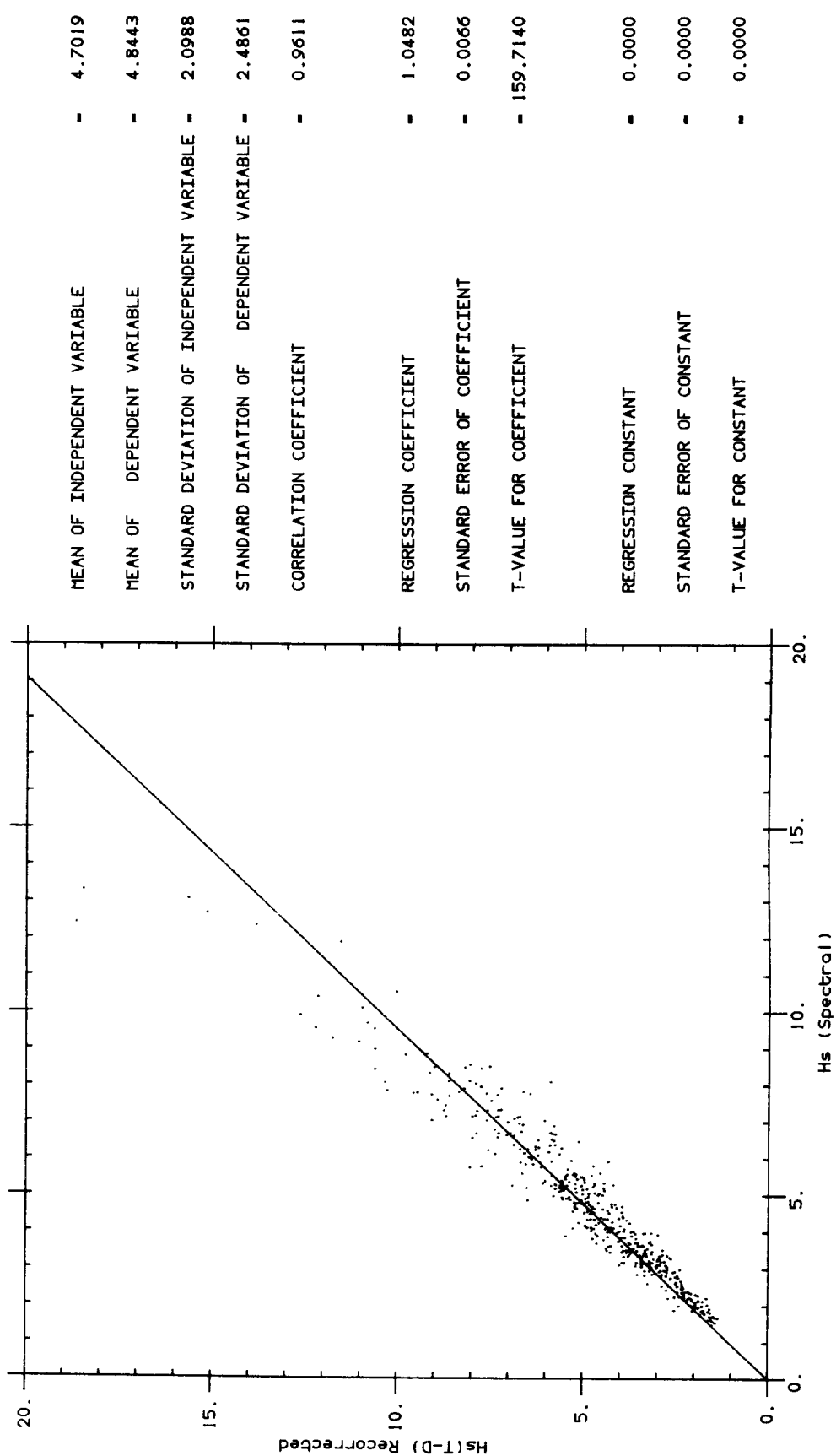


Fig. 8.3.2

SEVEN STONES, FEBRUARY - APRIL 1985

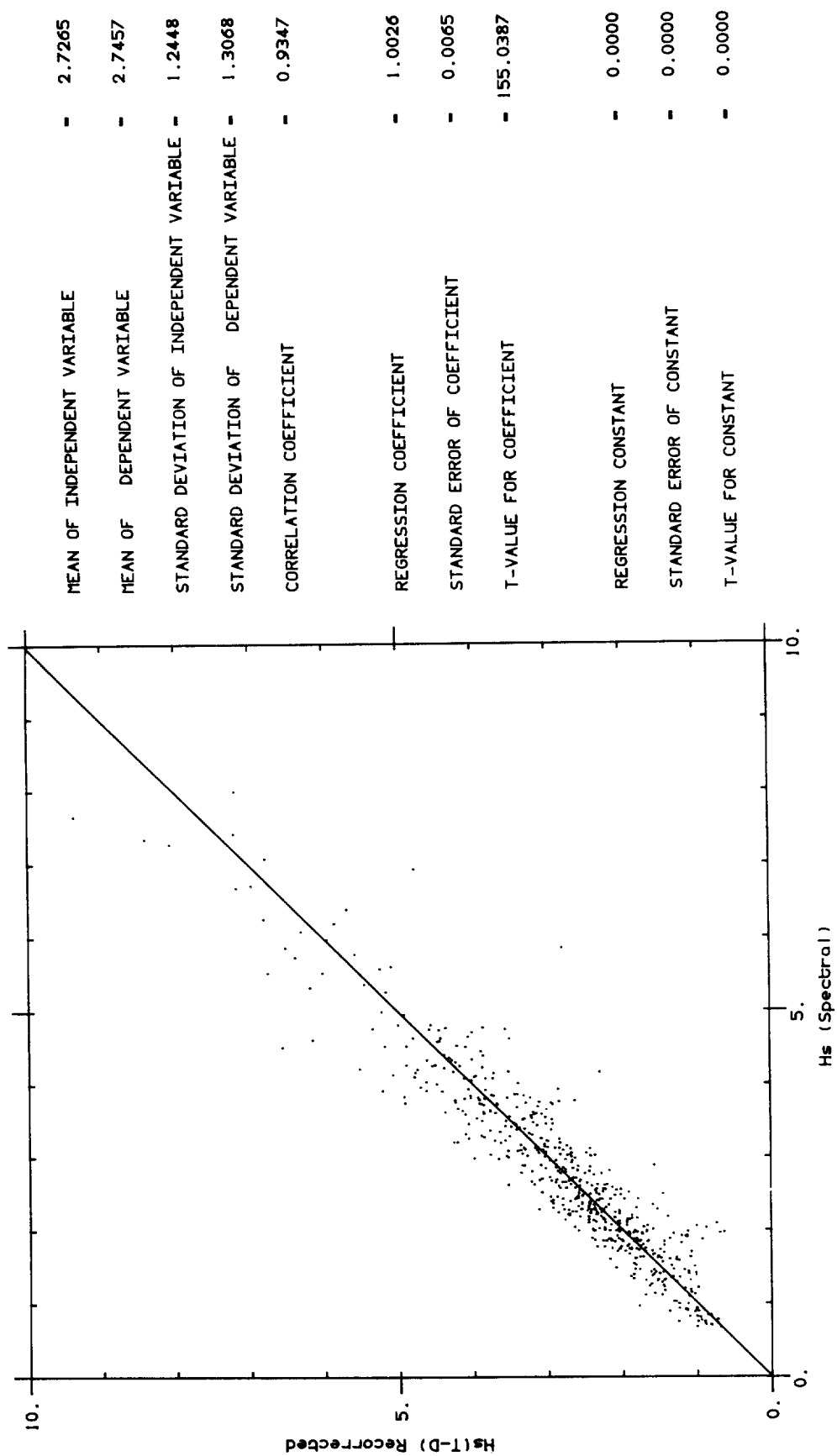


Fig. 8.3.3

DOWSING LV, JULY-SEPTEMBER 1985

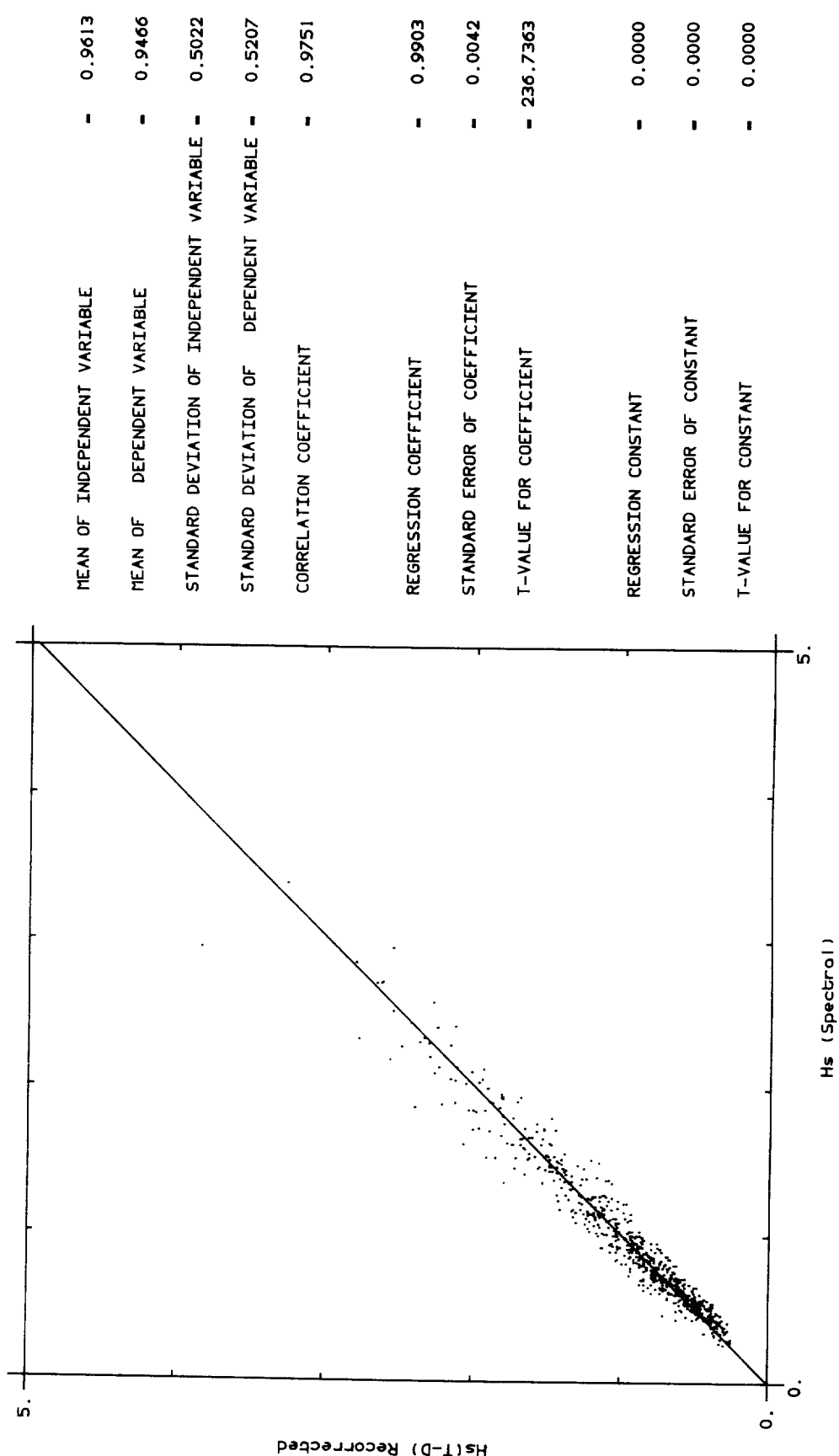


Fig. 8.3.4

CHANNEL LV, MARCH-MAY 1986

